

Design and synthesis of multivalent glycoconjugates for lectin binding

Dissertation

to obtain the academic degree

Doctor rerum naturalium (Dr. rer. nat.)

Submitted to the Department of Biology, Chemistry, Pharmacy
of Freie Universität Berlin

by

Pallavi Kiran

December 2018

The following project was carried out within the research group of Prof. Dr. Rainer Haag from **September, 2014** until **December, 2018** at the Institute of Chemistry and Biochemistry of the Freie Universität Berlin.

The first one year of studies has been supported by Sonderforschungsbereich (SFB 765 „Multivalenz in Chemie und Biochemie“), Freie Universität Berlin and final three years have been funded by an EU- Innovative Training Network, Multi-App.

1. Reviewer: Prof. Dr. Rainer Haag, Freie Universität Berlin
2. Reviewer: Dr Jens Dornedde, Charité-Universitätsmedizin Berlin

Day of defense: 20.12.2018

Dedicated to My Family

Acknowledgements

I want to express my deep gratitude to my Doctoral supervisor Prof. Dr. Rainer Haag for his scientific support and the opportunity to conduct this research in his group. He has also provided insightful discussions about the research. I appreciate all his contribution of ideas, time, and funding to make my Ph.D. experience productive and stimulating

I would especially like to thank Dr. Jens Dervedde for his consent to be the second reviewer of my thesis and taking part in subsequent defense procedure.

Furthermore, I am very thankful to Prof. Dr Andreas Hermann his sincere support and to allow me to conduct biological assay in his lab.

I would also like express my deep sense of thanks and gratitude to Dr. Sumati Bhatia for her valuable guidance, motivation, and constant support for the successful completion of project. Her guidance helped me in all time of research and writing this thesis.

I am grateful to all the cooperation partners I have been working with during my Ph.D, especially Prof. Dr. ir. Jurriaan Huskens, Prof. Dr. ir. Luc Brunsveld, Prof. Dr. Bettina G. Keller (Freie Universität Berlin), Prof. Dr. Wolfgang Maison (Universität Hamburg), Dr. Daniel Lauster (Humboldt-Universität zu Berlin), Dr. Stevel Aleksić (Freie Universität Berlin), and Dr. Susanne Liese (University of Oslo). I am especially grateful to the MULT-APP ITN for providing financial assistance, all the PIs for their helpful suggestions and comments during my progress report presentation and the PhD students, Daniele, Eva, Carlos, Maria, Petr, Wilber, and Isabell, for their good advice and friendship.

I expand my thanks to all the present and past group members of Haag group for their support and providing a nice working environment. I thank Jutta Hass and Eike Ziegler for taking care of my scholarships and official documentation and Dr. Pamela Winchester for proof reading. I thank Dr. Wiebke Fischer for always helping me. I also acknowledge Gaby Hertel, Katharina Goltsche, Cathleen Schlesener, Marleen Selent, Anja Stöshel, and Andrea Schulz for taking care of chemical ordering, GPC measurements, and help in measurements. I thank Dr. Florian Paulus and Daniel Stöbner for the synthesis of dendritic polyglycerol and MALDI TOF measurements. I would also like to thanks Dr. Kai Ludwig for the cryo TEM imaging. Furthermore, I would like to cordially thank Dr. Stephan Block, Dr. Luis Cuellar Camacho, Dr. Katharina Achazi, Dr. Nadine Rades, Dr. Virginia Wycisk, Chuanxiong Nie, Matthias Müller, Maiko Schulze, and Michael Tully for fruitful discussions in the subgroup seminar. I would specially like to thanks Dr. Badri Prashad for his supports and suggestions.

I am immensely grateful to my office and lab mates, Antara Sharma, Yong Hou, Qingcai Zhao, Karolina Walker, Fang Du, Pradeep Dey, Kim Silberreis, Manoj Muthalaya, Svenja Ehrmann, Alexander Oehrl, Katharina Huth, Magdalena Czuban, Guy Guday, Paria Pouyan, and Era Kapourani for keeping friendly lab and office environment. Also, I would like to thank Katherina for the translation of the short summary of my thesis.

I would like to extend huge, warm thanks to my friend Shalini, who always was beside me during the inevitable ups and downs of conducting my research to motivate and for her constant love and care. I feel lucky to have all the friends who helped me in different stages of my life. I mention few names Sreekant, Abhishek, Sirisha, Kiran, Gautam, and Rikesh.

I thank the service of core facility BioSupraMol for various NMR and mass measurements.

Financial support for this work was provided by the Sonderforschungsbereich (SFB 765 „Multivalenz in Chemie und Biochemie“), Freie Universität, Berlin and EU-Innovative Training Network, Multi-App.

Last but not least I would like to pay high regards to all my family members for their sincere encouragement, inspiration, and moral support. I feel lucky to have my parents' affections and blessings with me, which help me to get all the success in my life. I truly thank my elder brother Amit Anand and my sister Rashmi Kiran, and I acknowledge my husband Abhishek for his faith in me that I can finish this PhD. I truly thank my husband for his love, support, and cheering me up in stressful situations.

Table of Contents

1. Multivalency	1
1.1 Terms and definition of multivalency.....	1
1.2 Application of multivalency in biological and synthetic systems.....	2
1.3 Scaffolds for multivalent ligand.....	5
1.4 Polyglycerol based scaffolds.....	6
2. Lectin binding by multivalent glycoconjugates	9
2.1 Influenza virus and hemagglutinin.....	9
2.2 C-type lectins.....	16
2.2.1 MBL.....	17
2.2.1.1 MBL and complement system.....	18
2.2.1.2 Inhibitors for MBL pathway.....	20
2.2 DC-SIGN	21
3 Motivation and Objective	24
4 Publication and manuscript	
4.1 Exploring Rigid and Flexible Core Trivalent Sialosides for Influenza Virus Inhibition.....	26
4.2 Synthesis and comparison of linear and hyperbranched multivalent glycosides for C-type lectin binding.....	82
5 Summary and conclusion	108
6 Outlook	111
7 Abstract and Kurzzusammenfassung	112
8 References	114

9 Appendix.....	121
9.1 List of abbreviations.....	121
9.2 Publications and Conference Contributions.....	124
9.3 Curriculum vitae.....	126

1. Multivalency

1.1 Terms and definition of multivalency

Multivalency is an important phenomenon in various biological processes to achieve reversible and strong non covalent interaction between two components, i.e., ligand and receptor.^[1] A receptor can be defined as a molecule or protein that binds to the ligand using the binding pocket present on their surface.^[2]

Multivalency can be divided into three categories, namely, bivalency with two interactions between the different species ($i = 2$), oligovalency ($i \leq 10$) with a discrete number of interactions and polyvalency ($i \geq 10$) with a large number of interactions between the two species (the exact number of which is often unknown).^[2]

Multivalency can convert inhibitors with low affinity (K_d affinity \sim mM–M) to ones with high avidity (K_d avidity \sim nM) and/or biological “activity”^[2-3]. The affinity of a monovalent interaction is defined by its dissociation constant (K_d affinity); this constant usually has units of concentration (typically, molarity). Avidity (K_d avidity) is defined as the dissociation constant of a polyvalent interaction ($K_{d,N}$).

To achieve multivalent binding, the understanding of thermodynamics of interaction i.e., enthalpy (ΔH) and entropy (ΔS) is very important.^[4] In an ideal case the enthalpy of binding of a multivalent system is more favourable than that of the monovalent interaction, with little or no corresponding increase in the unfavourable translational and rotational entropy of binding. The enthalpy of interaction of a multivalent ligand with a multivalent receptor is, in principle, additive, while the entropy of interaction is not.^[2] However in some cases, the binding of one ligand to a receptor with a given enthalpy may cause the next ligand to bind to its receptor with greater enthalpy; that is, the value of $\Delta H^{\text{avg}}_{\text{poly}}$ in this case is more negative (more favorable) than the value of ΔH_{mono} .^[2] This can be explained on the basis of *effective molarity* (*EM*). Effective molarity is an important parameter and hence it is called the hallmark for multivalency.^[5] The first binding interaction between the polyvalent ligand and polyvalent receptor may change concentration of ligand that will be experienced by the neighbouring free receptor binding site. When this so-called effective concentration is more than the actual concentration of ligand in solution, the intramolecular multivalent binding interaction are more favoured. However, when the effective concentration of ligand at the receptor binding site is less than that in solution then the binding occurs in an intermolecular manner. The *effective molarity* (*EM*) is described by equation (1) where K_n is the association constant for the n-valent interaction and b is a

statistical factor showing the number of association and dissociation pathways during the interaction.^[4]

$$EM = \left(\frac{Kn}{bK_i^n} \right)^{1/(n-1)} \quad (1)$$

Another thermodynamic term i.e., enhancement factor (β) is defined as the ratio of the multivalent binding constant [K_{multi}] (binding a multivalent ligand to a multivalent receptor) with the monovalent binding constant [K_{mono}] (binding of monovalent ligand to multivalent receptor).^[3]

1.2 Application of multivalency in biological and synthetic system

Multivalent interactions are very important in various biological processes.^[1b, 3, 6] As described above, an important function of multivalent interactions in biological systems is enhancing weak interactions. One example of multivalent receptor is the pentameric cholera toxin (CT). CT is composed of one A-subunit with a noncovalently associated pentameric ring of B-subunits (AB_5) (Fig. 1). The B-subunits attaches to the membrane ligand, ganglioside GM1 at the intestinal cell surface with a high affinity and leads to the transport of CT into the cytoplasm, which consequently leads to the acute watery diarrhea.^[7] This is a good system to study the design of multivalent ligands as five ligand can bind to CT.

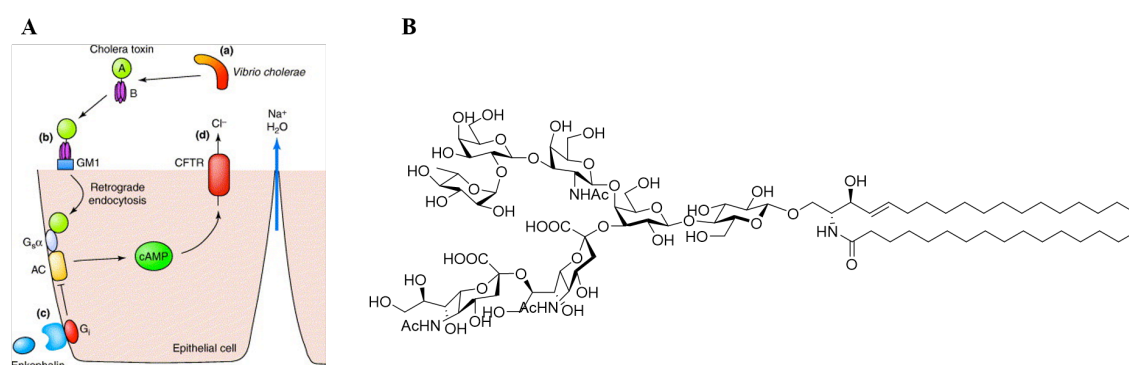


Figure 1. A) Mechanism of binding of cholera toxin to epithelial cells of the intestine. Adapted with permission from ref. ^[8] Copyright 2005 Cell Press. B) Structure of gangliosides GM1.^[9]

Another well explored example of strong lectin-carbohydrate interactions between polyvalent surfaces are selectins and their carbohydrate ligands. Selectin is a C-type lectin

Introduction

like glycoproteins that mediates the rolling of leukocytes during inflammatory processes. The rolling of leukocyte is mediated by the interaction of multiple E- and P-selectins present in the endothelial cell and sialyl Lewis^X (sLe^X), which is a tetrasaccharide ligand on the surface of leukocytes.^[10] Also, the L-selectin which is expressed on the surface of leukocyte, binds to the sLe^X present on endothelial cell.^[11] These process leads to extravasation of leukocytes into the inflamed tissue, which eventually leads to severe tissue damage (Fig. 2).^[12]

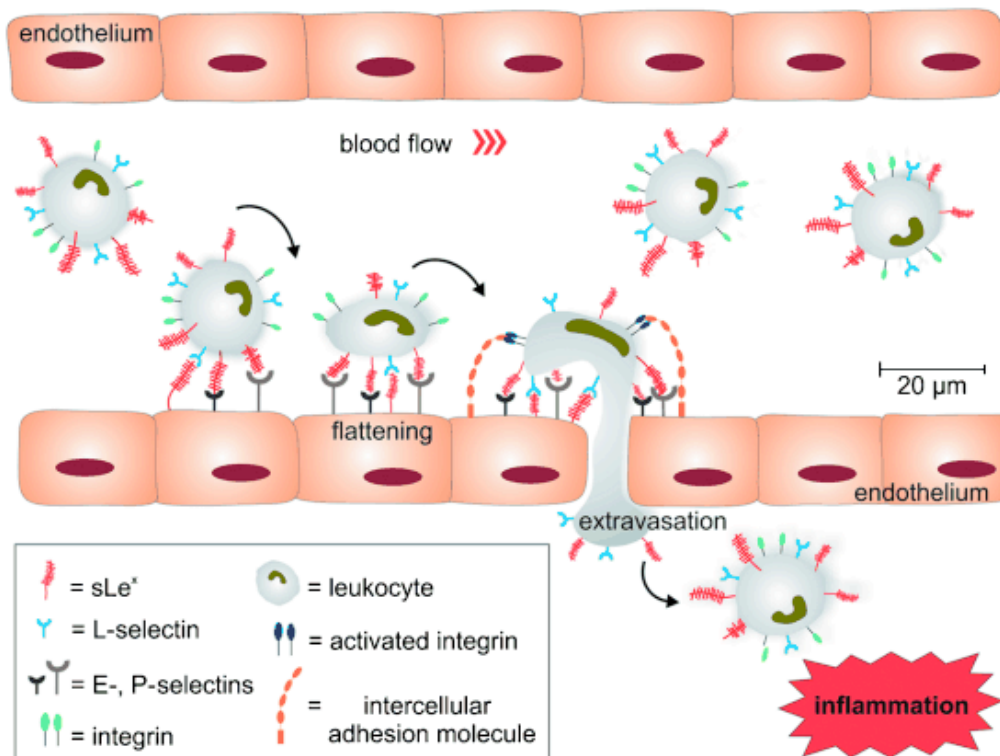


Figure 2. Recruitment of leukocytes to the vascular endothelium cell followed by extravasation of leukocytes at the inflamed tissue. Adapted with permission from ref.^[1a] Copyright 2012 WILEY-VCH.

Viral attachment to the cell surface occurs due to multivalent interaction. The binding of influenza virus to the epithelial cell^[13] is a very good example of multivalent interaction. The influenza virus attacks a target cell through multivalent interactions between multiple trimers of hemagglutinin (HA) with multiple components of sialic acid residues on the target cell surface (Fig. 3).^[3, 11]

Introduction

First application in the development of multivalent inhibitors was the synthesis of multivalent sialosides for binding with hemagglutinin on influenza virus.^[3, 13b] These inhibitors were composed of linear polyacrylamide (PAA) backbone, which was functionalized with sialic acid (SA) residues for specifically binding with hemagglutinin on influenza virus. The multivalent presentation of SA on PAA inhibited hemagglutination 10^4 to 10^5 times more strongly than did a similar concentration of methyl sialosides for influenza A X-31.^[13b]

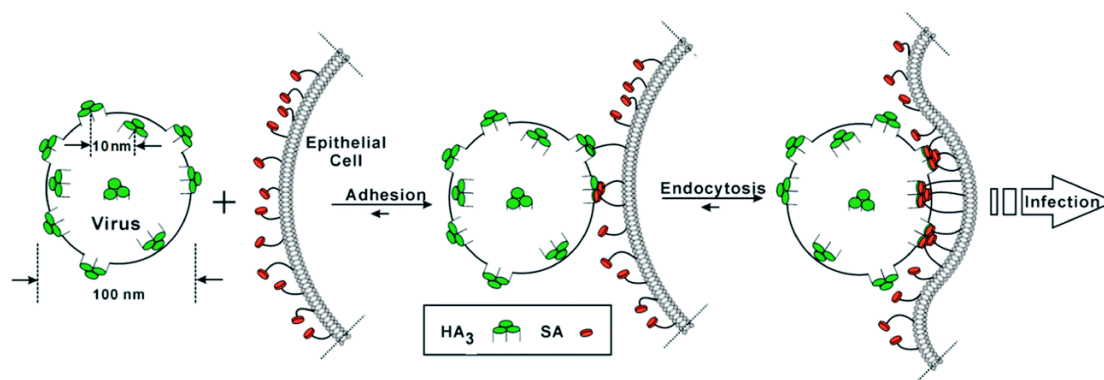


Figure 3. Multivalent interactions of trimeric haemagglutinin (HA₃) on influenza virus with sialic acid (SA) residues on cells leading to endocytosis and infection. Adapted with permission from ref.^[14] Copyright 2014, Royal Society of Chemistry.

CT has a low affinity with monovalent sugar and with the dissociation constants (K_d) in the millimolar range.^[15] Hol, Fan, and co-workers explored a series of multivalent ligand targeting cholera toxin and heat-labile *E. coli* enterotoxin. They used a semi-rigid pentacyclen scaffold for the design of pentavalent and decaivalent galactoside based inhibitors and observed a large enhancement in binding (10^5 - 10^6).^[16] One of the interesting constructs reported by Fan and co-workers was MNPG based galactosides where five copies of *m*-nitrophenyl- α -D-galactoside abbreviated as MNPG was attached on semi-rigid pentacyclen core via a flexible linker. The pentameric MNPG showed 100-times greater inhibition than the monovalent galactose.^[15b]

Thoma et al developed a series of multivalent polylysine conjugated with sLeX to inhibit the E-selectin mediated cell-cell interaction. Although the monovalent sLeX had an IC_{50} value in the millimolar range, the multivalent counterpart had IC_{50} value of 50 nM. The multivalent presentation of low affinity ligands showed 700-fold improved potency more than the monovalent ligand.^[17]

1.3 Scaffolds for multivalent ligand

Designing of a successful multivalent architecture requires, consideration of not only the intrinsic affinity of each ligand to the receptor but also the degree of flexibility, the extent of hydration, and the size of scaffold.^[2] The purpose of scaffold is to serve ligands attached by linkers to the multivalent receptor site (Fig. 4). A rigid scaffold can be used to avoid loss of conformational entropy upon complexation.^[2] Two types of scaffolds commonly used for the design of multivalent ligands are randomly-coil linear polymers or spherical architecture (e.g., hyperbranched or dendritic polymers). The linear polymers can have high impact on the viscosity, whereas the spherical polymers have negligible effect on the viscosity of the solution.^[2] Linear polymers offer flexibility and good water solubility, which makes it an appropriate platform for the design of multivalent ligands. The flexibility of the polymers can be varied using flexible or rigid backbone. Polyacrylamides (PAA) has been used by numerous researchers to make flexible backbone.^[13] For instance, sialic acid (SA) functionalized PAA has been used for influenza virus inhibition.^[18] Kiessling et al. has reported β -glucose containing linear poly(7-oxanorbornene) polymer that was prepared by ROMP (ring-opening metathesis polymerization) for concanavalin A (Con A) binding.^[19] Poly(p-phenylene ethynylene) (PPE) functionalized with mannose has been used for detection of *E. coli* by multivalent interactions.^[20] Other important multivalent scaffold architectures are glycopolymers with different carbohydrate functionalization to natural architectures, for example dextrans, chitosans, hyaluronic acids and heparins.^[1a] Sugar functionalized chitosan have been evaluated for various cell recognition studies. Several cell specific carbohydrates for example mannose,^[21] fucose,^[21b] galactose,^[21b, 22] lactose^[21a] were introduced into chitosan backbones and have been used to study the interaction of cells with microorganisms. Various carbohydrate functionalized dendrimers have been examined for the inhibition of hemagglutinin or for the binding to lectins caused by either bacteria or lectins. Poly(amidoamine) (PAMAM) or poly(ethylenimine) (PPI) based dendrimers were used as a scaffold for the multivalent presentation of ligands.^[23] Cloninger and co-workers prepared and investigated mannose conjugated PAMAM dendrimers (G1 up to G6) for the Con A-induced hemagglutination inhibition of erythrocytes.^[24] The glycodendrimers (G4-G6) with more than 50 mannose residues per dendrimer were efficient inhibitors of hemagglutination with significant enhancement because larger dendrimers were able to bind bivalently to Con A.^[24b] An application of dendrimers as therapeutics is the poly-L-lysine (PLL) dendrimer based drug called VivaGel[®] developed by Starpharma (Australia). It is a fourth-generation dendrimer

Introduction

(SPL7013) covered with naphthalene disulfonate, which is believed to bind with the virus by electrostatic interactions and thus preventing its attachment to the host cells. This polymer is currently under clinical development as a topical vaginal gel to prevent the infection of sexually transmitted HIV *in vivo*.^[25]

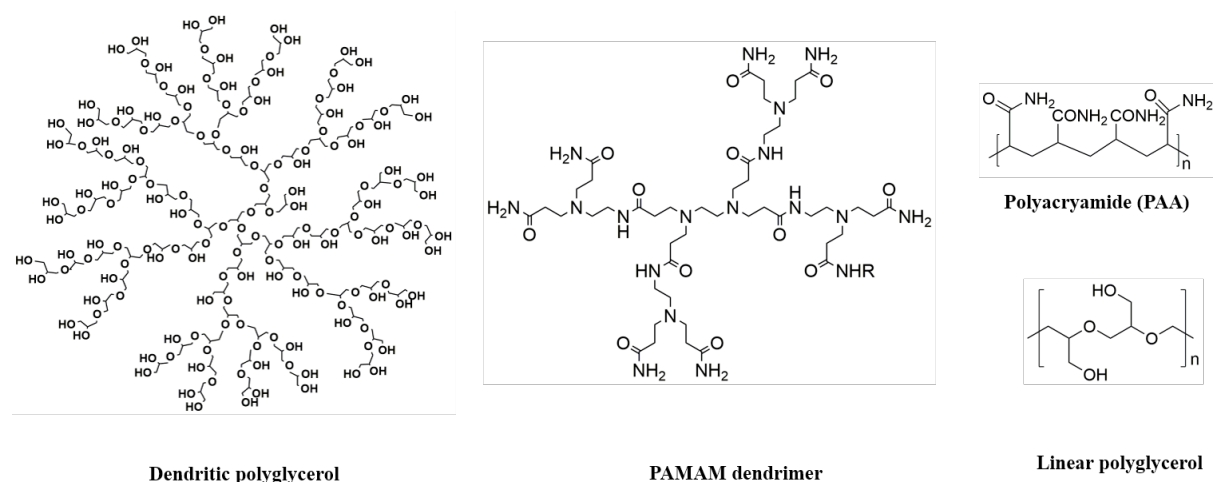


Figure 4. Structures of commonly used scaffolds for the multivalent display of ligand.

1.4 Polyglycerol based scaffolds

Polyglycerols polymers are a potent class of scaffold for the multivalent display of ligands, because of their good water solubility, biocompatibility, low toxicity, high number of hydrophilic functional groups, and a highly flexible aliphatic polyether backbone.^[13b, 26] Kim and Webster were the first ones to introduce the term “hyperbranched polymers” in 1980 to define dendritic macromolecules synthesized by AB_m -type polycondensation.^[27] Unlike most dendrimers, which are prepared in multistep syntheses, hyperbranched polymers can be synthesized in single step and are considered the “poor cousins of dendrimers” because of their high polydispersity.^[28] Hyperbranched polymers do not show entanglements, due to which they have very low bulk viscosities in comparison to linear polymers. Molecular weight (M.Wt.), degree of branching (DB), and polydispersity (PDI) are the three fundamental parameters to characterize the hyperbranched polymers. Control of these parameters are essential for the development of complex macromolecular architectures.^[28a]

Polyglycerols can be produced by various polymerization methods. Kim and Webster reported the synthesis of hyperbranched polymers by the most common method i.e., polycondensation of AB_m type monomers, which strongly affects the DB and molecular

Introduction

weight distribution of the polymer.^[27a] A second method, reported by Fréchet and co-workers used self-condensing vinyl polymerization (SCVP), where the vinyl monomer bearing an initiating group was used.^[29] The disadvantages of using these methods were that the obtained polymers have broad molecular weight distribution and very high PDI. A third method reported by Sunder et al in 1999 is the ring opening multibranching polymerization (ROMBP) where cyclic AB₂-type monomers were used.^[30] This type of polymerization was carried out by anionic ring opening polymerization of commercially available glycidol by making use of partially deprotonated trifunctional core-initiator. In this method, hPG was synthesized in a one-step process starting with a slow addition of glycidol to partially deprotonated trimethylolpropane (TMP). Due to fast polymer exchange that occurs during polymerization the different chain ends (primary and secondary alcohols) grow simultaneously, which gives rise to a branched structure (Fig. 5). The molecular weight of polymers obtained by this method, which can be adjusted by the ratio of monomer to initiator and PDI, is typically low. Brooks et al reported similar biocompatibility profiles of hPG and polyethylene glycol (PEG).^[31] However, hPG has slightly higher thermal and oxidative stability in comparison to PEG.^[26b, 31-32] Considering these remarkable features, hyperbranched PGs is a suitable material for biomedical applications.

As described above, polymerization of glycidol leads to the formation of hPG, but linear polyglycerol (LPG) can also be obtained, when the protected glycidol is used as a monomer followed by removal of the protective group in the post polymerization step (Fig. 5). Typical monomers used for the LPG synthesis are trimethylsilyl glycidyl ether (TMSGE), ethoxyethyl glycidyl ether (EEGE), tert-butyl glycidyl ether (*t*BGE), and allyl glycidyl ether (AGE).^[33] EEGE is the most commonly used for the synthesis of LPG due to easy removal of acetal protecting group under mild acidic condition.^[33] Typical low molecular weight PGs are obtained with initiators such as potassium tert-butoxide (t-BuOK),^[34] potassium 3-phenylpropanoate (PPOK),^[35] alkoxy ethanolates and potassium methoxide (MeOK)^[36]. Taton et al was the first one to report the synthesis of LPG by anionic ring-opening polymerization of EEGE using CsOH as an initiator with high molecular weight (approx. 30kDa).^[37] Typically, anionic polymerization of protected glycidol like EEGE is carried out using an initiator which leads to the formation of protected LPG. Tetraoctyl ammoniumbromide (NOct₄Br) could be used as initiators and triisobutylaluminum (^tBu₃Al) for the activation of monomer as reported previously in the literature.^[38] In the second step,

Introduction

acetal protection is removed by acid-catalyzed reaction which leads to the formation of LPG (Fig.5).^[33]

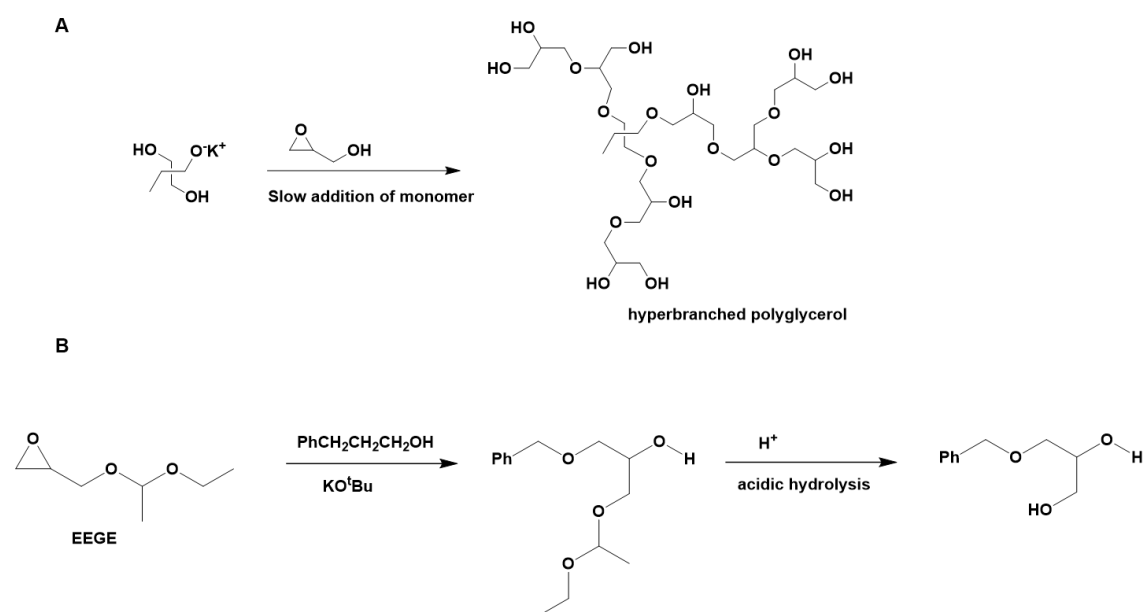


Figure 5. Synthesis of A) hyperbranched^[30] and B) linear polyglycerol^[35b] by anionic ring opening polymerization.

2. Lectin binding by multivalent glycoconjugates

2.1 Influenza virus and hemagglutinin

The influenza viruses belongs to the class of Orthomyxoviridae family of viruses and it is characterized by single-stranded RNA genome of negative polarity, which is contained within an enveloped virion as eight different RNA segments.^[39] There are four types of influenza virus namely A, B, C and D.^[40] The influenza A viruses are responsible for major pandemics that mostly cause higher mortality rates than seasonal influenza epidemics. In the last century, influenza A viruses have caused four major pandemics, the most severe one was 1918 Spanish pandemic which caused approximately 40 million death worldwide.^[41] The other three pandemic includes 1957 Asian pandemic, 1968 Hong Kong pandemic, and the 2009 H1N1 pandemic.^[42] The H5N1 virus (bird flu) that was first detected in Hong Kong in 1997 has been reported to cause serious human disease and caused high mortality rate.^[42d] In contrast, the 2009 H1N1 virus (swine flu) was able to do human-to-human transmission but was a relatively milder disease with a lower mortality rate.^[43] The virion envelope of influenza A viruses are decorated with two major surface glycoproteins, hemagglutinin (HA) and neuraminidase (NA), as well as integral membrane protein (M2 ion channel protein) (Fig. 6).^[44] Influenza A viruses are divided into subtypes based on antigenic HA and NA subtypes i.e., 18 HA (H1-H16) and 11 NA (N1-N9) antigenic subtypes have been found to circulate so far.^[45] The major subtypes of influenza A that have affected human population during seasonal epidemics are H1N1, H2N2, and H3N2.^[40b, 42d] HA molecules mediate the attachment of virus to sialylated glycan receptors on the host cells, and thus release the viral ribonucleoprotein particles into the cytoplasm. NA catalyzes the cleavage of the glycosidic bond of terminal sialic acid on the host surface and facilitates the release of the virion (Fig. 6).^[46]

Influenza A viruses undergo constant evolution through mutation of virus itself and re-assortment of viral genomes from different strains.^[47] It undergoes constant point mutation at antigenic sites over time as the virus replicates. These are called antigenic drift. These genetic changes can occur at the surface protein of influenza A virus (IAV) such as HA or NA. As a consequence, the body's immune system are unable to recognize those viruses and the immune protection will no longer be effective against virus which will cause viral infection.^[48] The exchange of genetic material between coinfecting viruses that is called reassortment, is another process by which influenza virus undergoes evolution.^[49] The reassortment occurs when IAVs infect the same host and same cell within the host.^[49c]

Introduction

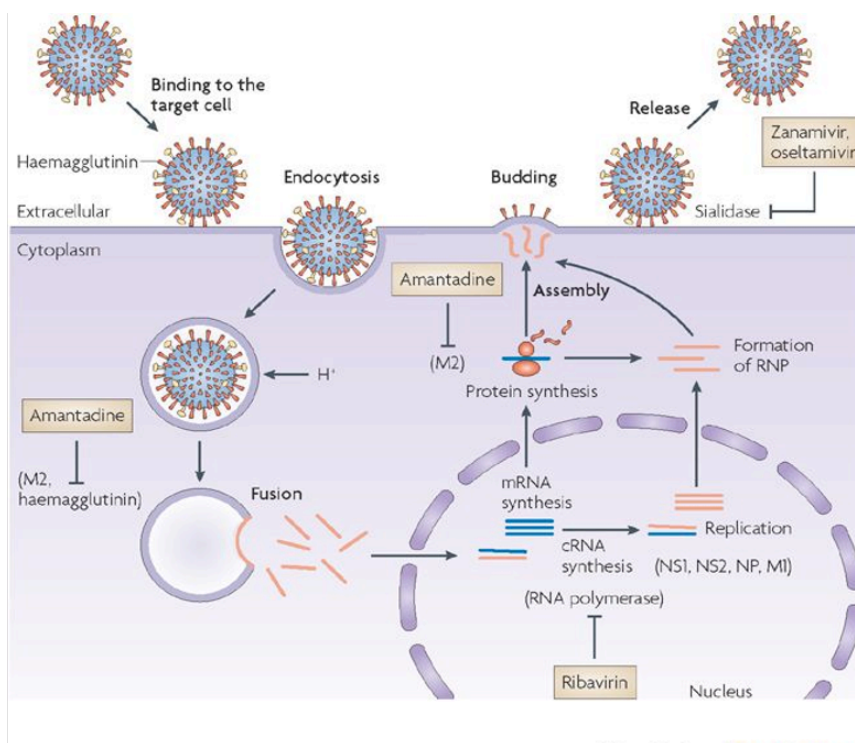


Figure 6. Schematic diagram showing the viral replication process. Adapted with permission from ref.^[50] Copyright 2007 Nature Publishing Group.

Influenza virus has eight different segments of virus, the reassortment of virus leads to new antigenic pattern called antigenic shift.^[51] It is a special case of reassortment. As described above, antigenic drift is natural mutation over a long period of time which causes loss of immunity contrasts with antigenic shift. Antigenic drift occurs in influenza A, B and C whereas antigenic shift occurs only in influenza A virus. Two of the major pandemics in 20th century, i.e., 1957 and 1968 pandemic flue, emerged due to reassortment between human IAV and avian influenza virus,^[47a, 52] whereas 2009 swine flu outbreak was due to reassortment of human, swine, and avian influenza virus.^[47a] Other than mutation and reassortment, IAVs can undergo mutation by relatively rare means called recombination.^[47a] Recombination occurs through two mechanisms, one is non homologous recombination, which happens between two different RNA fragments.^[53] The other method of recombination known as homologous recombination in influenza virus. It involves in template switching of RNA molecules that coinfect a single cell. Homologues RNA recombination rarely occurs.^[54] Due to these genetic drifts of influenza virus there is urgent

Introduction

need for development of new vaccine and drugs production against seasonal influenza viruses each year.^[55]

As hemagglutinin is the major surface antigen of influenza A viruses, it is primary source of natural immunity and key target in vaccination. It plays an important role in the development of human pandemic influenza viruses.^[55] HA exists as a trimer of identical subunits, and has a cylindrical shape with approximate length of 135 Å and radius of 35-70 Å.^[56] It is present as spike-like protein on the surface of influenza virus. Each monomer of HA molecule contains a globular head domain and a stem domain. The receptor binding site is located on globular domain.^[57] The receptor for influenza virus spikes i.e., HA is sialic acid (SA) containing molecules on the cell's surface.^[44, 58] However, there are a number of chemically different forms of sialic acids, which are based on glycosidic linkage of SA and the next sugar of the side chain, the influenza virus varies in its affinity for SA.^[44] The human IAVs (e.g., H3N2) prefer to bind sialic acid with α 2,6-glycosidic linkage to galactose.^[59] Whereas, viruses of avian origin (e.g., H5N1) preferentially binds to SA with α 2,3 glycosidic linkage to galactose.^[60] Neuraminidase (NA) is another major membrane protein which is embedded on the surface of influenza virus.^[61] It exists as a mushroom-shaped tetramer of identical subunits and it extends approximately 60 Å from the surface of the virus. NA is an enzyme that catalyzes the hydrolysis of glycosidic bond during the process of viral replication, specifically terminally linked sialic acid from glycoprotein saccharide chains and removes SA from the cellular glycoproteins. As a result, the virus is released from the membrane and move off to infect other cells and spread the infection.^[62]

Currently, two different strategies are used to control the spread of influenza virus namely, vaccines and small molecule based antiviral drugs. Vaccines are in the first line of defense against influenza, however, production of sufficient quantities of vaccine with appropriate antigens takes 6 months, therefore antiviral drugs are important countermeasure to reduce the effect of influenza virus infection.^[63] Two classes of anti influenza drugs are currently available to treat influenza infections i.e., M2 ion channel inhibitors (amantadine and rimantadine) and neuraminidase inhibitors (NAIs: oseltamivir, zanamivir, peramivir, and laninamivir). The M2 ion channel inhibitors block the influx of protons through M2-proton channel so that uncoating and release of genetic material into the cytoplasm are inhibited. NAIs block the sialidase, and hence inhibit the release mechanism of virus. However, IAV rapidly developed resistance against these classes of drugs due to mutation of viral components. Most of the circulating IAV has developed resistance for M2 ion channel

Introduction

inhibitors.^[45c, 64] Thus, NAIs are the only remaining class of drugs to prevent influenza A and B virus infection. Hence development of new anti-IAVs drug is very important to protect the population against influenza virus.

An alternative approach for the prevention of influenza virus infection is to target HA which mediates the entry process.^[65] The inhibition of HA will block the initial step of viral infection.^[66] Until now, various types of anti-influenza compound targeting HA have been reported, including small molecules, monoclonal antibodies, peptides and proteins.^[67] The crystal structure of HA reported by Wiley and co-workers has led to an extensive search for small molecules that can bind to HA with high affinity.^[68] No compound targeting HA has been reported as a drug yet.^[44, 69] This is mainly due to weak interaction of HA to its natural ligand SA.^[70] Also the binding affinity of HA with monovalent SA is very weak (10^{-3} M) and it requires high concentration of monovalent SA.^[70] Several polymeric multivalent sialosides have been reported in the literature, which show strong binding to HA.^[71] Whitesides and co-workers have reported a series of polyacrylamides presenting α -C-glycosidic Neu5Ac group as a side chain for the inhibition of IAV. The best copolymer inhibited HA approximately 10^4 - 10^5 times more strongly than did a similar concentration of α -methyl sialoside.^[13a] Although high molecular weight PAA polymer based sialosides reported by Whiteside's group were extremely effective against virus, but due to toxicity of PAA based material, various other synthetic scaffolds continue to be investigated.^[18] A variety of multivalent polymers functionalized with sialic acid have been reported in literature which show more enhancement in binding affinity than its monovalent counterpart.^[13a, 71-72] As mentioned before, commercially available dendrimers such as PAMAM related scaffolds have been explored for multivalent display of sugars.^[23] Kwon and co-workers reported the importance of optimal ligand density and spacing between the ligand for the design of effective IAV inhibition. They used spherical PAMAM scaffold and decorated with 6'-sialyllactose (6SL) to prepare a series of multivalent IAV inhibitors. The most potent candidate among the series was G4 based 6SL-PAMAM conjugates with dissociation constant of 1.6×10^{-7} M. *In vivo* application of these conjugates protected 75% of mice from H1N1 and successfully prevented the loss of weight for infected animals.^[73] Recently, Bhatia and co-workers reported the importance of architecture and optimal ligand densities for the development of multivalent IAV inhibitors. PGs (LPG and dPG) were used as scaffolds for the multivalent display of SA and LPGSA with 40% ligand density was the most potent candidate with a dissociation constant in low micromolar range (Fig. 8A).

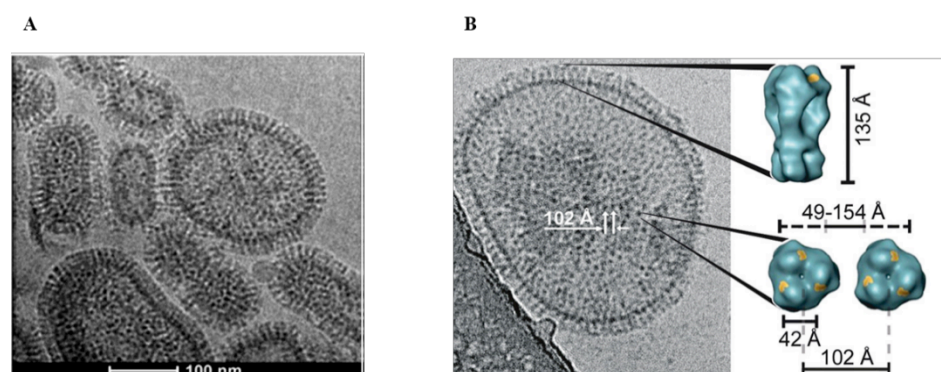
Introduction

Also, *in vivo* application of LPGSA and NAI i.e., oseltamivir carboxylate showed synergistic inhibitory effect and efficiently prevented IAV infection.^[26c]

Papp et al, investigated synthesized dendritic polyglycerol based nanogels (nPG) and functionalized it with sialic acid with diameters in the range of 25-100 nm for influenza virus inhibition (Fig. 8B). The ligand density and size of nanoparticles were optimized, and they found that larger particle i.e., 50 nm sized nPG with 12% ligand density was the most potent candidate showed up to 80% inhibition of viral activity (IAV/X31) at low micromolar concentration.^[74] Also, glycerol based dendrons (1 nm) were functionalized with sialic acid and were covalently attached to gold based nanoparticles (AuNPs) in different size range (2 nm and 14 nm). The sialylated AuNPs with a 14 nm size were highly efficient for the inhibition of influenza virus, whereas, the 2 nm AuNPs did not have any significant impact on inhibition of influenza virus. This work highlighted the importance of matching particle size for efficient infection inhibition.^[26d]

In this direction, Lauster et al developed a new class of polyglycerol-based peptide conjugates for the inhibition of IAV (Fig. 8C). In this study they used two types of peptide which binds to CRD domain of HA namely PeB and PeB^{GF} to synthesize a series of multivalent polyglycerol-based peptide with different molecular weight of PG-scaffold. They found that PG-PeB^{GF} conjugates had higher affinity in comparison to PG-PeB based construct when tested for *in vitro* assay i.e., in HAI and MST based experiment. In contrast, PG-PeB conjugates was more potent as multivalent inhibitor for *in vivo* model.^[75]

Typically, HA is uniformly distributed on the surface of influenza virus having approximately 400-500 copies of HA trimer. The Cryo-TEM imaging suggested 4-5 nm average distance between the binding site on single HA trimer, however a 10-12 nm distance between the midpoints of two adjacent HA trimers (Fig. 7).^[76] Design of multivalent sialosides with an optimal spacing in between the ligands to target hemagglutinin trimeric glycoprotein with high affinity has also been explored using trivalently functionalized scaffolds.



Introduction

Figure 7. Schematic diagram showing A) Cryo-TEM image of human IAV (X31/H3N2) presenting the HA trimer. Adapted with permission from ref.^[76a] Copyright 2016 American Chemical Society. B) The average distance between the receptor binding site of two adjacent HA trimer and inter-trimeric distance. Adapted with permission from ref.^[76b] Copyright 2017 American Chemical Society.

Waldman and co-workers reported trivalent SA decorated glycopeptide conjugates to target HA trimer of IAV (Fig. 9B). To reduce the overall flexibility of trivalent sialosides and minimize the entropic cost required during binding, they chose conformationally stiff peptide-based spacers instead commonly used ethylene glycol oligomers. The best tripodal compound had low nanomolar binding affinity ($K_d = 450$ nM) against H5 of avian influenza which was 4000-fold higher in comparison with monovalent Neu5Ac α 2Me. Thus they obtained the interaction strength between bi- (500-fold) and trivalent (300 000-fold) ligands.^[69] Ohta and co-workers reported cyclic peptide based scaffold for the trivalent presentation of sialyllactose [Neu5Ac α (2,3)Gal β (1,4)Glc] to target trimeric HA protein (Fig. 9C). The highest affinity glycopeptide based inhibitor were obtained when all the three ligands were pointing outward from the cyclic peptide ring so that 3 sugar can reach the binding pockets of HA trimer simultaneously to have multivalent effect ($K_d = 0.65$ mM).^[77]

Bandlow et al, explored two different type of scaffold namely flexible PEG based and rigid self-assembled DNA/PNA based scaffold for the bivalent display of α 2,6-linked sialyllactose (Sialy-LacNAc) ligand at distance of 23-101 Å to target the HA trimer of IAV/X31 (Fig. 9A). They investigated that although the end to end distance of ligand was 50 Å for the PEG based construct which should be ideally suitable to bridge the distance of receptor binding site on HA but due to flexible nature of PEG based scaffold, effective concentration of ligand at the second binding site was significantly much lower (100 μ M) than the binding affinity of monovalent ligand ($K_d = 3$ mM). However, DNA based construct having end to end distance in the similar range (52 Å) as that of PEG spacer, it had 100-times more effective concentration in comparison to PEG based construct. This shows the bimodal relationship of distance-affinity for the interaction with HA IAV with Sialy-LacNAc ligand DNA/PNA based scaffold.^[76b]

These examples suggest that the use of conformationally stiff peptide-based spacers for the design of multivalent inhibitors would be a good choice to attain a high affinity multivalent

Introduction

inhibitor due to minimal loss in conformational and rotational entropy up on binding with receptor.^[76a, 78] Yamabe and co-worker also focused on the spatial arrangement of SA binding sites and designed 2,3-SL functionalized three-way junction (3WJ) DNA architecture where topology of the inhibitor was like the SA binding sites. The best candidate was 3WJ DNA with three 2,3-SL and it has 8.0×10^4 -fold higher binding affinity for IAV in comparison to 2,3-SL.^[79]

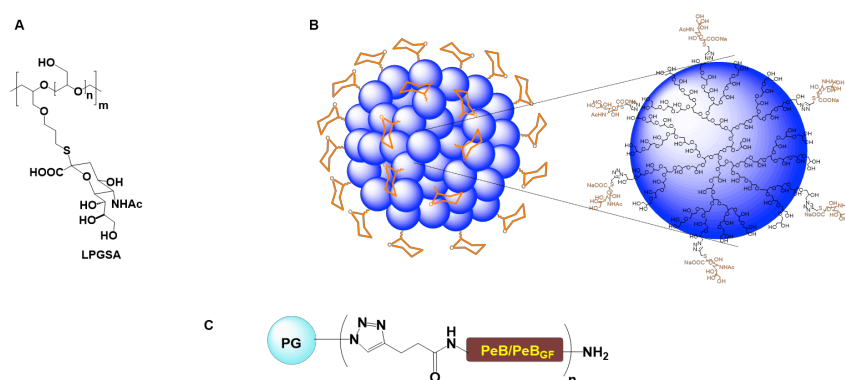


Figure 8. Polyglycerol based sialosides synthesized by A) Bhatial et al.^[26c] B) Papp et al.^[74] C) Lauster et al.^[75] Architecture B) adapted with permission from ref.^[76a] Copyright 2016 American Chemical Society.

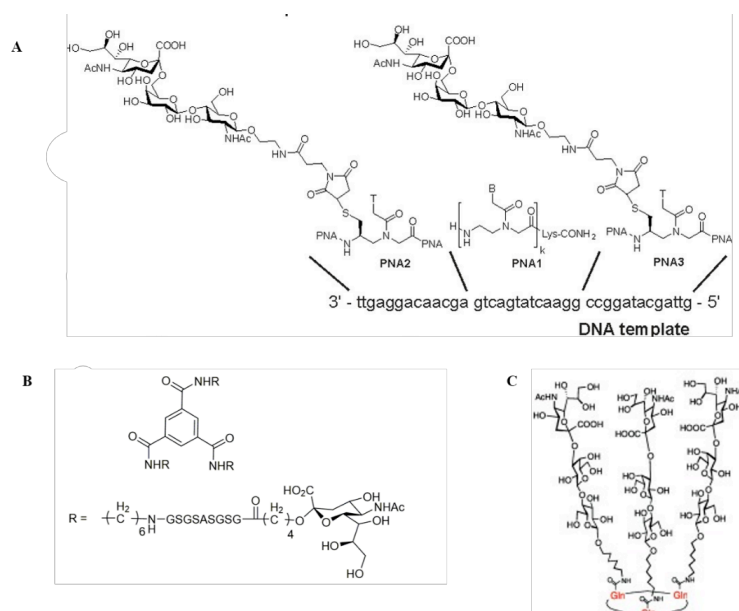


Figure 9. Different peptide based scaffold for HA trimer of influenza virus A) divalent DNA.PNA based sialyllactosides reported by Bandlow et al.^[76b], B) trivalent peptide based

sialosides reported by Waldman et al.^[69] and C) cyclicglycopetide based trivalent sialosides reported by Ohta et al.^[77]

2.2 C-type lectins

The C-type lectins (CTL) were amidst the first animal lectins recognized and approximately more than 1000 proteins were found to have C-type lectin-like domains (CTLDs).^[80] Originally the C-type designation for these molecules originates from their dependence on Ca^{++} for sugar binding through their conserved residues within CTLD.^[81] The carbohydrate binding activity of CTLs is mediated by a highly conserved module called carbohydrate recognition domain (CRD). However, the CTLDs of many C-type lectins is not compulsorily restricted to bind carbohydrates or Ca^{++} . CTLs and proteins with CTLD are present in all organisms. Based on the organization of domain, CTLDs are divided into 17 groups.^[80, 82] In mammals CTLs are divided into two types based on the molecular structure of C-type lectin receptors (CLRs) i.e., transmembrane proteins and soluble proteins (Fig. 10A). For example, DC-SIGN belongs to the class of transmembrane protein and MBL belongs to the class of soluble protein which will be discussed in the next section. These proteins usually oligomerize into homodimers, homotrimers, and higher order of oligomers, which enhance their binding ability for multivalent ligands.^[83] However, all the CTLDs have similar structural homology still they have different specificity for binding the different type of carbohydrates. CTLs have diverse functionality including cell adhesion and as a signaling receptor for various immune function such as pathogen recognition and inflammation.^[84]

The structural analysis of C-type carbohydrate recognition using mannanose binding proteins (MBP) of serum showed that CRD of CTLs have a hydrophobic core and disulfide bonds that represent the overall characteristic of domain.^[85] C-type CRD of MBPs bind to several different sugars containing adjacent equatorial hydroxyl group like hydroxyl group at 3 and 4 positions of mannose, glucose, fucose, N-acetylglucosamine (GlcNAc) due to presence of EPN (Glu-Pro-Asn) motif where 3 and 4 hydroxyl groups of sugar directly coordinate with Ca^{++} and form H-bond. In addition to this, it also binds with galactose-type sugars where 4 hydroxyl group is at axial position such as galactose and N-acetylgalactosamine (GlaNAc) due to presence of QPD (Gln-Pro-Asp) motif at CRD (Fig. 10B).^[81, 86]

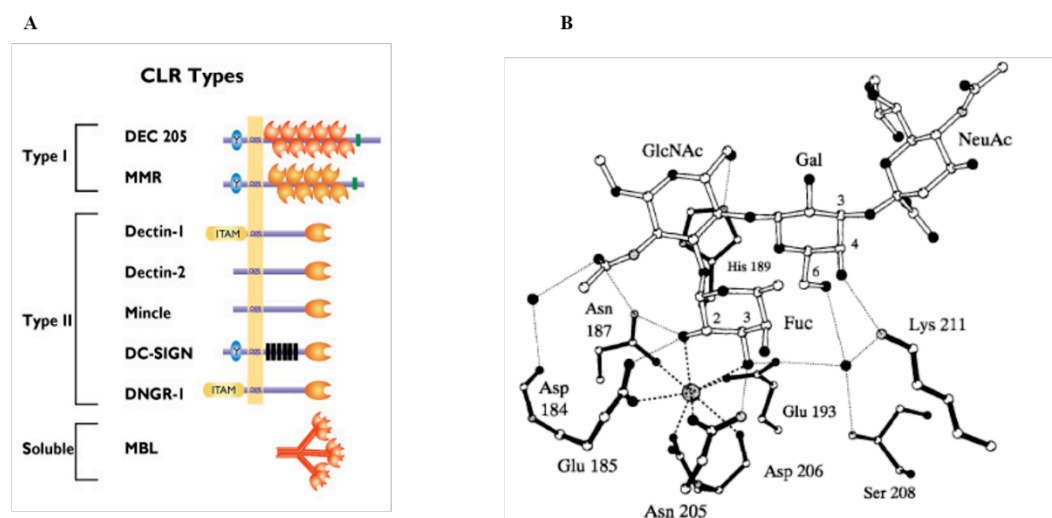


Figure 10. A) Diagram showing the different types of C-type lectin receptor.^[87] and B) Binding of sLe^x at CRD of MBL-A. White, black, small grey and large grey spheres are representing carbon, oxygen, nitrogen, and calcium, respectively. Coordination bonds are shown as thick dashed lines, and H-bonds as thin dashed line. Adapted with permission from ref.^[88] Copyright 1997 Elsevier Ltd.

2.2.1 MBL

Mannose binding lectin or mannan binding lectin (MBL) is a member of collectin family which plays an important role in innate immune system.^[89] MBL has a bouquet like structure and exist in various oligomeric forms ranging from dimers to hexamers. These oligomers are built of subunits that consist of three identical peptide chains of about 32 kDa each. Each chain is made up of a cysteine rich N terminal, collagen-like domain, a hydrophobic neck region and a Ca⁺⁺-dependent carbohydrate recognition domain (CRD).^[90] The collagenous domain of three polypeptides chains are held together by disulfide bonds to form triple helical structure (Fig. 11A).^[91] The MBL carry two calcium ions, named as sites 1 and 2.^[92] The calcium ion at site 2 form coordination bonds with the 3 and 4 OH group of “mannose type” sugar as mentioned in the previous section. The hydroxyl group has 2 lone pairs of electrons and 1 proton free for non-covalent interactions. One of the two lone pair of electrons of OH group is utilized in forming coordination bond with calcium ion and the other tend to form H-bond acceptor for amine functionality of two asparagine (Asn) residues. The Asn residue uses its free oxygen to form coordination bond with calcium ion. The proton is involved in forming the H-bond with carboxyl group of the side

Introduction

chain. Thus, it gives pentagonal bipyramidal geometry (Fig. 10B). However, when there is no sugar available for binding, these positions are occupied by water molecules, showing that these water molecules are displaced upon carbohydrate binding.^[86a] Due to hydrophobic interface between neck and carboxyl terminal pf CRD, the distance between receptor binding site is 45 Å (human) and 53 Å (rat) in the trimer.^[86c, 90a]

MBL has been known to bind with a wide range of pathogens including bacteria, viruses (e.g., HIV, HSV, IAV) yeasts (*C. albicans*), fungi and protozoa decorated with carbohydrates molecules.^[93] MBL binds to various mannose type carbohydrate moieties specifically mannose, fucose, glucose, N-acetyl-D-glucosamine, and N-acetyl-mannosamine.^[94] Selectivity of human MBL (hMBL) for these sugars binding is N-acetyl-D-glucosamine > mannose > N-acetyl-mannosamine and fucose > glucose.^[95] MBL is involved in the activation of lectin complement pathway (will be discussed in next section) and enhancement of opsonophagocytosis.^[96] It is also shown to be involved in the promotion of apoptosis and regulation of inflammation.^[90a]

2.3.1 MBL and complement system

Complement system is a part of innate immune system.^[89, 95, 97] It consists of many plasma proteins which interact with one another to opsonize the microorganisms and induce a cascade of inflammatory reaction that support the host to combat the infection. There are three pathways of complement activation: classical pathway, alternate pathway and mannose binding lectin pathway (MBL pathway).^[98] The classical pathway is triggered upon direct binding of a protein complex known as the complement component 1q (C1q), to the surface of microorganism.^[99] The second pathway i.e., alternative pathway is activated when a spontaneously activated complement component attaches to the microbial surface.^[98]

The MBL pathway is activated upon binding upon MBL binding sugar rich pathogen surface.^[100] A family of two serine protease: **m**annan-binding lectin- associated **s**erine protease (MASPs) namely MASP-1, MASP-2 and MASP-3 are reported to be associated with MBL. Furthermore, a small molecular weight (19 kDa) protein called **s**mall **M**BL-associated **p**rotein (sMAP) or **M**BL-associated **p**rotein of **19** kDa (MAp19) are also found in the complex. When the MBL complex attaches to the surface of pathogen, it leads to the activation of MASP-1 and MASP-2 which further cleave the blood protein C4 (C4a and C4b) and C2 (C2a and C2b). The C4b then attaches to the pathogen surface forming the complex with C2b and initiate the formation of C3-convertase. The subsequent complete

Introduction

cascade mediated by C3-convertase leads to the formation of membrane attack complex (MAC), which results in the formation of pore in the lipid bilayer membrane that disrupt the integrity of membrane. This ultimately kills the pathogens by destroying the H^+ -gradient across the cell membrane of pathogen (Fig. 11B).^[101]

There are 3 different ways by which the complement system safeguard against the microbial infection. First, opsonization of pathogens. In this process, the activated complement proteins attach covalently to the surface of microbes and it can be then recognized by phagocyte bearing receptor that signal for phagocytosis. Second method utilizes the complement proteins to act as chemoattractant which leads to the recruitment of more phagocytes at the site of complement activation which further causes phagocytosis. Third, the MAC or terminal complement complex (TCC) is formed on the surface of pathogen which create pores on the cell membrane of microbes leading to cell lysis and death of pathogens.^[102]

Although MBL has important role for the protection against pathogen infection, an excess of MBL activation could be injurious, because of an uneven proinflammatory response causing additional tissue damage.^[103] High level of MBL activity have demonstrated inflammatory autoimmune diseases like Systemic Lupus Erythematosus, causing organ damage. Moreover, increased level of MBL serum concentration and complement activity is responsible for transplant rejection, myocardial reperfusion ischemic injury, diabetic nephropathy, cerebral ischemia injury, traumatic brain injury (TBI) and other cellular injury.^[104] Thus, high level of MBL activation contribute to tissue damage and hence inhibition of the lectin pathway in chronic condition is necessary for the protection of human health.

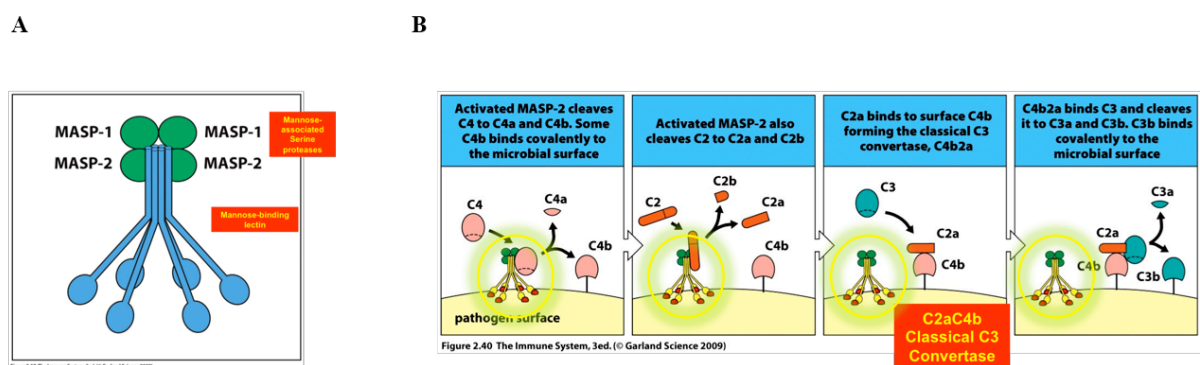


Figure 11. A) Structure of the MBL oligomer, and B) mechanism of complement activation by the MBL pathway.

2.2.1.2 Inhibitors for MBL pathway

Many reports showing the therapeutic benefits of using inhibitors to reduce the activation of the complement pathway has been demonstrated in the literature. For example, recombinant soluble complement receptor type-1 (sCR1) has been shown to decrease the infarct volume by more than 40%.^[105] Furthermore, during the clinical trial, sCR1 was given to the patients suffering myocardial ischemia (MI), resulted in the recovery from ischemic contractile failure of the heart.^[106] Moreover, monoclonal antibodies (mAbs) were designed to inhibit the complement cascade at C5 or C5a and C1 esterase inhibitor (C1-INH) for the inhibition of the complement system to avoid spontaneous activation have been shown in literature to decrease injury, improved organ function IR raised the survival rate in various animal model for human disease.^[107]

There are large number of proteins and antibodies for the inhibitory effect against various complement components have been documented in the literature. Jordan et al demonstrated the use of mAbs (P7E4) for the inhibition of C3 deposition in heart during MBL pathway, which further reduced the infarct size and tissue injury, neutrophil accumulation, proinflammatory gene expression (e.g., ICAM-1, IL-6, and VCAM-1).^[108] Pavlov et al designed a novel mouse model expressing hMBL and showed that mAbs 3F8 prevented the deposition of C3 and further decreases infarct size and inhibit thrombogenesis. Additional inhibitors for MBL complex have been designed and used in IR models.^[109] Natural, endogenous inhibitor namely MBL/ficolin -associated protein-1 (MAP-1), when used at pharmacological doses removes MASP-1, -2 and -3 from MBL complex and inhibit lectin pathway activation and prevent myocardial dysfunction in mice having MI/R.^[110] Not much has been reported on synthetic inhibitors against MBL pathway so far. Orsini et al has reported Polyman2, a dendritic system with multivalent display of mannose residue which has effectively reduced the infarct volumes during cerebral injury.^[111] Similar dendritic mannosides were explored by Blasio et al for the inhibition of MBL pathway showing a dose dependent inhibition of rhMBL for example Polyman2 has $IC_{50} = 270 \mu\text{M}$, Polyman9 has $IC_{50} = 136 \mu\text{M}$ and Polyman31 has $IC_{50} = 62 \mu\text{M}$ (Fig. 12).^[112]

Introduction

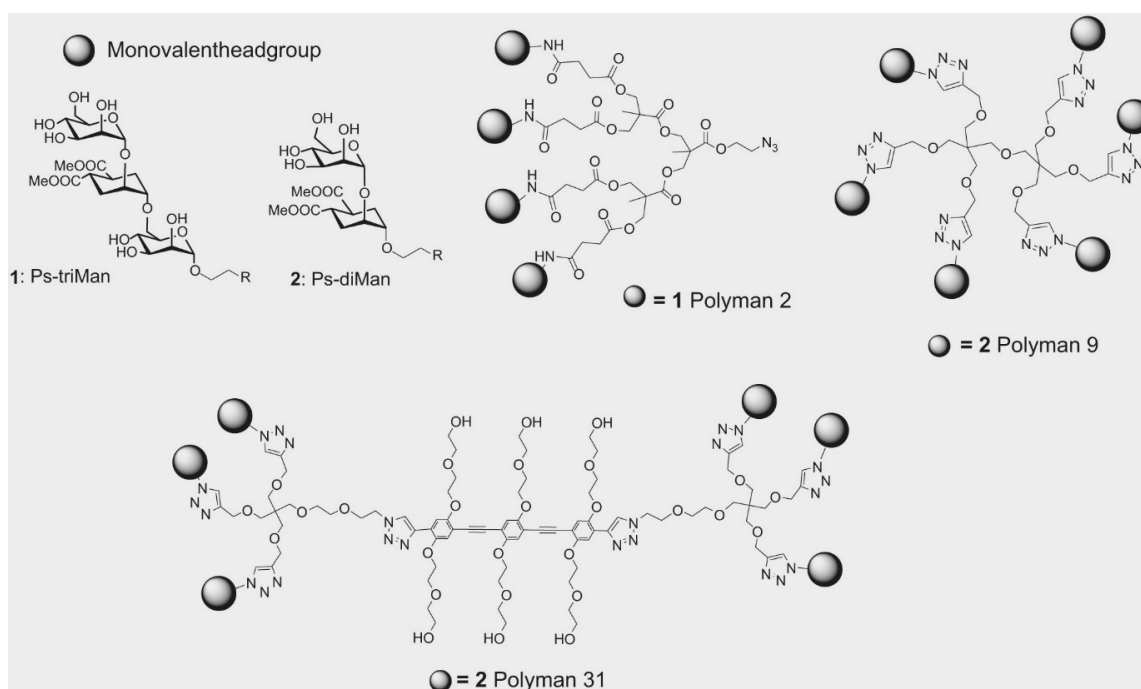


Figure 12. Structures of the glycodendrons reported by Stravalaci for MBL binding: Polyman2, Polyman9, and Polyman31.^[112b]

2.2.2 DC-SIGN

DC-SIGN (dendritic cell-specific intercellular adhesion molecule-3-grabbing non-integrin) is a C-type lectin receptor and belongs to the class of type II integral membrane protein and it is involved in both innate and adaptive immune system. It binds to the sugar in a calcium dependent fashion and serves as a cellular adhesion receptor and is involved in binding with a wide spectrum of microorganisms.^[113] For example, DC-SIGN bind to viruses (Ebola virus, hepatitis C virus, Dengue virus, HIV-1, HIV-2 and SARS coronavirus), bacteria (*Mycobacterium tuberculosis* and *Helicobacter pylori*), and parasites (*Leishmania* and *Schistosoma*).^[114]

DC-SIGN consist of three structurally distinct domains: a cytosolic tail domain, a transmembrane segment, and an extended extracellular domain (ECD) which project the CRD region up to 320 Å above the cell membrane so that it can interact with pathogens.^[115] The ECD is further divided into two structurally and functionally distinct domains: the neck repeat region, which play very important role in the formation of tetramers of the receptors and the carbohydrate recognition domain (CRD) which facilitate the binding of microbes in a calcium-dependent fashion (Fig. 13A).^[116] The CRD in DC-SIGN interacts with two classes of glycans: N-linked highly mannosylated oligosaccharides such as (Man)₉(GlcNAc)₂, which is a branched oligosaccharide that is available in multiple copies

Introduction

on the surface of several pathogen and specifically on gp120 envelop protein of HIV (Fig. 13B). DC-SIGN also interact with branched, fucosylated oligosaccharides having terminal fucose unit, for instance Lewis antigens.^[117] High mannosylated glycans are present on various enveloped viruses such as HIV, however fucosylated glycans are commonly present on parasites.^[118] The oligosaccharide's binding with DC-SIGN occurs by coordination of residual sugars of oligosaccharides to the calcium binding site present on the surface of protein as mentioned before. In addition to promoting the infection process, DC-SIGN plays an important role in immunoregulation process that have attracted the attention of many researcher to exploit DC-SIGN as a potentially new target in immunotherapy.^[119]

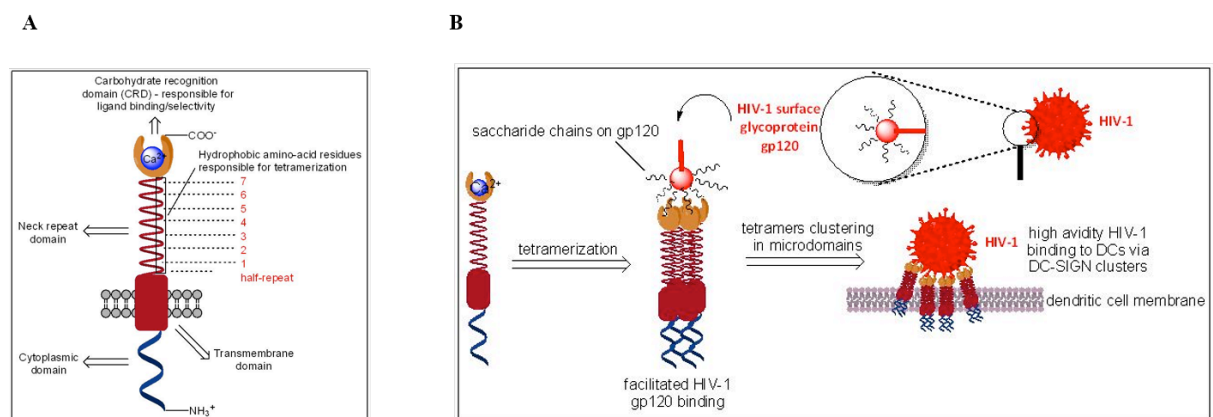


Figure 13. A) Structure of DC-SIGN showing Ca⁺⁺ dependent CRD domain, a neck region, a transmembrane region and cytoplasmic tail, and B) Tetramerization of DC-SIGN and further clustering which allow high binding avidity which influences pathogen binding (e.g., HIV-1 binding).^[120]

Since CRD of DC SIGN receptors is exploited by large number of highly opportunistic pathogens and cause infection to the host cell. Therefore, development of anti-infective agents for DC SIGN is extremely important.^[119]

The binding of monosaccharides with the CRD of DC SIGN are very weak i.e., K_i (L-fucose) = 6.7 mM and K_i (D-mannose) = 13.1 mM being the highest binding amongst monosaccharides.^[121] To overcome this, several multivalent carbohydrate architectures have been reported in literature. Rojo et al were the first one to report the multivalent glycoconjugates against DC-SIGN. They synthesized G3 Boltron-type dendrimers for the multivalent presentation of 32 copies of mannose and found that it strongly inhibited the DC-SIGN facilitated Ebola pseudo typed virus infection at very low concentration, with

Introduction

$IC_{50} = 337$ nM. But the relatively long synthesis and instability of the scaffold were strong drawbacks of this synthetic approach.^[122]

Recently Becer et al have synthesized a library of glycoconjugate decorated with different ratio of mannose and galactose to investigate the binding inhibition of DC-SIGN to gp120 glycoprotein. The glycoconjugate with 100% mannose was most potent candidate with IC_{50} value of 37 nM which is 40 times better affinity in comparison to mannose.^[123]

Sattin et al designed tetravalent construct displaying 4 copies of pseudo-trimannoside which inhibited HIV-1 transfection to CD4+ T lymphocytes with approximately >94% inhibition at 100 μ M concentration. The tetrameric dendron having four unit of D-mannose were tested for the purpose of comparison, and they found that the control molecule failed to prevent the trans infection of HIV-1 with almost comparable potency (65% inhibition at 100 μ M).^[122]

3 Motivation and Objective

Seasonal influenza is the major cause of human death worldwide every year. Developing new class of antiviral drugs is essential because of high mutation rate and increased resistance of influenza strains against available drugs. An approach to develop high affinity inhibitors of influenza virus is optimizing trivalent sialosides to target three receptor binding sites on the hemagglutinin trimers and thus efficiently inhibiting virus -cell attachment during the initial stage of infections. Several trivalent sialosides have been explored previously to target HA trimers of influenza virus. But selection of the architecture and the linker is associated with disadvantages, for example, protein-based ligands can have autoimmune response inside the body and the peptide-based ligand is associated with the stability issue at biological pH. Scale of such constructs for advanced therapeutic use is also tedious.

Our objective in the first part of this thesis is optimizing trivalent synthetic architecture using OEG spacer to target HA trimer of IAV/X31. The OEG spacer will be used as a linker because of their biocompatibility and good water solubility. We will use functionalisable rigid and flexible core which has the possibility to attach trivalent ligands with the large scaffolds to afford multimeric presentation of ligands for influenza inhibition. We will synthesize tripodal architecture with rigid and flexible core on which monomeric ligand i.e. SA will be attached to target the HA trimer. The adamantane core will be considered as rigid core due to restriction in the degree of freedom and the commercially available and highly economic 4-(((benzyloxy)carbonyl) amino)-4-(2-carboxyethyl) heptanedioic acid abbreviated as Tris will be used as a flexible core. MD simulation data will be used to determine the length of OEG spacer to bridge the distance between receptor binding site on HA trimer and the core of scaffold. Labelled microscale thermophoresis (MST) will be used to study the binding affinity of trivalent sialosides with the IAV-X31. Rhodamine (R18) will be used to label the intact X31 virus. To analyse the effect of valency (2 vs 3 SA) on affinity value, a divalent adamantane based sialosides shall be synthesized using the similar procedure as described for trivalent system.

C-type lectin inhibitors are therapeutically interesting for several biomedical applications. In the second part of thesis, our objective is to design biocompatible and water-soluble polyglycerol based multivalent glycoconjugates to target two very interesting class of C-type lectin namely MBL and DC-SIGN. They bind to various carbohydrates specially mannose type ligand having equatorial hydroxyl group at 3 and 4 position presents on various microorganism and are involved in various infectious process. So far, mostly

Motivation and Objective

branched architectures have been implied for lectin binding. Here we will compare linear and branched architectures with chemical structure and linkage. Herein, we will use linear and hyperbranched PG based scaffolds for multivalent display of mannose and fucosyllactose. Carbohydrates will be assembled on PGs using very simple and easy, copper copper-assisted click chemistry between alkyne-functionalized PGs and azide-functionalized sugar molecules. To analyze the size of glycoconjugates, dynamic light scattering (DLS) technique shall be used. Further on, the degree of functionalization be determined by NMR spectroscopy and CHN elemental data. Surface plasmon resonance (SPR) binding analysis and non-labelled MST techniques will be used to study molecular interactions of glycoconjugates with DC-SIGN and MBL, respectively.

4 Publication and manuscript

In the following section the published article and submitted manuscript are listed and the contributions of the author are specified.

4.1 Exploring Rigid and Flexible Core Trivalent Sialosides for Influenza Virus Inhibition

Pallavi Kiran,^[+] Sumati Bhatia,^[+] Daniel Lauster, Stevan Aleksić, Carsten Fleck, Natalija Peric, Wolfgang Maison, Susanne Liese, Bettina G. Keller, Andreas Herrmann, Rainer Haag* *Chem. Eur. J.* **2018**, 24, 1–14.^[124]

^[+] authors contributed equally.

<https://doi.org/10.1002/chem.201804826>

Abstract

Herein, the chemical synthesis and binding analysis of functionalisable rigid and flexible core trivalent sialosides bearing oligoethylene glycol (OEG) spacers interacting with spike proteins of influenza A virus (IAV) X31 is described. Although the flexible Tris- based trivalent sialosides achieved micromolar binding constants, a trivalent binder based on a rigid adamantane core dominated flexible tripodal compounds with micromolar binding and hemagglutination inhibition constants.

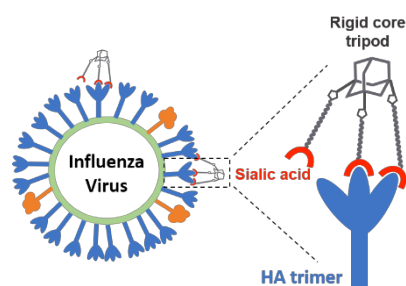


Figure 14. Adapted with permission from Kiran et al.^[124] Copyright 2018 Wiley- VCH Verlag GmbH & Co. KGaA, Weinheim.

Author's contributions: In this publication the author contributed to the synthesis, characterization, the data evaluation, binding assays as well as the draft of the manuscript.

4.2 Synthesis and comparison of linear and hyperbranched multivalent glycosides for C-type lectin binding

Pallavi Kiran, Shalini Kumari, Jens Dervedde, Sumati Bhatia*, Rainer Haag* to be submitted.

[P. Kiran, S. Kumari, J. Dervedde, R. Haag and S. Bhatia, *New J. Chem.*, 2019.] - Reproduced by permission of The Royal Society of Chemistry (RSC) on behalf of the Centre National de la Recherche Scientifique (CNRS) and the RSC Copyright (2019) New Journal of Chemistry.

Abstract

Lectins belongs to diverse class of protein that binds to carbohydrate residues of the glycoproteins present on the cell surface. There are two interesting types of calcium dependent lectin i.e., Mannose-binding lectin (MBL) and DC SIGN which are involved in various infectious processes and in the regulation of the immune response. MBL is a serum protein which activates the lectin complement pathway upon binding with the glycan epitopes on the surface of pathogens or altered self-cell. High level of complement pathway activation leads to tissue injury and organ failure after ischemia reperfusion.

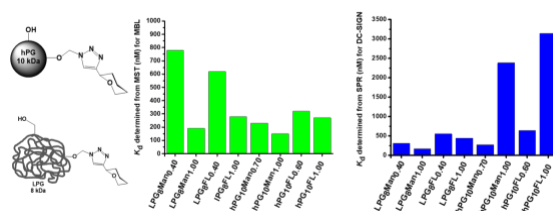


Figure 15. Binding affinity of LPG- and hPG- based carbohydrates for A) MBL and B) DC-SIGN dimer. Author's contributions: In this manuscript the author contributed to the synthesis, characterization, the data evaluation, binding assays as well as the draft of the manuscript.



Journal Name

COMMUNICATION

Synthesis and comparison of linear and hyperbranched multivalent glycosides for C-type lectin binding

Pallavi Kiran^a, Shalini Kumari^a, Jens Dervedde^b, Sumati Bhatia^a,* Rainer Haag^a,*Received 00th January 20xx,
Accepted 00th January 20xx

DOI: 10.1039/x0xx00000x

www.rsc.org/

Linear and hyperbranched polyglycerol based mannosides and fucosyllactosides were developed as nanomolar binders of Mannose binding lectin (MBL) and DC-SIGN using Label free microscale thermophoresis (MST) and surface plasmon resonance (SPR) techniques, respectively. While there was a small preference for hyperbranched polyglycerol in the case of MBL inhibitors, a clear advantage of ligand presentation on linear polyglycerol scaffolds for DC-SIGN was observed.

Lectins are ubiquitous carbohydrate binding proteins^[2] which are involved in many biological processes, including cell signalling, cell - cell interaction, and the immune response to pathogens.^[3] C- type animal lectins are the largest and most distinct amongst lectin families.^[4] They have conserved motifs in carbohydrate recognition domain (CRD) that bind sugars in a Ca²⁺ dependent manner.^[3b, 5] Soluble C-type lectins can recognize glycan epitopes on the surface of pathogens and thereby tag invaders for a further immune response. A function of immune cell bound C-type lectins is the direct pathogen recognition.^[6] Mannose binding lectin (MBL) is a soluble calcium dependent serum protein.^[7] An intrinsically coiled-coil region which trimerizes the protein and a collagen-like domain are responsible to generate various oligomeric forms including dimers, trimers, tetramers, pentamers, and hexamers.^[8] MBL binds to the sugar residues e.g., mannose, fucose, glucose, N-acetyl-D-glucosamine and N-acetyl-mannosamine on the surface of various pathogens e.g., viruses, bacteria, fungi, and parasites.^[9] Agglutination of these microbes mediated by oligomeric MBL allows the clearance of pathogens through phagocytosis.^[10] Binding of MBL to pathogens also activates the

lectin pathway of the complement system. Consequently, a cascade of specific proteolytic events generates active proteins that contribute to pathogen elimination and includes the generation of pro-inflammatory stimuli to recruit leukocytes.^[8a] On the contrary, a high level of complement activity has been associated with chronic inflammatory diseases, transplant rejections, and diabetic nephropathy.^[11] The complement system might play an important role in tissue damage and impaired organ function after ischemia-reperfusion (IR). In the case of IR, MBL deposition on autologous cells has been observed which results in cell clearance, enhanced vascular permeability, blood clotting, and increased inflammation.^[12] Thus, developing MBL inhibitors to dampen the complement activity on demand is desirable.

Dendritic Cell-Specific Intercellular adhesion molecule-3-Grabbing Non-integrin (DC-SIGN) is a type II trans-membrane C-type lectin which is involved in the recognition of oligosaccharides on the surface of viruses (e.g., HIV, Ebola), fungi (e.g., *Candida albicans*, *A. fumigatus*), bacteria (*M. tuberculosis*, *S. pneumonia*) and parasites (*Leishmania*).^[13] DC-SIGN binds to highly mannosylated glycans which are presents on several pathogens including HIV-1.^[14] It also binds to fucosylated glycans such as Lewis oligosaccharides.^[15] Interestingly, MBL can also bind with gp120 on HIV virions and can block their entry by DC-SIGN.^[16]

Multivalent ligand presentation is effective for converting inhibitors of low affinity ($K_{d,affinity} \sim \text{mM} - \mu\text{M}$) to the ones of with high avidity ($K_{d,avidity} \sim \text{nM}$).^[17] The binding affinity (K_d) of mannose binding lectin (MBL) to mannose as determined by NMR titration was $\sim 3 \text{ mM}$ and thus can be improved by design of multivalent inhibitors.^[1] To the best of our knowledge, only Simoni and coworkers have reported the multivalent mannosylated glycodendrimers for the inhibition of MBL mediated injuries.^[18] But several reports on using antibodies against MBL have been published. For the protection against IR related myocardium injury, for example, Jordan et al developed the monoclonal antibodies (mAbs; P7E4 and 14C3.74) against rat MBL (rMBL). They showed that antibody (P7E4) blocked the

^a *Institut für Chemie und Biochemie, Freie Universität Berlin, Takustr. 3, 14195 Berlin, Germany.*

^b *Charité-Universitätsmedizin Berlin, corporate member of Freie Universität Berlin, Humboldt-Universität zu Berlin, and Berlin Institute of Health; Institute of Laboratory Medicine, Clinical Chemistry and Pathobiochemistry, CVK Augustenburger Platz 1, 13353 Berlin, Germany*

Electronic Supplementary Information (ESI) available: [details of any supplementary information available should be included here]. See DOI: 10.1039/x0xx00000x

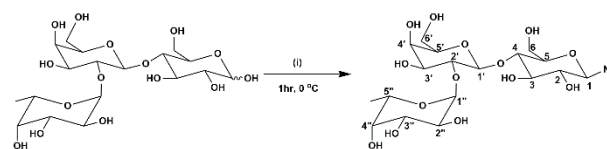
lectin pathway in a concentration-dependent manner with approximately 80% inhibition at 10 $\mu\text{g}/\text{mL}$ P7E4.^[19] Working in this directions Pavlov et al has presented an animal model i.e., mouse expressing functional hMBL and showed that mAbs 3F8 inhibited C3 deposition.^[20]

On the other hand, several dendritic multivalent inhibitors of DC-SIGN have been reported and only one report on using linear polymer scaffold has been published by Becer et. al.^[21] In all cases there was however no direct comparison of linear and dendritic scaffolds with respect to their lectin binding affinities, which might be relevant for an optimal ligand presentation.

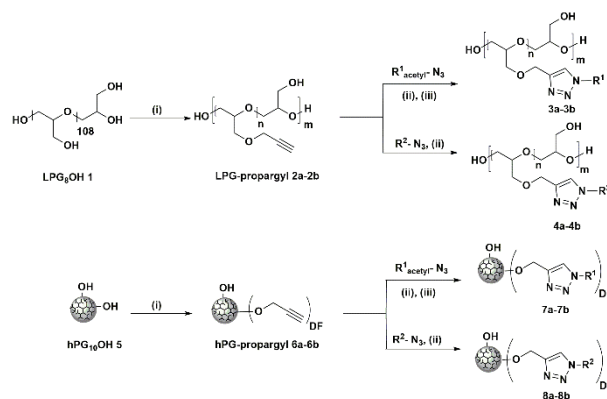
Linear and hyperbranched polyglycerols are water soluble, biocompatible, and easily functionalizable polymer scaffolds. Recently we have compared linear and hyperbranched polyglycerol based multivalent sialosides for influenza virus binding.^[22] In this manuscript, we report the synthesis of linear and hyperbranched polyglycerols based multivalent mannosides and fucosyllactosides where the carbohydrate residues are present on different polymer backbones with varying ligand densities in a multivalent fashion. These synthesized multivalent glycosides have been evaluated for the binding with MBL and DC-SIGN using microscale thermophoresis (MST) and surface plasmon resonance (SPR) respectively, achieving potent nanomolar binders of MBL and DC-SIGN.

The β -azido functionality at the anomeric position of 2'-Fucosyllactose was introduced by one step conversion using 2-chloroimidazolium salt affording 2'-fucosyllactose azide by a slightly modified procedure from the one reported in literature (Scheme 1).^[23] 8 kDa linear polyglycerol^[24] (LPG₈OH **1**) and 10 kDa hyperbranched polyglycerol^[25] (hPG₁₀OH **5**) were propargylated using propargyl bromide as described below. The propargylated polyglycerols were coupled with 2-Azido mannose derivative and 2'-fucosyllactose azide using CuI-catalyzed Huisgen click chemistry to obtain two different degrees of functionalization (DF) affording multivalent glycosides LPG₈Man **3a-b** (DF = 0.40 and 1.00), LPG₈FL **4a-b** (DF = 0.40 and 1.00), hPG₁₀Man **7a-b** (DF = 0.70 and 1.00) and hPG₁₀FL **8a-b** (DF = 0.60 and 1.00) (Scheme 2). All intermediates and final products were characterized by spectroscopic techniques (see SI). The DF of all glycoside polymers was determined by ¹H NMR and the overall molecular weight was calculated based on the parent PG backbone.

Size distribution profiles of all glycosides and the parent polyglycerol polymers were determined by dynamic light scattering (DLS) technique in phosphate buffer saline (PBS, pH 7.4) at a concentration of 1 mg/mL (Table 1). The hydrodynamic diameter (D_h) for LPG₈OH **1** was similar to hPG₁₀OH **5**.^[26] This shows that the used LPG and hPG scaffolds are equal in their size. However, it should be noted that the LPG had a lower molecular weight (8 kDa) as compared to the dendritic analogue (10 kDa), which explains the increased swelling of the linear random coil structure.^[22] Compact globular morphologies for the LPG based multivalent glycosides were earlier reported.^[22]



Scheme 1. Synthesis of 2'-fucosyllactose azides by using DMC (i) 2-Chloro-1,3-dimethylimidazolium chloride (DMC), DIPEA, NaN₃, D₂O, 0 °C.



Scheme 2. Synthesis of LPG and hPG based multivalent mannosides and fucosyllactosides derivatives. (i) NaH, propargyl bromide, dry DMF, 0 °C to RT. (ii) CuSO₄·5H₂O, Na ascorbate, DMF, 40 °C (iii) 2M NaOH.

Therefore, assuming spherical morphologies for both hPG and LPG based mannosides and fucosyllactosides, ligand density per nm² was calculated for all the synthesized constructs based on the observed D_h values in volume distribution profiles (Figure 1). An increase in D_h was observed with increasing glycoside residue density for both the LPG and hPG based polymer backbones. However, increase in size was slightly more for the fucosyllactoside derivatives than the mannoside derivatives (Table 1).

All synthesized multivalent constructs and the non-functionalized polymer were assessed for their binding affinity against Mannose binding Lectin (MBL) and DC-SIGN using microscale thermophoresis (MST) and surface plasmon resonance (SPR) biophysical techniques, respectively.

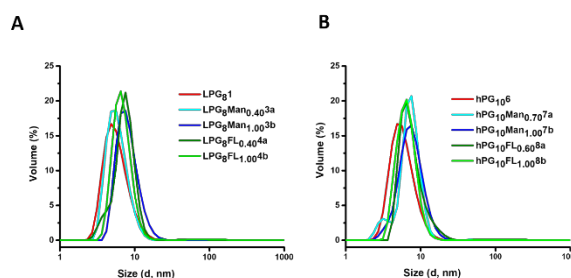


Figure 1. Size analysis of the linear and hyperbranched polyglycerol based glycoconjugates by DLS. The volume distribution profiles of **A**) linear polyglycerol (LPG₈OH **1**), linear polyglycerol mannosides (**3a-b**) and linear polyglycerol fucosyllactosides (**4a-b**); **B**) hyperbranched polyglycerol (hPG₁₀OH **5**), hyperbranched polyglycerol mannosides (**7a-b**) and hyperbranched polyglycerol fucosyllactosides (**8a-b**) as observed by DLS at concentration of 1 mg/ml in aqueous PBS (pH 7.4, 150 mM NaCl) at 25 °C.

MST is a powerful technique to study the quantitative interaction between the biomolecules and small ligands with very low sample consumption.^[27] Label-free MST technique utilizes the intrinsic fluorescence of the proteins to study the molecular migration on applying temperature gradient.^[28] The dissociation constants (K_d) is evaluated from the changes in the thermophoretic behaviour resulting from binding of the ligand to the biomolecules.^[29] First concentration of MBL in aqueous buffer (PBS⁺⁺, pH 7.4) was optimized for the required intrinsic fluorescence signal which depends on the available tryptophan residues in the protein. Then the synthesized multivalent glycosides were titrated against the free MBL protein. We observed apparent K_d values in low micromolar range 0.15–0.77 μM for the multivalent constructs. Affinity was high for the high ligand densities. For LPG₈Man (**3a-b**) and LPG₈FL (**4a-b**), affinity increased up to four times and two times respectively with high ligand density of 1 ligand/nm². The hyperbranched glycopolymers i.e. hPG₁₀Man (**7a-b**) and hPG₁₀FL (**3a-b**) has affinity in the low micromolar range i.e. 0.15 – 0.30 μM . Interestingly we observed that the affinity was nearly 0.2–0.3 μM for the constructs with the ligand density approaching 1 ligand/nm². This also means that the fully functionalized multivalent mannosides and fucosyllactosides were more potent than the partially functionalized ones. The parent nonfunctionalized LPG₈OH **1** and hPG₁₀OH **5** did not substantially bind with the MBL. Mannan (from *Saccharomyces cerevisiae*, which is a branched mannose polysaccharide was purchased from Sigma Aldrich) was used as a positive control and showed an affinity value of 9.51 μM .

Overall, the fully functionalized hPG₁₀Man_{1.0} **7b** was evaluated as the most potent candidate with $K_d = 0.152 \mu\text{M}$ for the MBL dimer.

The binding affinities (K_d) of all the synthesised glycoconjugates with DC-SIGN were determined by SPR technique. Glycoconjugates were used as analyte and flowed over protein A sensor chip immobilised with DC-SIGN. The dissociation constant at equilibrium was evaluated from single cycle kinetics measurement of individual polymer. No big difference in binding affinities was observed for the low and high ligand density on linear polyglycerol mannoside or fucosyllactoside conjugates. Binding affinities of all the constructs were less than 1 μM . In contrast to linear glycoconjugates, affinity decreases with increase in DF on hyperbranched polymers. hPG₁₀Man_{0.70} **7a** ($K_d = 0.27 \mu\text{M}$) bound with DC-SIGN nine times stronger than hPG₁₀Man_{1.0} **7b** ($K_d = 2.38 \mu\text{M}$). Also, hPG₁₀FL_{0.60} **8a** ($K_d = 0.64 \mu\text{M}$) bound approximately five times more strongly than hPG₁₀FL_{1.0} **8b** ($K_d = 3.14 \mu\text{M}$). Thus, the influence of ligand density was more pronounced for hyperbranched polymers than the linear ones although the LPG₈Man_{1.0} **3b** was the most potent with $K_d = 0.157 \mu\text{M}$. The unfunctionalized hPG₁₀OH **6** did not substantially bind with DC-SIGN. Man₉GlcNAc₂ was used as a positive control and showed binding in nanomolar range ($K_d = 10 \text{ nM}$) (Table 1)

Table 1 Characterization and dissociation constant (K_d) of mannose and fucosyllactose

Polymer	(%)			nm		K_d (μM)
LPG ₈ OH 1	-	-	6.2±0.3	0.30	-	No binding
LPG ₈ Man _{0.40} 3a	39	36	6.4±0.4	0.46	0.32	0.78±0.3
LPG ₈ Man _{1.0} 3b	108	100	8.4±0.3	0.41	0.90	0.19±0.1
IPG ₈ FL _{0.40} 4a	42	39	8.2±1.3	0.60	0.35	0.62±0.3
IPG ₈ FL _{1.0} 4b	108	100	9.1±1.0	0.40	0.90	0.28±0.1
hPG ₁₀ OH 5	-	-	6.3±0.5	0.31	-	No binding
hPG ₁₀ Man _{0.70} 7a	92	68	8.2±0.3	0.30	0.74	0.23±0.1
hPG ₁₀ Man _{1.0} 7b	135	100	9.1±1.0	0.57	1.08	0.15±0.1
hPG ₁₀ FL _{0.60} 8a	81	60	9.4±0.3	0.44	0.64	0.32±0.2
hPG ₁₀ FL _{1.0} 8b	135	100	11.1±0.5	0.58	1.08	0.27±0.1
Man-9-Glycan	-	-	-	-	-	-
Mannan	-	-	-	-	-	9.51±14.8
Mannose	-	-	-	-	-	2900±1000 [#]

^aPost functionalized molecular weight calculated by using the Mn of the polyglycerol core and the experimental degree of functionalization (DF).

^bNumber of ligands per polymer was calculated from the DF by ¹H NMR.

^cDetermined by ¹H NMR analysis.

^dDetermined from DLS in aqueous buffer (PBS, pH 7.4), the values represent the means of at least three measurements ± standard deviation of the volume distribution profile.

The surface area of the backbone: LPG₈ (A_{2nm}) = 120, hPG₁₀ (A_{2nm}) = 125.

[#] Determined by NMR titration of rat CRD of MBL and mannose.^[11]

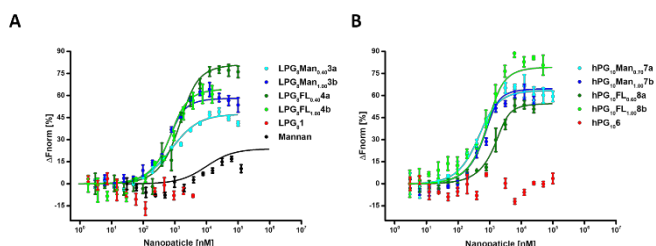


Figure 2. MST dose–response curves of glycoconjugates. A) linear PG based Man (**3a–b**) and FL (**4a–b**), B) hyperbranched PG based Man (**7a–b**) and FL (**8a–b**). All systems are titrated against MBL (100 μ M). Each graph displays data merged from three independent experiments.

Conclusion

We compare almost similar molecular weight linear and hyperbranched polyglycerol based multivalent glycoconjugates for C-type lectin binding. We observed that ligand density of 1 ligand/ nm^2 for the linear and hyperbranched PGs was crucial to achieve high binding affinity against MBL. Comparison of linear and hyperbranched PG glycoconjugates revealed a clear advantage of high ligand density for MBL binding and the ligand presentation on LPG scaffold for DC-SIGN binding. While the hyperbranched PG based hPG₁₀Man_{1.0} **7b** appeared to be the most potent candidate against MBL with K_d of 152 nM, against DC-SIGN was the LPG₈Man_{1.0} **3b** with K_d of 157 nM which is approximately 23,000-fold more active than the monovalent mannose ($K_d = 3.5$ mM). Overall, PG based glycoconjugates are worth exploring for MBL and DC-SIGN binding inhibition. Such glycoconjugates will be effective for drug design, drug discovery, and therapeutic investigations for C-type lectins. Commercially available divalent lectins were used in this study, and we expect the affinity values to be even stronger on using native proteins.

Acknowledgement

The authors would like to acknowledge the SFB765 (DFG) and the ITN Multiapp (EU Marie Curie Action) for financial support.

Supplementary Information

Synthesis, GPC profiles for hPGOH and LPGOH, NMR spectra, SPR sensogram, intensity and number distribution profiles.

Conflicts of interest

There are no conflicts to declare

References

- [1] S. T. Iobst, M. R. Wormald, W. I. Weis, R. A. Dwek, K. Drickamer, *The Journal of biological chemistry* **1994**, *269*, 15505-15511.
- [2] a) H. Lis, N. Sharon, *Chemical Reviews* **1998**, *98*, 637-674; b) W. I. Weis, K. Drickamer, *Annual Review of Biochemistry* **1996**, *65*, 441-473; c) C. Lee, R. T. Lee, *Accounts of Chemical Research* **1995**, *28*, 321-327.
- [3] a) H. S. N. Jayawardena, X. Wang, M. Yan, *Analytical chemistry* **2013**, *85*, 10277-10281; b) K. Drickamer, *Curr Opin Struct Biol* **1999**, *9*, 585-590.

- [4] K. J. Clemetson, J. M. Clemetson, in *Platelets (Third Edition)* (Ed.: A. D. Michelson), Academic Press, **2013**, pp. 169-194.
- [5] a) K. Drickamer, M. E. Taylor, *Curr Opin Struct Biol* **2015**, *34*, 26-34; b) I. M. Dambuza, G. D. Brown, *Current opinion in immunology* **2015**, *32*, 21-27.
- [6] D. A. Wesener, A. Dugan, L. L. Kiessling, *Curr Opin Struct Biol* **2017**, *44*, 168-178.
- [7] E. C. van Asbeck, A. I. M. Hoepelman, J. Scharringa, B. L. Herpers, J. Verhoef, *BMC microbiology* **2008**, *8*, 229-229.
- [8] a) L. Nuytinck, F. Shapiro, *Personalized medicine* **2004**, *1*, 35-52; b) A. Miller, A. Phillips, J. Gor, R. Wallis, S. J. Perkins, *The Journal of biological chemistry* **2012**, *287*, 3930-3945.
- [9] a) A. M. Kerrigan, G. D. Brown, *Immunobiology* **2009**, *214*, 562-575; b) M. W. Turner, *Molecular immunology* **2003**, *40*, 423-429.
- [10] J. Bestebroer, C. J. C. de Haas, J. A. G. van Strijp, *FEMS Microbiology Reviews* **2010**, *34*, 395-414.
- [11] a) L. H. Bouwman, B. O. Roep, A. Roos, *Human Immunology* **2006**, *67*, 247-256; b) P. Hovind, T. K. Hansen, L. Tarnow, S. Thiel, R. Steffensen, A. Flyvbjerg, H. H. Parving, *Diabetes* **2005**, *54*, 1523-1527; c) M. Saraheimo, C. Forsblom, T. K. Hansen, A. M. Teppo, J. Fagerudd, K. Pettersson-Fernholm, S. Thiel, L. Tarnow, P. Ebeling, A. Flyvbjerg, P. H. Groop, *Diabetologia* **2005**, *48*, 198-202.
- [12] a) S. Fumagalli, M. G. De Simoni, *Stroke* **2016**, *47*, 3067-3073; b) L. J. Schlapbach, M. Mattmann, S. Thiel, C. Boillat, M. Otth, M. Nelle, B. Wagner, J. C. Jensenius, C. Aebi, *Clinical infectious diseases : an official publication of the Infectious Diseases Society of America* **2010**, *51*, 153-162.
- [13] a) Y. van Kooyk, T. B. Geijtenbeek, *Nature reviews. Immunology* **2003**, *3*, 697-709; b) J. J. Reina, J. Rojo, *Braz J Pharm Sci* **2013**, *49*, 109-124.
- [14] D. De Blasio, S. Fumagalli, L. Longhi, F. Orsini, A. Palmioli, M. Stravalaci, G. Vegliante, E. R. Zanier, A. Bernardi, M. Gobbi, M.-G. De Simoni, *Journal of Cerebral Blood Flow & Metabolism* **2016**, *37*, 938-950.
- [15] a) S. Cecioni, A. Imberty, S. Vidal, *Chemical Reviews* **2015**, *115*, 525-561; b) E. Van Liempt, A. Imberty, C. M. Bank, S. J. Van Vliet, Y. Van Kooyk, T. B. Geijtenbeek, I. Van Die, *The Journal of biological chemistry* **2004**, *279*, 33161-33167.
- [16] X. Ji, H. Gewurz, G. T. Spear, *Molecular immunology* **2005**, *42*, 145-152.
- [17] V. M. Krishnamurthy, L. A. Estroff, G. M. Whitesides, **2006**.
- [18] a) M. Stravalaci, D. De Blasio, F. Orsini, C. Perego, A. Palmioli, G. Goti, A. Bernardi, M. G. De Simoni, M. Gobbi, *Journal of biomolecular screening* **2016**, *21*, 749-757; b) F. Orsini, P. Villa, S. Parrella, R. Zangari, E. R. Zanier, R. Gesuete, M. Stravalaci, S. Fumagalli, R. Ottria, J. J. Reina, A. Paladini, E. Micotti, R. Ribeiro-Viana, J. Rojo, V. I. Pavlov, G. L. Stahl, A. Bernardi, M. Gobbi, M.-G. De Simoni, *Circulation* **2012**, *126*, 1484-1494.
- [19] E. Jordan James, C. Montalto Michael, L. Stahl Gregory, *Circulation* **2001**, *104*, 1413-1418.
- [20] V. I. Pavlov, Y. S. Tan, E. E. McClure, L. R. La Bonte, C. Zou, W. B. Gorsuch, G. L. Stahl, *The American journal of pathology* **2015**, *185*, 347-355.
- [21] C. R. Becer, M. I. Gibson, J. Geng, R. Ilyas, R. Wallis, D. A. Mitchell, D. M. Haddleton, *Journal of the American Chemical Society* **2010**, *132*, 15130-15132.
- [22] S. Bhatia, D. Lauster, M. Bardua, K. Ludwig, S. Angioletti-Uberti, N. Popp, U. Hoffmann, F. Paulus, M. Budt, M.

- Stadtmüller, T. Wolff, A. Hamann, C. Böttcher, A. Herrmann, R. Haag, *Biomaterials* **2017**, *138*, 22-34.
- [23] T. Tanaka, H. Nagai, M. Noguchi, A. Kobayashi, S.-i. Shoda, *Chemical Communications* **2009**, 3378-3379.
- [24] M. Gervais, A.-L. Brocas, G. Cendejas, A. Deffieux, S. Carlotti, *Macromolecules* **2010**, *43*, 1778-1784.
- [25] a) A. Sunder, R. Hanselmann, H. Frey, R. Mülhaupt, *Macromolecules* **1999**, *32*, 4240-4246; b) R. Haag, A. Sunder, J.-F. Stumbé, *Journal of the American Chemical Society* **2000**, *122*, 2954-2955.
- [26] M. Imran ul-haq, B. F. Lai, R. Chapanian, J. N. Kizhakkedathu, *Biomaterials* **2012**, *33*, 9135-9147.
- [27] M. Jerabek-Willemsen, C. J. Wienken, D. Braun, P. Baaske, S. Duhr, *Assay and drug development technologies* **2011**, *9*, 342-353.
- [28] S. Duhr, D. Braun, *Proceedings of the National Academy of Sciences* **2006**, *103*, 19678-19682.
- [29] S. A. I. Seidel, C. J. Wienken, S. Geissler, M. Jerabek-Willemsen, S. Duhr, A. Reiter, D. Trauner, D. Braun, P. Baaske, *Angewandte Chemie International Edition* **2012**, *51*, 10656-10659.

Supporting Information

Synthesis and comparison of linear and hyperbranched multivalent glycosides for C-type lectin binding

Pallavi Kiran^a, Shalini Kumari^a, Jens Dornedde^b, Sumati Bhatia^{a,*}, Rainer Haag^{a,*}

^aInstitut für Chemie und Biochemie, Freie Universität Berlin, Takustr. 3, 14195 Berlin, Germany. ^bCharité-Universitätsmedizin Berlin, corporate member of Freie Universität Berlin, Humboldt-Universität zu Berlin, and Berlin Institute of Health; Institute of Laboratory Medicine, Clinical Chemistry and Pathobiochemistry, CVK Augustenburger Platz 1, 13353 Berlin, Germany

*Corresponding author

Rainer Haag: haag@zedat.fu-berlin.de

Table of contents

1. Material and methods
2. Binding assay by microscale thermophoresis (MST)
3. Binding assay by surface plasmon resonance (SPR)
4. Synthesis and characterization of all intermediates and final compounds
5. ¹H and ¹³C spectra of all the intermediates and final molecules.
6. SPR binding isotherms derived from single-cycle kinetic measurements.
7. GPC data of linear and hyperbranched polyglycerols.

1 Material and methods

All the reagents and solvents were purchased from commercial suppliers and used without further purification unless stated otherwise. Reactions requiring dry or oxygen-free conditions were carried out under argon in Schlenk glassware. NMR spectra were recorded on JEOL ECP500, BRUKER AV500 and BRUKER AV700 spectrometers at 400 MHz, 500 MHz and 700 MHz for ^1H NMR spectra and 125 MHz and 175 MHz for ^{13}C NMR spectra, respectively. Chemical shifts are given in parts per million (ppm) in relation to deuterated solvent peak calibration. Infrared (IR) spectra were recorded with a Nicolet AVATAR 320 FT-IR 5 SXC (Thermo Fisher Scientific, Waltham, MA, USA) with a DTGS detector from 4000 to 650 cm^{-1} . A TSQ 7000 (Finnigan Mat) instrument was used for ESI measurements and a JEOL JMS-SX-102A spectrometer was used for the high-resolution mass spectra.

DLS measurements of the various polymers were conducted by using a Nano DLS particle sizer (Brookhaven Instruments Corp.) at 25 °C. Aqueous samples were filtered through 0.2 mm filters prior to analysis. Water of Millipore quality was used in all experiments.

NS0-derived recombinant human DC-SIGN/CD209 Fc Chimera Protein, CF and HEK293-derived recombinant human MBL Protein, CF were purchased as dimers from R & D Systems Biotechnology company, US. 2'-Fucosyllactose was purchased from Carbosynth. 2-Azidoethyl-2,3,4,6-tetra-O-acetyl- α -D-mannopyranoside was purchased from Apollo scientific.

2 Label-free microscale thermophoresis (MST)

Label-free microscale thermophoresis was used to measure the binding interactions between MBL and PG based glycoconjugates according to the following protocol. For each measurement, a dilution series with constant MBL concentration but varying ligand concentrations was prepared in PBS⁺⁺. No significant ligand-derived autofluorescence was detected at 280 nm wavelength. The final MBL concentration was 100 μM . All measurements were performed at 22 °C. The thermophoretic movement of fluorescent MBL was monitored with a laser on for 30 s and off for 5 s keeping the MST power at 20% and LED power at 20%. Fluorescence was measured before laser heating (F_{Initial}) and after 30 s of laser irradiation (F_{Hot}). The K_d values were then calculated

from three independent thermophoresis measurements using the NanoTemper software (NanoTemper Technologies, Munich, Germany).

3 Surface Plasmon Resonance (SPR)

Experiments were performed on a Biacore X100 instrument (GE Healthcare Europe, Freiburg, Germany) at 25 °C, using HBS-Ca-Mn buffer (10 mM HEPES, pH 7.4, 150 mM NaCl, 0.1 mM CaCl₂ and 0.01 mM MnCl₂) in all cases. DC-SIGN, Fc Chimera Protein (R & D Systems Biotechnology company, US) was immobilised on a protein A sensor chip (GE Healthcare, final response 1700 RU), whereas the reference lane was left unfunctionalized. Each cycle consisted of a 120 s period of sample contact time (association phase) followed by a 600 s dissociation phase. All sample measurements were analysed with single cycle kinetics. Therefore, a concentration series of each sample was measured in triplicates. The determination of K_d values was performed with response unit (RU) data points taken at 15 s before injection stop using built-in software of the Biacore X100. Corresponding binding isotherms were plotted.

4. Synthesis and characterization of all intermediates and final compounds

2'-Fucosyllactose azide

2'-Fucosyllactose (0.07 g, 0.143 mmol) was dissolved in deuterium oxide (1 mL). Diisopropylethylamine (0.25 ml, 1.43 mmol), NaN₃ (0.092 g, 1.73 mmol) and DMC (0.071 g, 0.43 mmol) were added to the above mixture and the reaction mixture was stirred for 1 h at 0 °C. After 1 h, the solvent was evaporated under high vacuum, DMF was added and it was centrifuged, and supernatant was collected. This centrifugation step was repeated 3-4 times and all the supernatant were collected and concentrated in vacuo. It was then dissolved in water and passed through pre-neutralized resin column (Dowex H). All the fraction was collected and dialysed in water to give the pure product. (0.071g, 0.139 mmol, Yield = 97.41 %). **¹H NMR (500 MHz, D₂O):** δ = 5.30 (d, J = 2.95 Hz, 1H, H-1'), 4.85 - 4.83 (1H, m), 4.64 (d, J = 7.55 Hz, 1H, H-1'), 4.31 (quart, J = 6.4 Hz, 1H, H-4"), 4.09 - 3.66 (m, 14H), 3.43 (t, J = 8.8 Hz, 1H, H-2), 1.32 (d, J = 6.15 Hz, 3H, -CH₃); **¹³C NMR (125 MHz, D₂O):** δ = 100.4, 99.6, 90.2, 77.4, 76.5, 75.4, 74.5, 73.8, 72.8, 71.9, 69.8, 69.3, 68.4, 67.1, 61.3, 60.2, 15.5; **IR (film):** ν = 3368.07, 2930.31, 2119.39, 1251.07, 1075.12, 1040.41 cm⁻¹.

LPG₈Propargyl_{0.40} 2a

Dried LPG (0.200 g, 1.08 mmol OH to be functionalized) was dissolved in dry DMF (10 mL) and cooled to 0 °C. To the stirred solution of LPG in dry DMF at 0 °C, NaH (0.054 g, 2.15 mmol, 2 eq., 95%) was added. After addition ice bath was removed and the reaction mixture was allowed to stir at room temperature for 3 hours and cooled down again to 0 °C. The propargyl bromide (0.278 mL, 3.22 mmol, 3 eq.) in dry DMF (1 mL) was added slowly to the reaction mixture and stirred at room temperature overnight. The excess of NaH was quenched by the dropwise addition of water while keeping the reaction flask in an ice bath. The DMF was removed under reduced pressure and the resulting mixture was dialyzed in MeOH to afford LPG-propargyl (0.180 g, 0.018 mmol, Yield = 73.17 %). Degree of propargylation was quantified by ¹H NMR, DF = 0.40. **¹H NMR (500 MHz, CD₃OD):** δ = 4.22 (s, 2H, OCH₂C≡CH), 3.71 - 3.55 (m, 13H, LPG backbone), 2.90 (s, 1H, C≡CH); **¹³C NMR (125 MHz, CD₃OD):** δ = 81.57, 80.90, 80.01, 76.33, 70.88, 62.79, 59.43; **IR (film):** ν = 3397.96, 3281.29, 2917.77, 2874.38, 2113.6, 1713.3, 1644.98, 1460.81, 1352.82, 1072.23 cm⁻¹.

LPG₈propargyl_{1.00} 2b

Similar procedure as for **2a**: LPG (0.235 g, 3.17 mmol OH to be functionalized) was propargylated using NaH (0.16 g, 6.35 mmol, 2 eq., 95%) and propargyl bromide (0.081 mL, 9.52 mmol, 3.0 eq.). DF = 1.00. (0.231 g, 0.0194 mmol, Yield = 66.57 %). **¹H NMR (500 MHz, CD₃OD):** δ = 4.18 (s, 2H, OCH₂C≡CH), 3.65 - 3.57 (m, 5H, LPG backbone), 2.48 (s, 1H, C≡CH); **¹³C NMR (125 MHz, CDCl₃):** δ = 79.99, 78.70, 74.80, 69.87, 58.66; **IR (film):** ν = 3285.14, 2919.7, 2114.58, 1357.64, 1033.66, 952.66.

hPG₁₀Propargyl_{0.60} 6a

Similar procedure as for **2a**: hPG (0.198 g, 1.60 mmol OH to be functionalized) was propargylated using NaH (0.081 g, 3.2 mmol, 2 eq., 95%) and propargyl bromide (0.0413 mL, 4.8 mmol, 3.0 eq.). DF = 0.60 (0.190 g, 0.0145 mmol, Yield: 73.64 %). **¹H NMR (500 MHz, CD₃OD):** δ = 4.36 (s, 1H, sec OCH₂C≡CH), 4.23 (s, 1H, primary OCH₂C≡CH), 3.89 - 3.60 (m, 8H, hPG backbone), 2.91 (s, 1H, C≡CH); **¹³C NMR (125 MHz, CD₃OD):** δ = 81.51, 79.95, 78.08, 76.43, 74.05, 72.45, 71.21, 70.74, 59.48, 58.49; **IR (film):** ν = 3420.14, 3284.18, 2919.70, 2114.56, 1092.48, 1032.69 cm⁻¹.

hPG₁₀Propargyl_{1.00} 6b

Similar procedure as for **2a**: hPG (0.227 g, 3.06 mmol OH to be functionalized) was propargylated using NaH (0.155 g, 6.13 mmol, 2 eq., 95%) and propargyl bromide (0.078 mL, 9.19 mmol, 3.0 eq.). DF = 1.00. (0.259 g, 0.017 mmol, Yield: 75.51 %). ¹H NMR (500 MHz, CD₃COCD₃): δ = 4.37 (s, 1H, sec OCH₂C≡CH), 4.23 (s, 1H, primary OCH₂C≡CH), 3.87 - 3.60 (m, 5H, hPG backbone), 2.97 (brs, 1H, C≡CH); ¹³C NMR (125 MHz, CD₃COCD₃) : δ = 80.75, 80.17, 78.70, 76.58, 74.97, 71.35, 69.82, 58.23, 57.23, 29.02; **IR (film)**: ν = 3287.07, 2868.59, 2114.56, 1033.66 cm⁻¹.

LPG₈Man_{0.40} 3a

To a mixture of LPG₈Propargyl_{0.40} **2a** (0.023 g, 0.101 mmol of propargyl to be functionalized) and azido mannose (0.0465 g, 0.112 mmol) in DMF (15 mL), CuSO₄·5H₂O (0.005 g, 0.02 mmol) and sodium ascorbate (0.040 g, 0.203 mmol) solution in H₂O (2 mL) were added dropwise. The reaction mixture was degassed thoroughly with argon for 5-10 minutes and then allowed to stir for 2 days at 40 °C. The reaction was stopped, and solvent was removed under reduced pressure. 2M NaOH (7 mL) was added to the residue and stirred at room temperature for 4-5 hrs. The reaction mixture was neutralized by adding 2M HCl solution and dialyzed first against water and aqueous EDTA solution for 2 days and again using only water for 4 days. The solvent of the dialysis was changed thrice a day. The aqueous solution obtained after dialysis was lyophilized to afford LPG₈ Man_{0.40}. DF = 0.36. (0.046 mg, 0.002 mmol, Yield: 93.91%). DF = 0.36. ¹H NMR (500 MHz, D₂O): δ = 8.10 (s, 1H, C=CH), 4.64 (brs, 4H, CH₂CH₂Trz, TrzCH₂O), 4.04 – 3.52 (m, 22H, Man: H-1, H-2, H-3, H-4, H-5, H-6, CHH_aCH₂Trz, LPG backbone) 3.02 (s, 1H, CHH_bCH₂Trz); Elemental analysis: calcd (%): N 7.83%; found: N 6.36 %.

LPG₈Man_{1.00} 3b

Similar procedure as for **3a**: LPG₈Propargyl_{1.00} **2b** (0.020 g, 0.141 mmol of propargyl to be functionalized) and azido mannose (0.107 g, 0.257 mmol) were coupled using CuSO₄·5H₂O (0.008 g, 0.034 mmol) and sodium ascorbate (0.068 g, 0.342 mmol) assisted click reaction. Deprotection was performed by similar procedure as **3a** using 2M NaOH. (0.051 g, 0.016 mmol, Yield: 69.86%). DF = 1.00. DF = 1.00. ¹H NMR

(700 MHz, D₂O): δ = 8.13 (s, 1H, C=CH), 4.65 (brs, 4H, CH₂CH₂Trz, TrzCH₂O), 4.10 – 3.61 (m, 13H, Man: H-1, H-2, H-3, H-4, H-5, H-6, CHH_aCH₂Trz, LPG backbone), 3.11 (s, 1H, CHH_bCH₂Trz); Elemental analysis: calcd (%): N 10.23%; found: N 9.24 %.

LPG₈FL_{0.40} 4a

Similar procedure as for **3a**: LPG₈Propargyl_{0.40} (0.020 g, 0.089 mmol of propargyl to be functionalized) and 2'-fucosyllactose azide (0.054 g, 0.106 mmol) were coupled using CuSO₄·5H₂O (0.004 g, 0.178 mmol) and sodium ascorbate (0.035 g, 0.178 mmol) assisted click reaction. (0.048 g, 0.014 mmol, Yield: 72.72 %). DF = 0.39. ¹H NMR (700 MHz, D₂O): δ = 8.31 (s, 1H, C=CH), 5.80 (s, 1H, H-1), 5.35 (s, 1H, H-1''), 4.72 (brs, 2H, CH₂Trz), 4.61 (d, J = 7 Hz, 1H, H-1'), 4.26 (s, 1H, H-4''), 4.09 - 3.73 (m, 28H, FL: H-2, H-3, H-4, H-5, H-6, H-2', H-3', H-4', H-5', H-6', H-2'', H-3'', H-5'', LPG backbone), 1.28 (s, 3H, CH₃); Elemental analysis: calcd (%): N 5.34 %; found: N 5.61 %.

LPG₈FL_{1.00} 4b

Similar procedure as for **3a**: LPG₈Propargyl_{1.00} (0.020 g, 0.171 mmol of propargyl to be functionalized) and 2'-fucosyllactose azide (0.105 g, 0.205 mmol) were coupled using CuSO₄·5H₂O (0.008 g, 0.034 mmol) and sodium ascorbate (0.068 g, 0.342 mmol) assisted click reaction. (0.091 g, 0.013 mmol, Yield: 75.20%). DF = 1.00. ¹H NMR (700 MHz, D₂O): δ = 8.20 (s, 1H, C=CH), 5.70 (s, 1H, H-1), 5.26 (s, 1H, H-1''), 4.52 - 3.64 (m, 28H, FL: H-1, H-2, H-3, H-4, H-5, H-6, H-1', H-2', H-3', H-4', H-5', H-6', H-1'' H-2'', H-3'', H-4'', H-5'', LPG backbone), 1.18 (s, 3H, CH₃); Elemental analysis: calcd (%): N 6.27 %; found: N 5.45 %.

hPG₁₀Man_{0.70} 7a

Similar procedure as for **3a**: hPG₁₀Propargyl_{1.00} (0.020 g, 0.178 mmol of propargyl to be functionalized) and azidomannose (0.089 g, 0.214 mmol) were coupled using CuSO₄·5H₂O (0.008 g, 0.035 mmol) and sodium ascorbate (0.070 g, 0.356 mmol) assisted click reaction. Deprotection was performed by similar procedure as **3a** using 2M NaOH. (0.051 g, 0.016 mmol, Yield: 69.86%). DF = 0.68. ¹H NMR (700 MHz, D₂O): δ = 8.21 (s, 1H, C=CH), 4.68 (brs, 4H, CH₂CH₂Trz, TrzCH₂O), 4.10 – 3.62 (m,

16H, Man: H-1, H-2, H-3, H-4, H-5, H-6, $\text{CHH}_a\text{CH}_2\text{Trz}$, hPG backbone), 3.13 (s, 1H, $\text{CHH}_b\text{CH}_2\text{Trz}$ Elemental analysis: calcd (%): N 9.29%; found: N 9.02 %.

hPG₁₀Man_{1.00} 7b

Similar procedure as for **3a**: hPG₁₀Propargyl_{1.00} (0.055 g, 0.495 mmol of propargyl to be functionalized) and azidomannose (0.0309 g, 0.743 mmol) were coupled using $\text{CuSO}_4 \cdot 5\text{H}_2\text{O}$ (0.025 g, 0.099 mmol) and sodium ascorbate (0.196 g, 0.99 mmol) assisted click reaction. Deprotection was performed by similar procedure as **3a** using 2M NaOH. DF = 1.00. (0.155 g, 0.003 mmol, Yield: 77.6 %). **¹H NMR (700 MHz, D₂O)**: δ = 8.12 (s, 1H, C=CH), 4.65 (brs, 4H, $\text{CH}_2\text{CH}_2\text{Trz}$, TrzCH_2O), 4.10 – 3.87 (m, 13H, Man: H-1, H-2, H-3, H-4, H-5, H-6, $\text{CHH}_a\text{CH}_2\text{Trz}$, hPG backbone), 3.13 (s, 1H, $\text{CHH}_b\text{CH}_2\text{Trz}$); Elemental analysis: calcd (%): N 10.36%; found: N 10.78 %.

hPG₁₀FL_{0.60} 8a

Similar procedure as for **3a**: hPG₁₀Propargyl_{0.60} (0.020 g, 0.124 mmol of propargyl to be functionalized) and 2'-fucosyllactose azide (0.082 g, 0.161 mmol) were coupled using $\text{CuSO}_4 \cdot 5\text{H}_2\text{O}$ (0.006 g, 0.024 mmol) and sodium ascorbate (0.049 g, 0.248 mmol) assisted click reaction. (0.0646 g, 0.001 mmol, Yield: 72.58 %). DF = 0.60. **¹H NMR (700 MHz, D₂O)**: δ = 8.21 (s, 1H, C=CH), 5.70 (s, 1H, H-1), 5.26 (s, 1H, H-1''), 4.52 - 3.65 (m, 27H, CH_2Trz , FL: H-2, H-3, H-4, H-5, H-6, H-1', H-2', H-3', H-4', H-5', H-6', H-2'', H-3'', H-5'', H-5'', hPG backbone), 1.18 (s, 3H, CH_3); Elemental analysis: calcd (%): N 5.84 %; found: N 6.21 %.

hPG₁₀FL_{1.00} 8b

Similar procedure as for **3a**: hPG₁₀Propargyl_{1.00} (0.015 g, 0.134 mmol of propargyl to be functionalized) and 2'-fucosyllactose azide (0.089 g, 0.173 mmol) were coupled using $\text{CuSO}_4 \cdot 5\text{H}_2\text{O}$ (0.006 g, 0.027 mmol) and sodium ascorbate (0.053 g, 0.267 mmol) assisted click reaction. DF = 1.00. (0.065 g, 0.0007 mmol, Yield: 73.03 %). **¹H NMR (500 MHz, D₂O)**: δ = 8.26 (s, 1H, C=CH), 5.77 (s, 1H, H-1), 5.34 (s, 1H, H-1''), 4.25 – 3.73 (m, 27H, CH_2Trz , FL: H-2, H-3, H-4, H-5, H-6, H-1', H-2', H-3', H-4', H-5', H-6', H-2'', H-3'', H-5'', H-5'', hPG backbone), 1.24 (s, 3H, CH_3); Elemental analysis: calcd (%): N 6.27 %; found: N 7.05 %.

5 ^1H and ^{13}C spectra of all the intermediates and final molecules.

1. $\text{LPG}_8\text{Propargyl}_{0.40}$ 2a

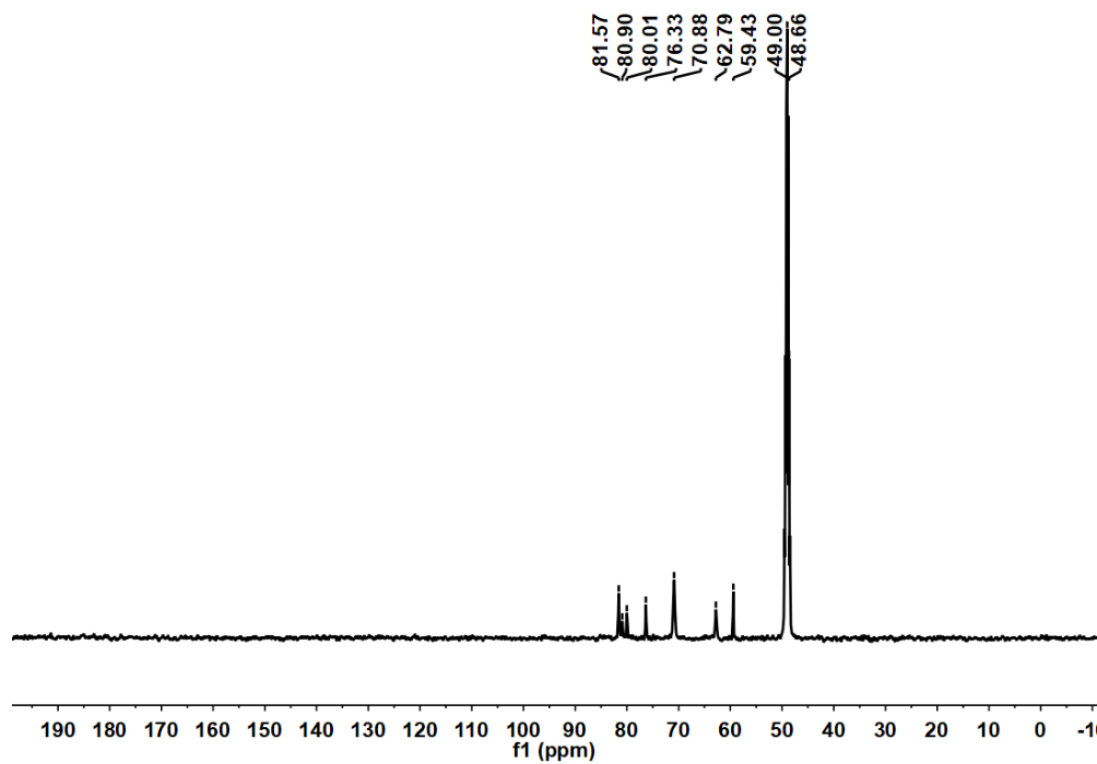
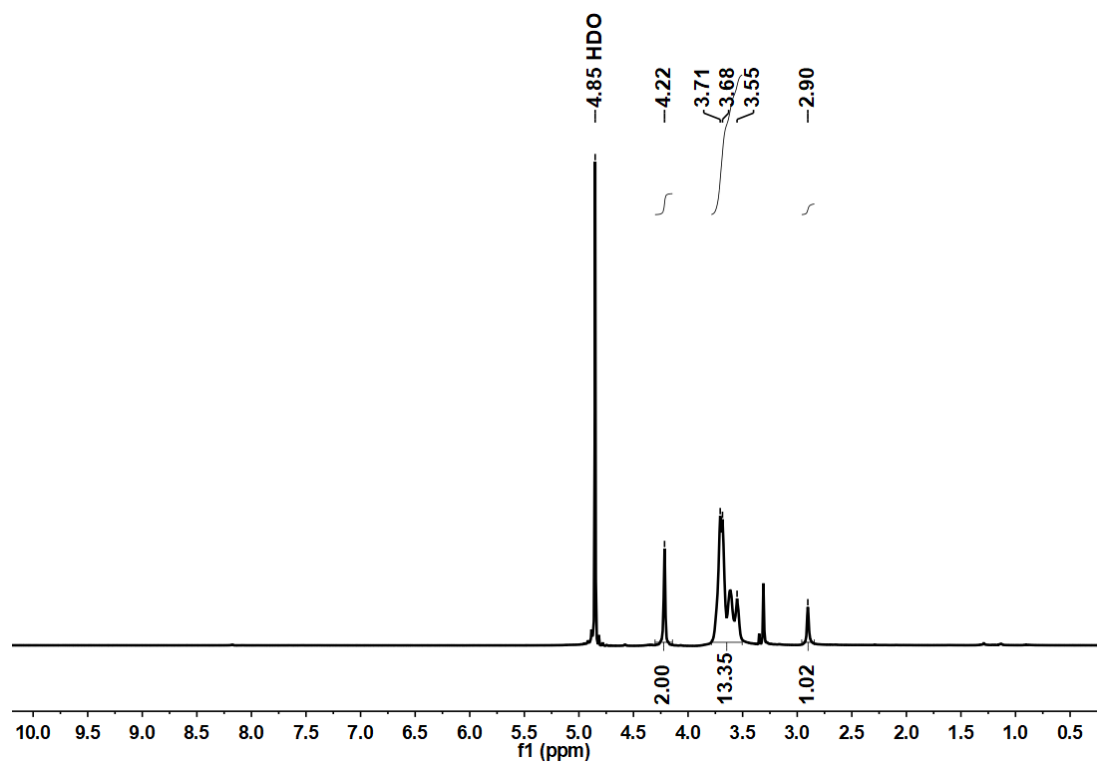


Fig. s1 ^1H and ^{13}C spectra of compound 2a

2. LPG₈Propargyl_{1.00} 2b

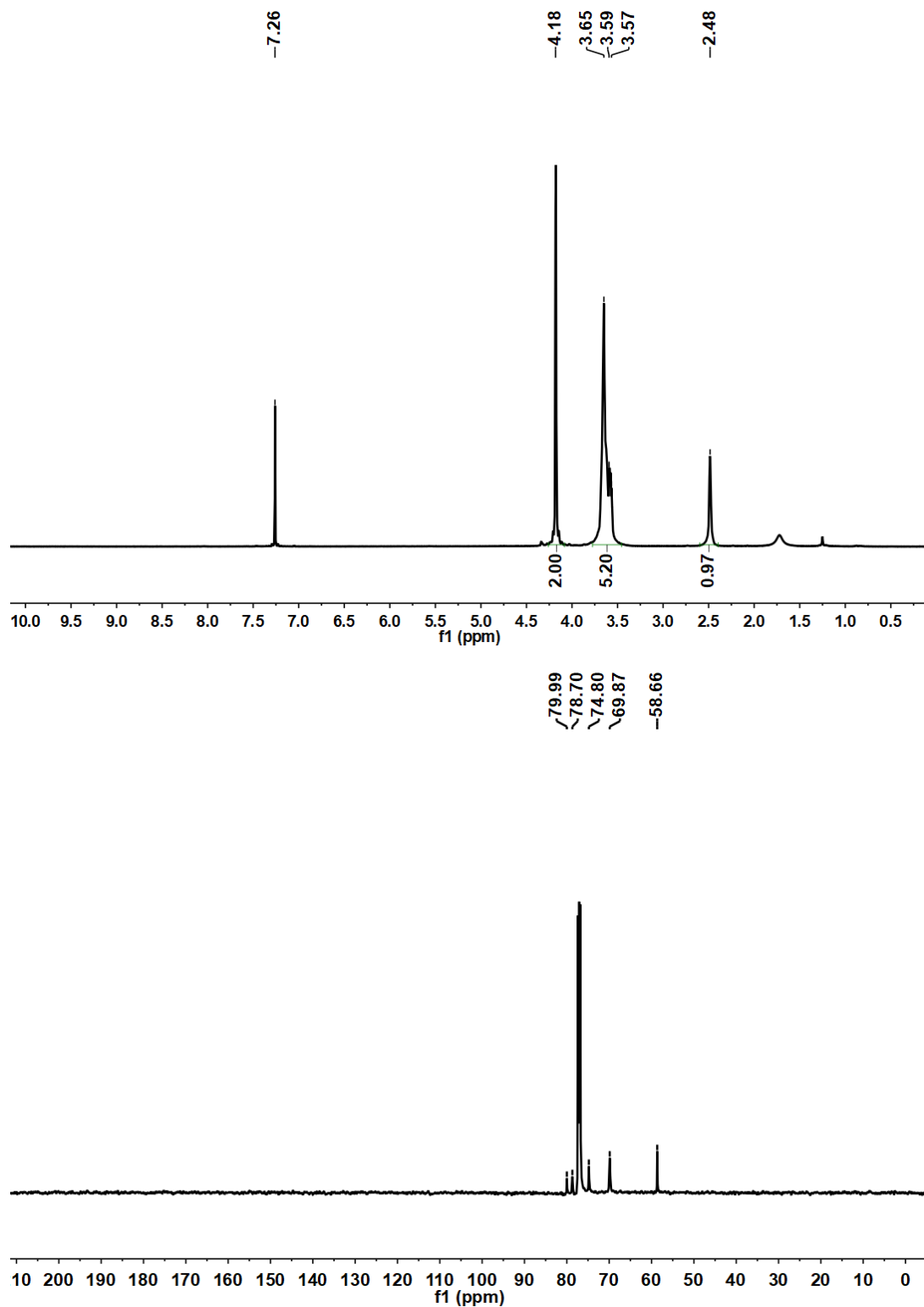


Fig. s2 ¹H and ¹³C spectra of compound 2b

3. hPG₁₀Propargyl_{0.60} 6a

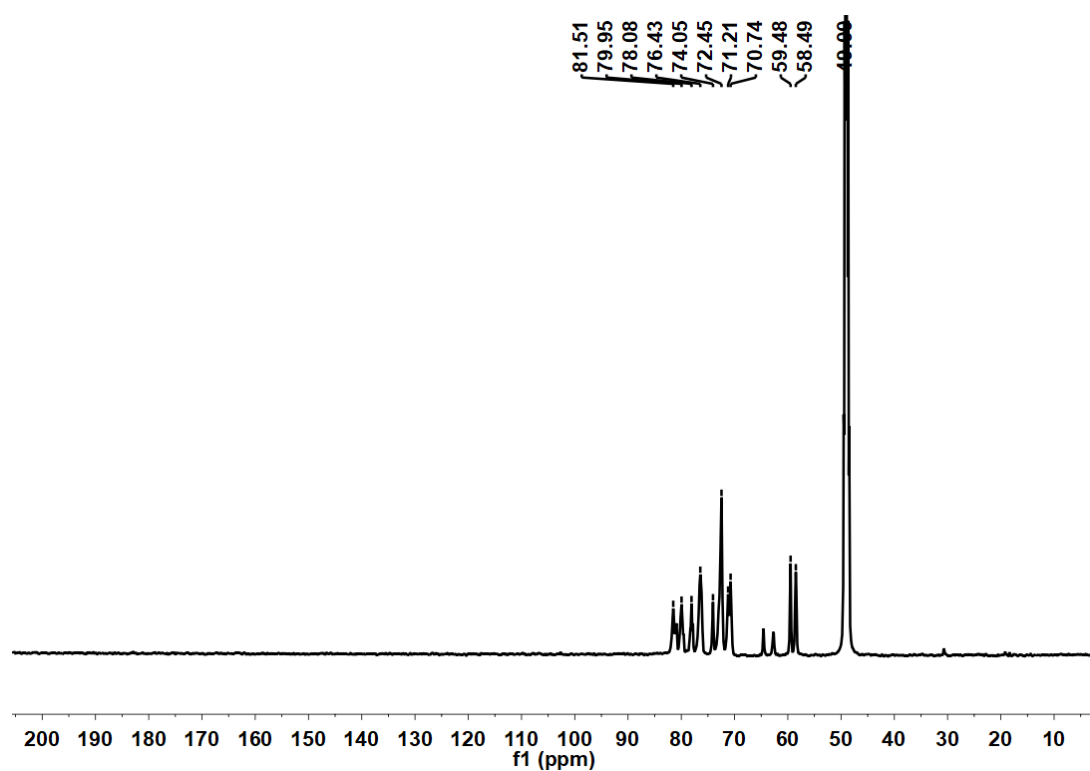
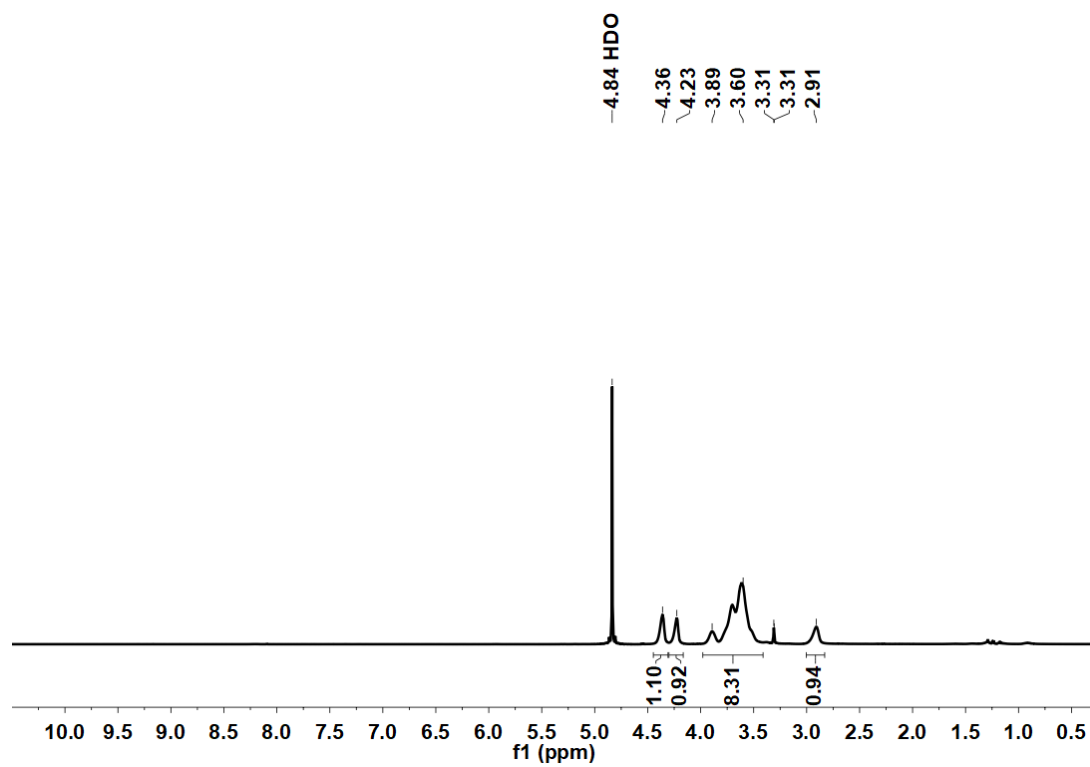


Fig. s3 ¹H and ¹³C spectra of compound 6a

4. hPG₁₀Propargyl_{1.00} 6b

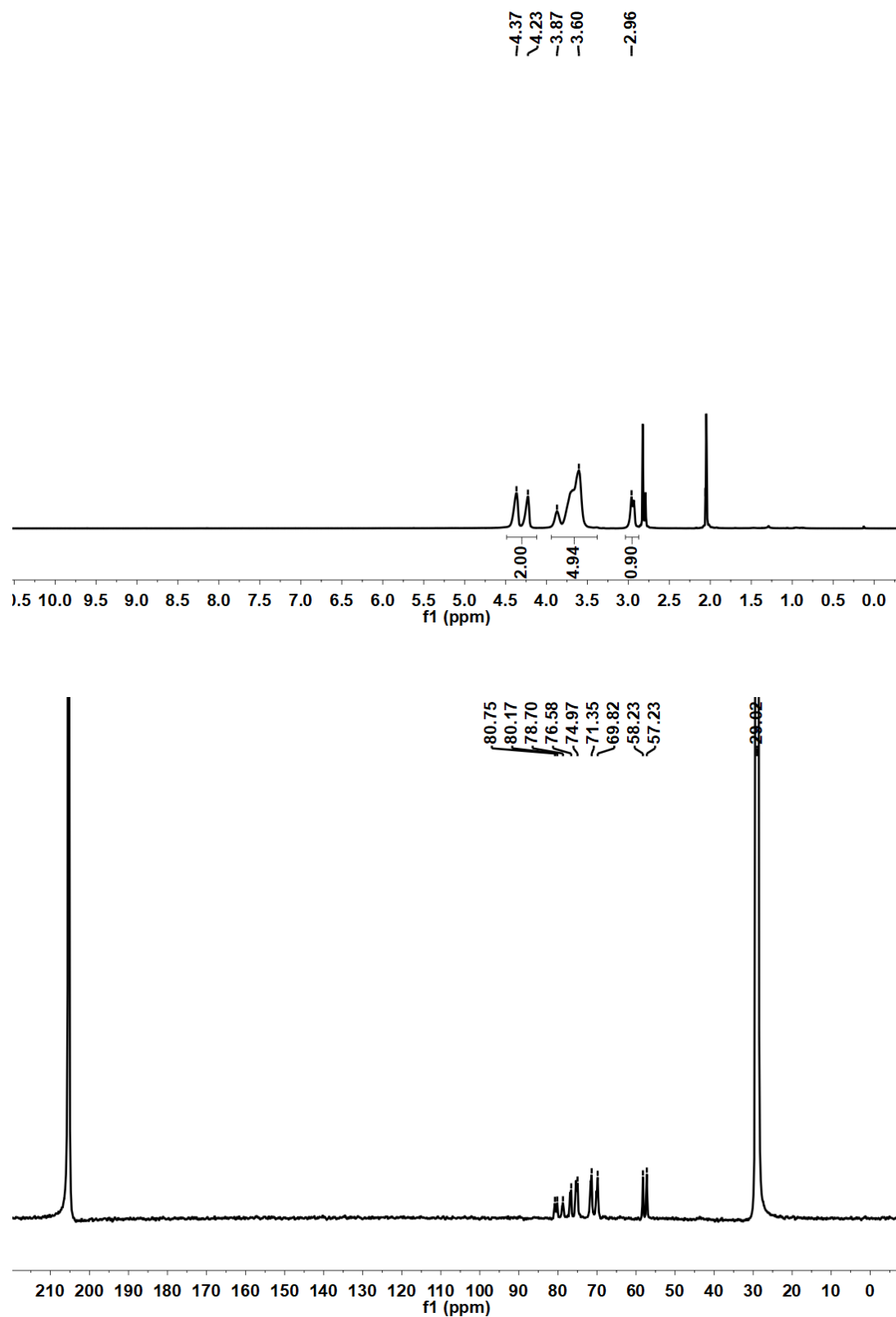


Fig. s4 ¹H and ¹³C spectra of compound 6b

5. 2'-fucosyllactose azide

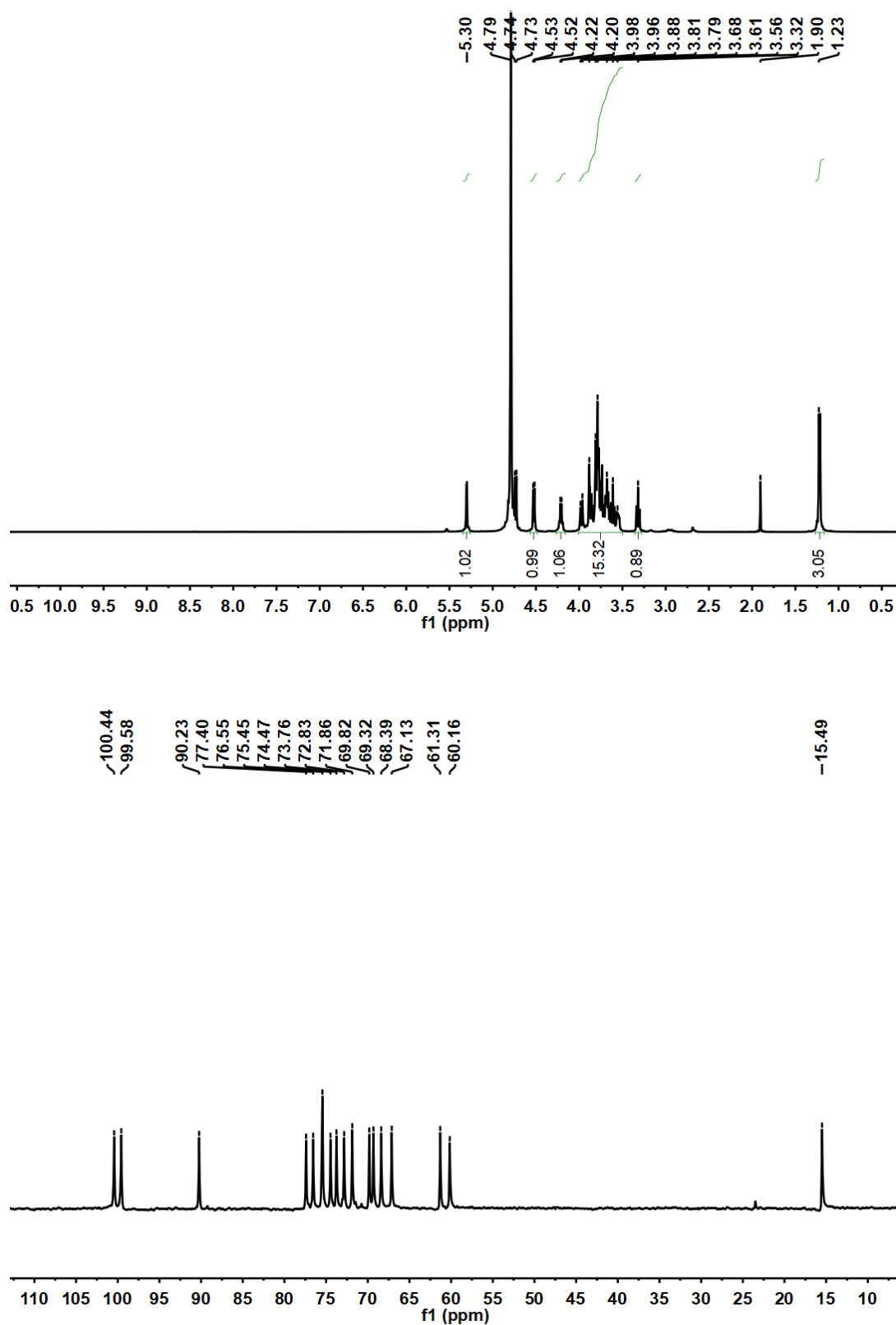


Fig. s5 ¹H and ¹³C spectra of 2'-fucosyllactose azide

6. LPG₈Man_{0.40} 3a

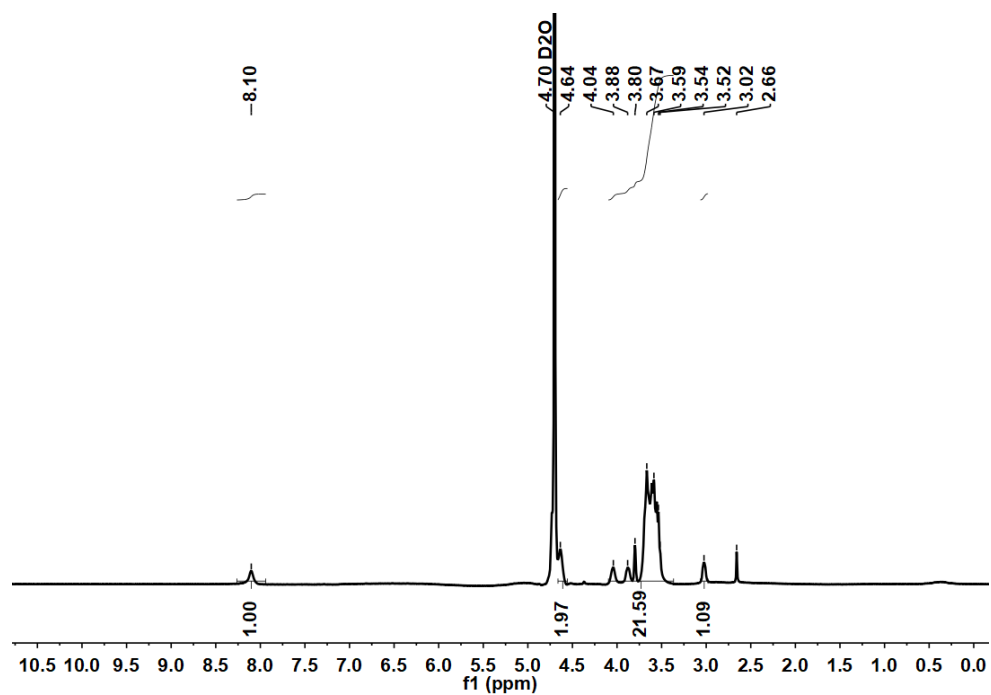


Fig. s6 ¹H spectra of compound 3a

7. LPG₈Man_{1.00} 3b

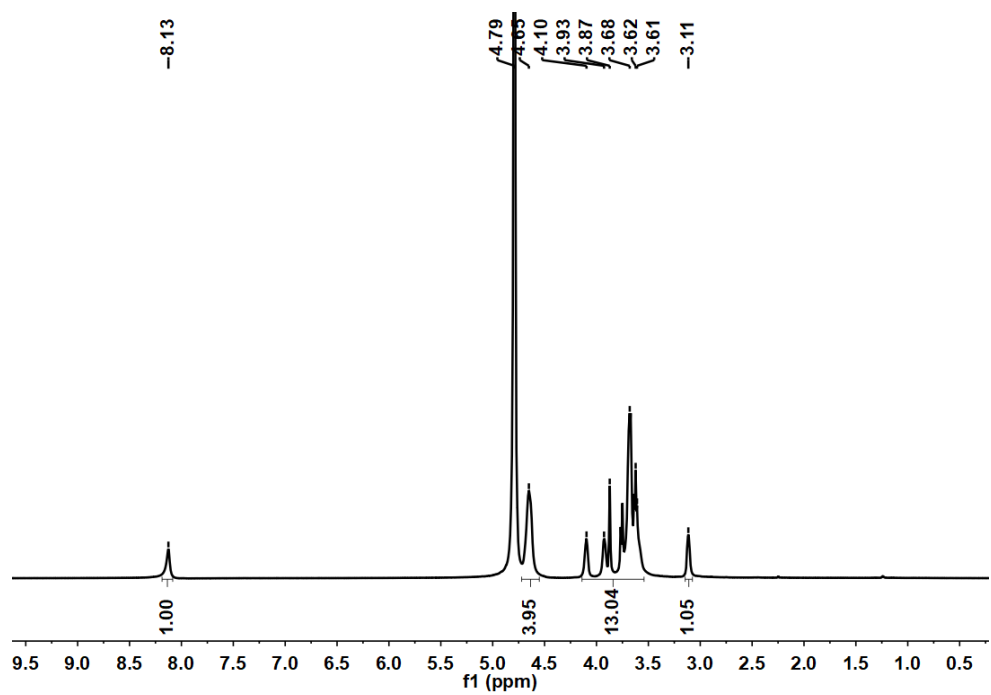


Fig. s7 ¹H spectra of compound 3b

8. LPG₈FL_{0.40} 4a

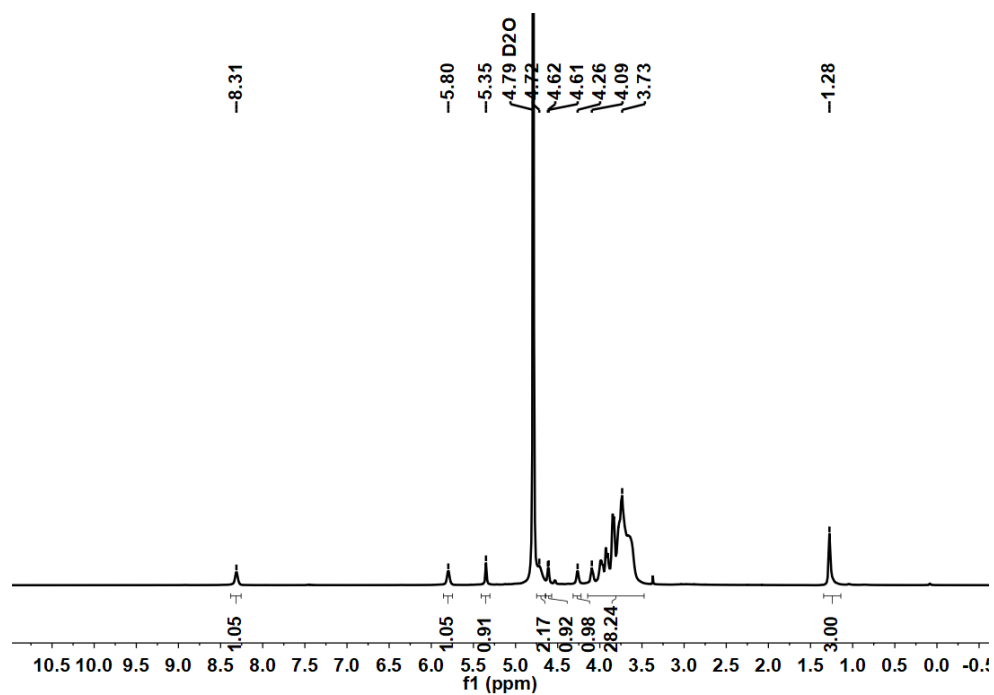


Fig. s8 ¹H spectra of 4a

9. LPG₈FL_{1.00} 4b

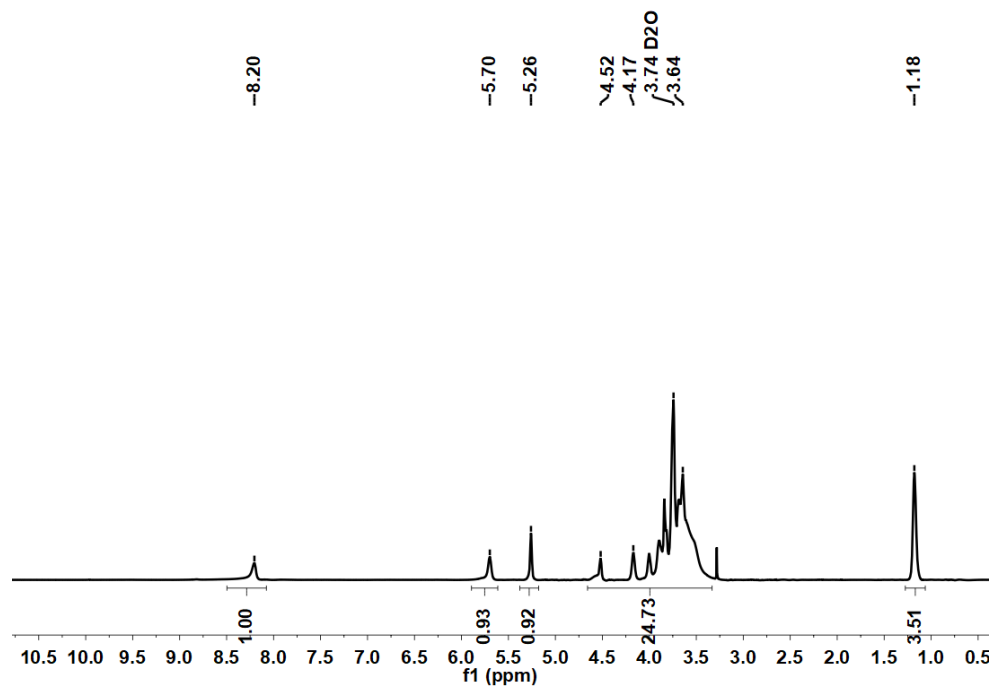


Fig. s9 ¹H spectra of compound 4b

10. hPG₁₀Man_{0.70} 7a

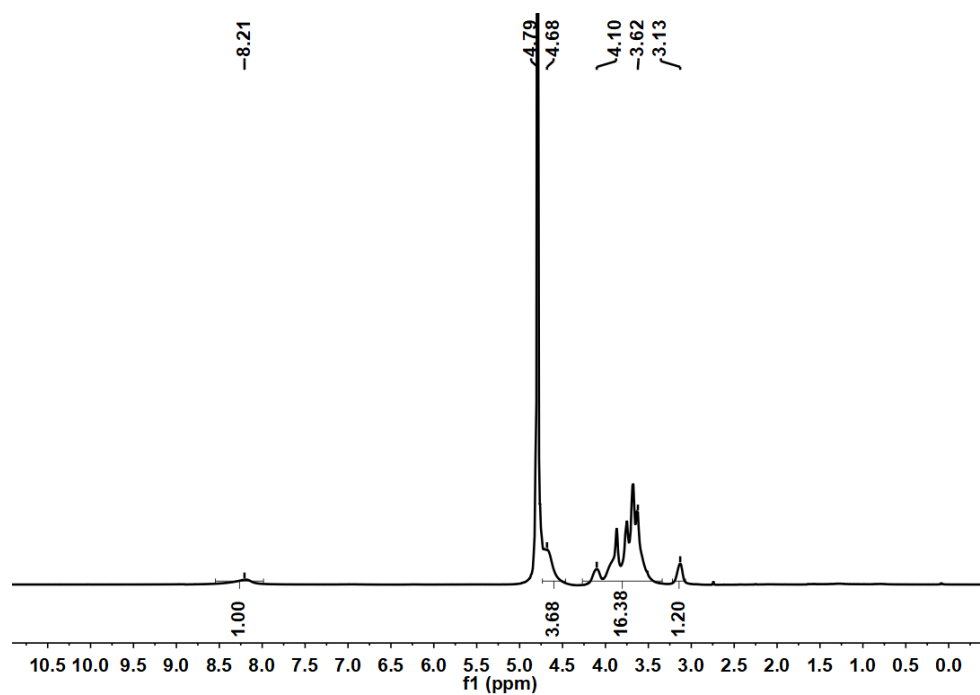


Fig. s10 ¹H spectra of compound 7a

11. hPG₁₀Man_{1.00} 7b

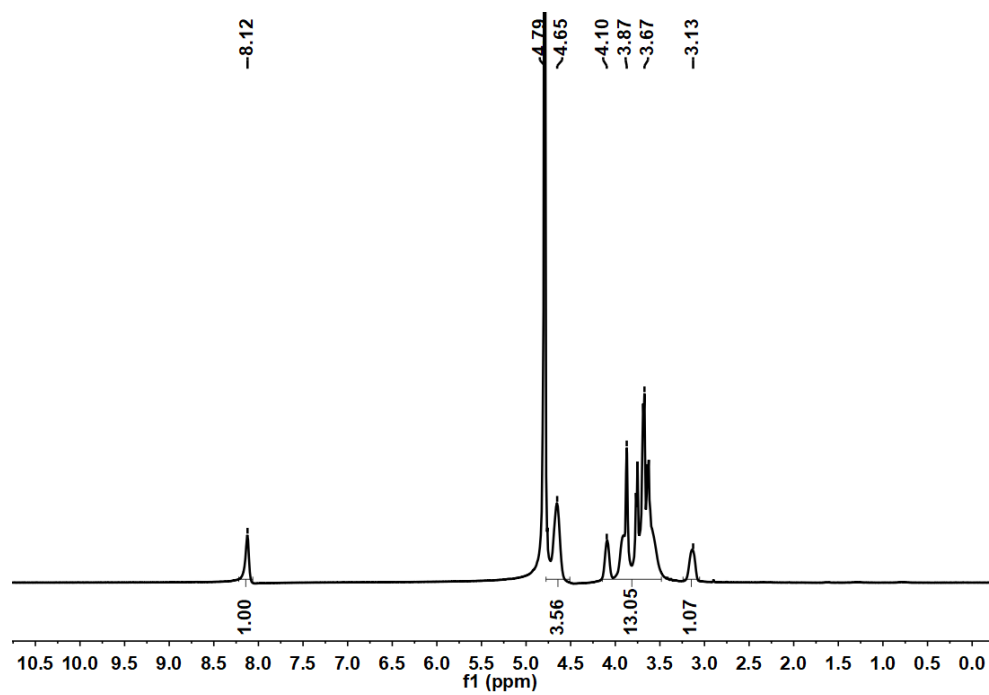


Fig. s11 ¹H spectra of compound 7b

12. hPG₁₀FL_{0.60} 8a

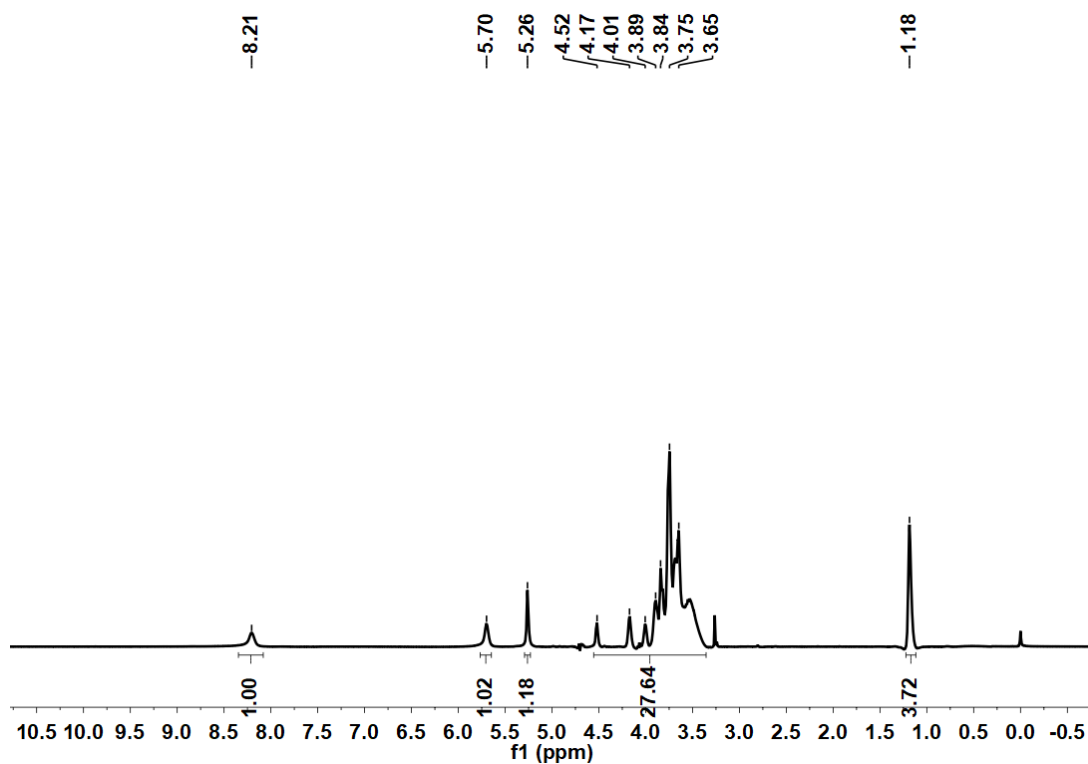


Fig. s12 ^1H spectra of compound **8a**

13. hPG₁₀FL_{1.00} 8b

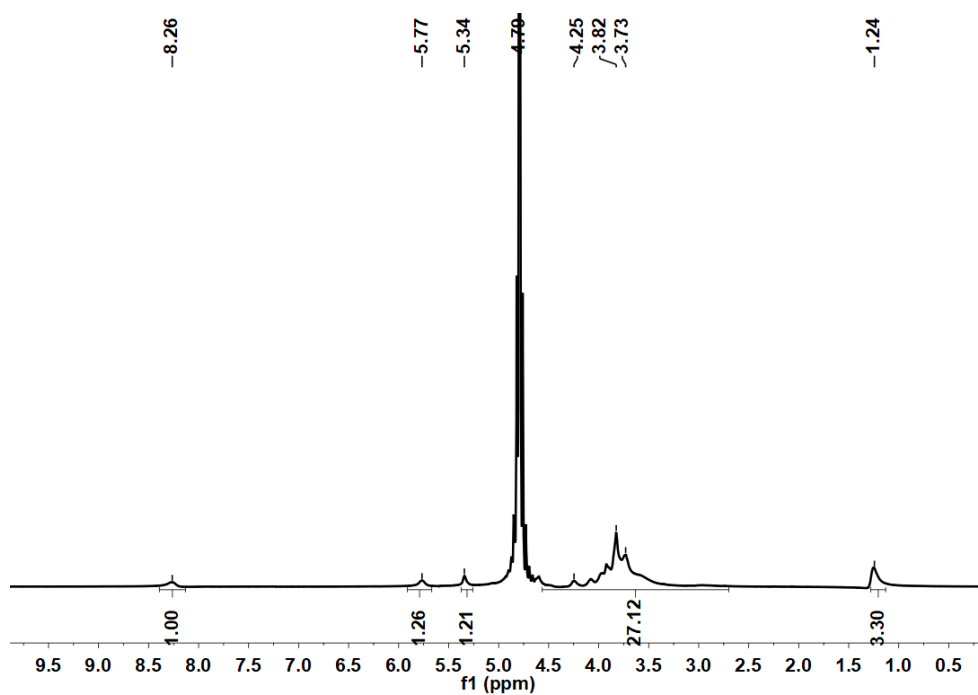


Fig. s13 ^1H spectra of compound **8b**

6 Resulting binding isotherms derived from single-cycle kinetic measurements

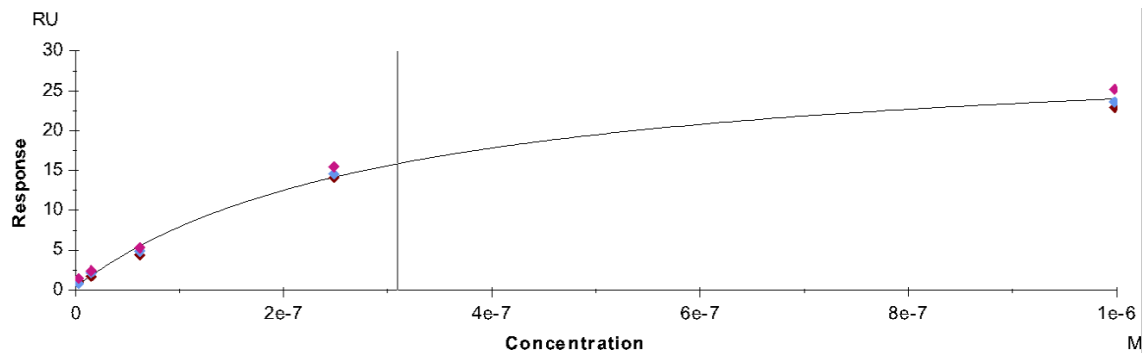


Fig. s14 Binding isotherm of compound 2a

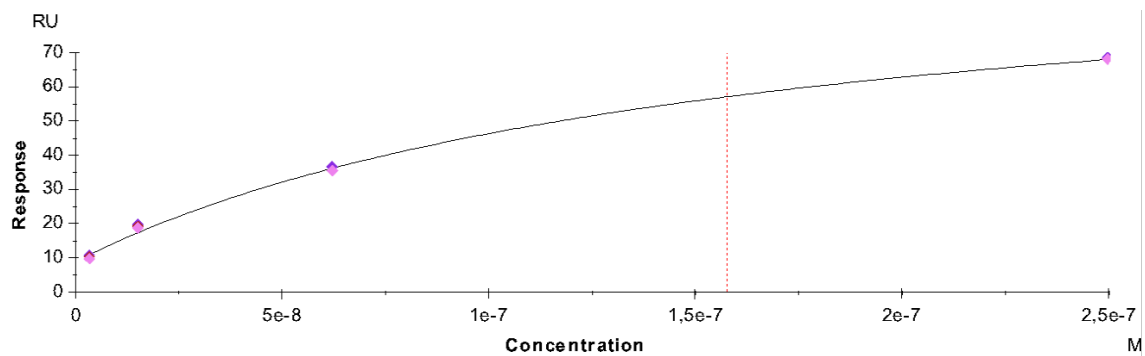


Fig. s15 Binding isotherm of compound 2b

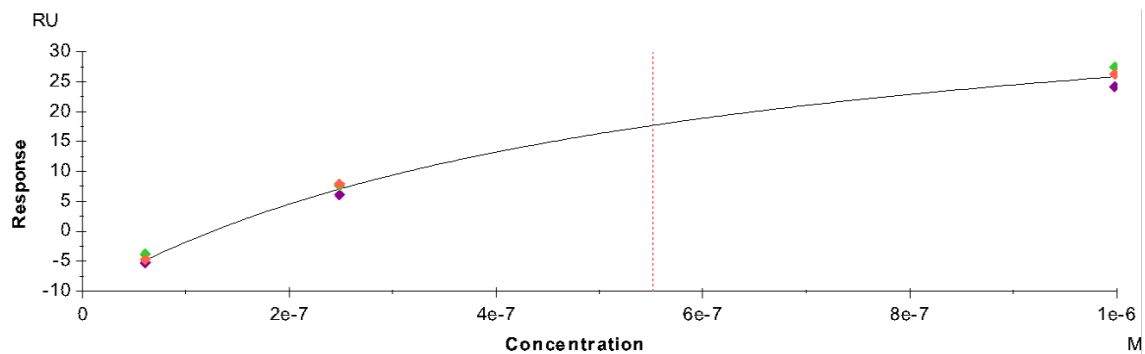


Fig. s16 Binding isotherm of compound 4a

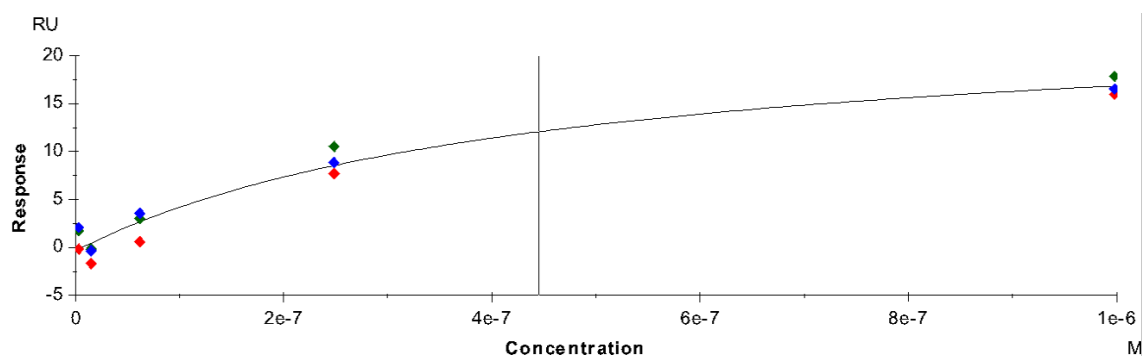


Fig. s15 Binding isotherm of compound **4b**

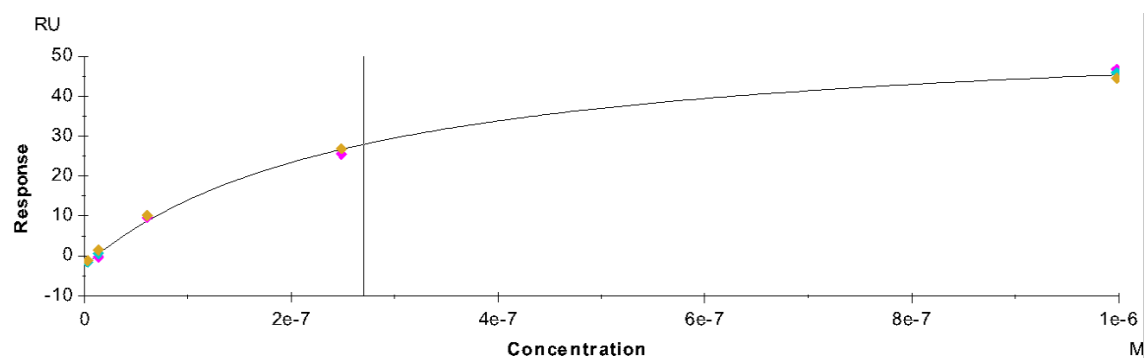


Fig. s16 Binding isotherm of compound **7a**

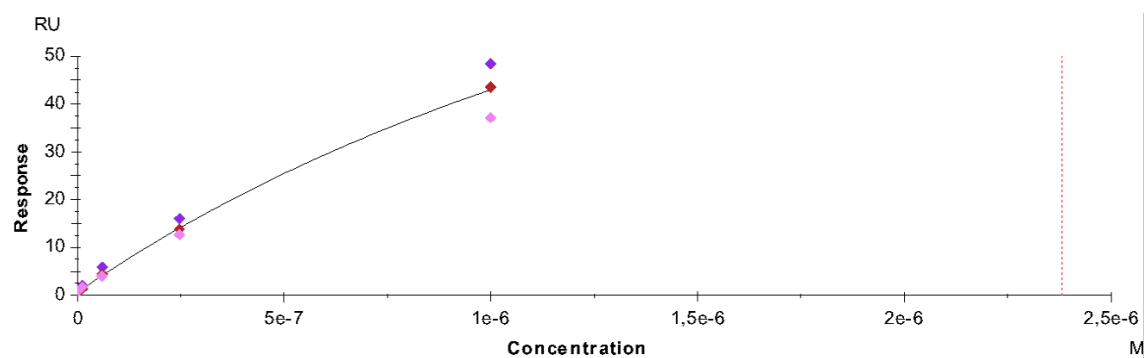


Fig. s17 Binding isotherm of compound **7b**

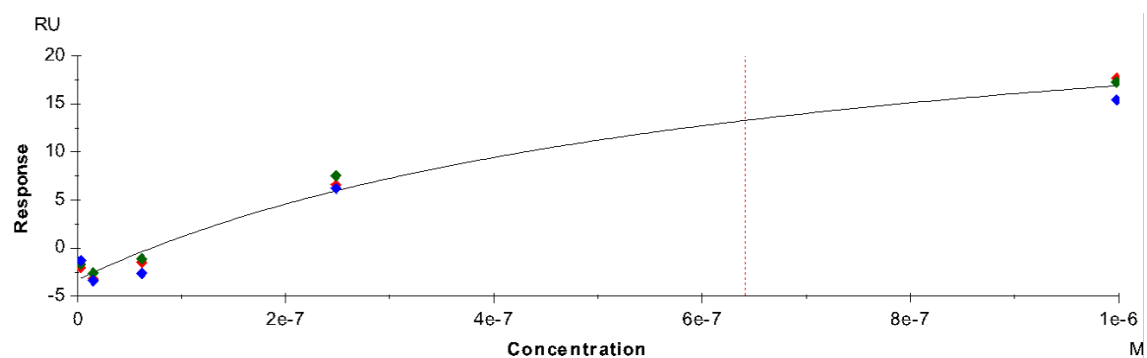


Fig. s18 Binding isotherm of compound **8a**

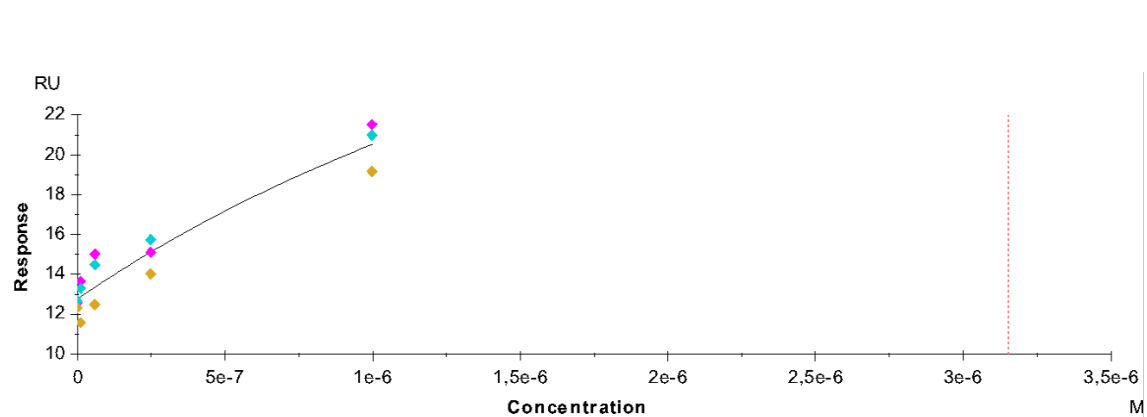


Fig. s19 Binding isotherm of compound **8b**

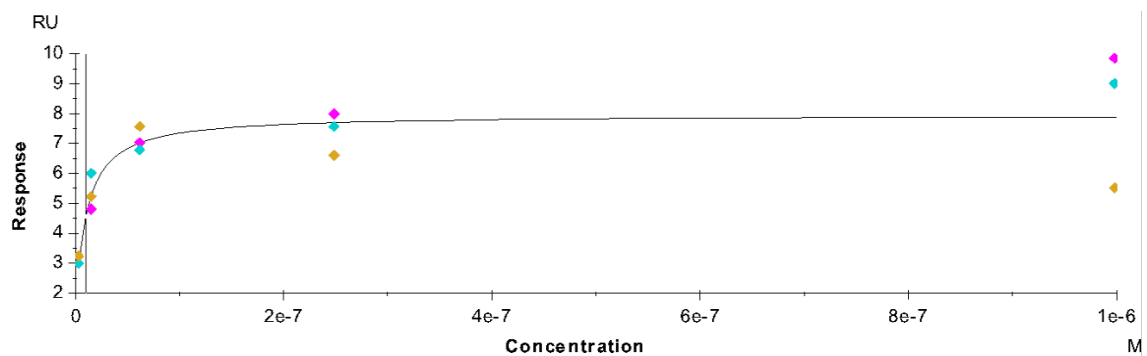


Fig. s20 Binding isotherm of compound **Man₉Glycan**

7.1 Gel permeation chromatography of hyperbranched and linear polyglycerol

$M_n = 10642$ g/mol, $M_w = 16633$ g/mol, $M_z = 24882$ g/mol, $D = 1.56$

Detector: RI, Eluent = H₂O, Flow rate = 1mL/min, GPC Colum = Suprema, Reference = Pullulan

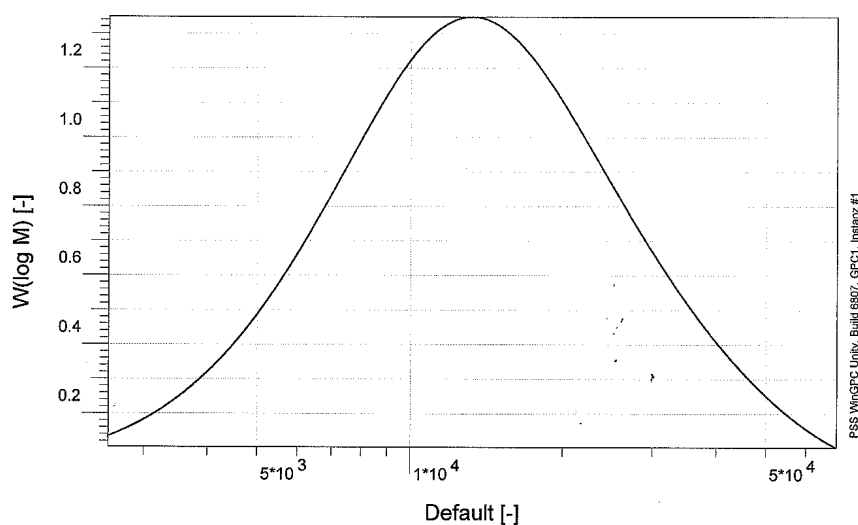


Fig. s21 GPC of compound **hPG₁₀OH**

7.2 Gel permeation chromatography of linear polyglycerol

$M_n = 6530$ g/mol, $M_w = 9298$ g/mol, $M_z = 12589$ g/mol, $D = 1.42$

Detector: RI, Eluent = H₂O, Flow rate = 1mL/min, GPC Colum = Suprema, Reference = Pullulan

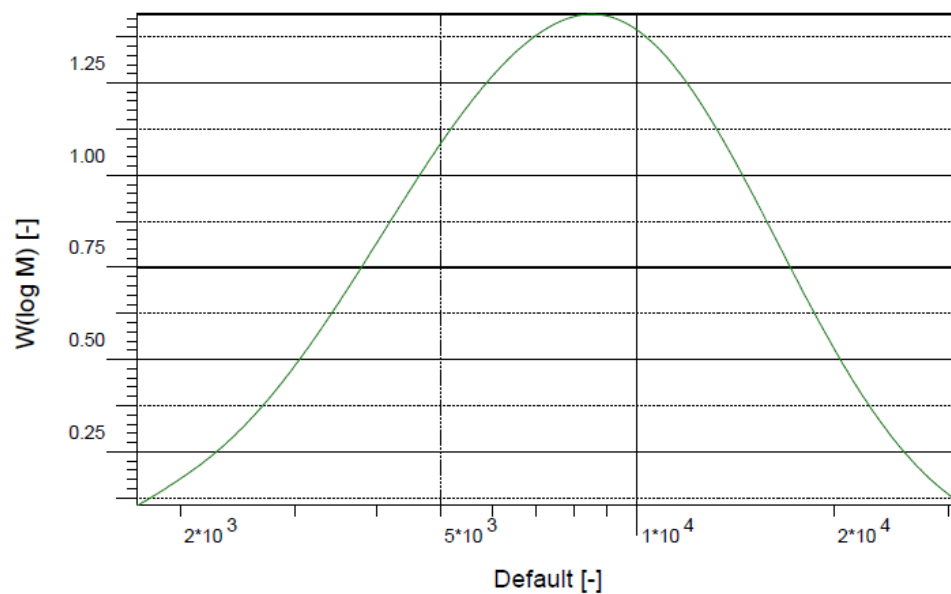


Fig. s22 GPC of compound LPG₈OH

5 Summary and conclusions

In the first part of the thesis we designed inhibitors for influenza A virus X31 (subtype Aichi). We targeted hemagglutinin (HA) which exist in homotrimeric form on the lipid membrane of the virus. Three receptor binding sites are present on the HA trimer which recognizes sialic acid residues on the host cell and cause viral infection. For this purpose, I prepared a series of trivalent sialosides to target the HA trimer. I choose trivalent rigid and flexible scaffold to develop the inhibitor. The commercially available 4-(((benzyloxy)carbonyl) amino)-4-(2-carboxyethyl) heptanedioic acid abbreviated as Tris was used as flexible core and for rigid system, adamantane core was used. Flexible oligoethylene glycol (OEG) of different lengths were used as spacer because of their biocompatibility and hydrophilicity. As per the MD simulation data, OEG should consist of 6-14 EG units to cover the distance between the center of scaffold to the ligand binding site on the HA.

Each of the synthesized tripodal sialosides were tested against IAV-X31 in hemagglutination inhibition assay. Non-functionalized scaffolds were used as negative control and did not show any binding inhibition in HAI assay. The adamantane based trivalent sialoside with hexaethylene glycol spacer namely $\text{cbzAd}(\text{EG}_6\text{SA})_3$ was the most potent compound with inhibition constant (K_i) in micromolar range. To test the dependence of binding affinity on the presence of 2 vs 3 ligand, the adamantane based divalent sialoside was also prepared and tested in HAI assay. The K_i values for the both trivalent and divalent sialosides in terms of tripod concentration were in micromolar range: 30 μM and 100 μM , respectively. This difference between the K_i value could be assigned to cooperativity factor as discussed in the previous section (section 1.1). In contrast, the HAI value of flexible Tris based trivalent sialosides was in millimolar range and 6.7 mM was the lowest K_i value for the flexible core compound with tetra ethylene glycol spacer i.e., $\text{cbzTris}(\text{EG}_4\text{SA})_3$.

All these compounds when tested for their binding affinity against rhodamine labeled IAV using labelled MST technique, showed dissociation constant in 58 and 71 μM for trivalent and divalent adamantane based sialosides respectively. This was in good comparison with the HAI values. However, for the flexible core based trivalent sialosides the binding affinity was also in micromolar range (16 μM) for $\text{cbzTris}(\text{EG}_4\text{SA})_3$. This could be attributed to non-specific binding of these compounds with the virus other than the HA which needs to be further investigated. In conclusion, rigid core adamantane based sialoside with EG_6 spacer was the most potent candidate among the series tripodal sialosides against IAV

Summary and Conclusion

which can be further used for the multimeric presentation of trivalent ligand on larger scaffolds to achieve high binding affinities against IAV.

In the second project, an easy approach i.e., copper assisted click chemistry was used for the development of linear and hyperbranched polyglycerol based glycoarchitecture with varying degree of ligand densities and binding affinity was evaluated for lectin binding. Mannose (Man) and fucosyllactose (FL) azides were used to decorate these glycoarchitecture. The hydrodynamic diameter of these glycoconjugates was analyzed using dynamic light scattering (DLS) technique and size was in the range of 6-11 nm. We observed an increase in size as the ligand density increases. Two types of C-type lectin namely MBL and DC-SIGN was used for this purpose.

All the synthesized PGs based mannosides and fucosyllactosides were tested for binding with rhMBL in a label-free MST technique where the intrinsic fluorescence of MBL protein due to tryptophan unit was utilized to analyze the molecular migration in the presence of applied temperature gradient. The dissociation constant of all the glycoconjugates was in low micromolar range. However, we observed a trend that the affinity was higher for high ligand density. With linear PG based mannosides and fucosyllactosides, the affinity increased 4 times and 2 times, respectively, with an increase in ligand densities (100% functionalization). In the case of hyperbranched PG based mannosides and fucosyllactosides, the binding affinity is still in low micromolar range, however, there was not any significant increase in binding affinity with increase of ligand densities. Non-functionalized PG scaffolds were used as a negative control did not show any binding upto 100 μ M.

Thus, we conclude that completely functionalized PGs scaffold with Man and FL showed to be potent binder for MBL in comparison to partially functionalized architecture. The most potent candidate against MBL was hPG₁₀Man_{1.0} with $K_d = 152$ nM.

Furthermore, the same set of compounds was also used to study the binding affinity of DC-SIGN using surface plasmon resonance spectroscopy (SPR) based binding assay. In this study DC-SIGN was immobilized on the protein A sensor chip and glycoconjugates were flowed over the chip as analytes. This study showed that all the glycoconjugates binds to DC-SIGN with a binding affinity less than 1 μ M. For LPG based glycoconjugate, there was not any big difference in K_d values with different degree of functionalization (DF). However, in the case of dendritic glycoconjugates the binding affinity was observed to decrease with increasing DF. Here also, unfunctionalized PG scaffold were tested for

Summary and Conclusion

negative control. Here, $\text{LPG}_8\text{Man}_{1.0}$ was the most potent candidate with a K_d value of 157 nM which was approx. 23,000-fold higher affinity than mannose residue ($K_d = 3.5$ mM).

In conclusion, these low molecular weights, PG based multivalent mannosides and fucosyllactosides with low binding affinity can be further optimized for C-type lectin.

6 Outlook

Design of trivalent sialosides with optimum linker length to target HA of influenza virus is a promising strategy for the development of anti-influenza agents. As described in this thesis, attaching sialic acid at the terminal position to block the receptor binding site of HA trimer which is present on the surface of influenza virus increases the binding potency in comparison to monovalent interaction of SA to HA. Trivalent sialosides prepared in this part have amino group functionality at the top of the core which can be exploited to attach the trivalent ligand system on the multivalent scaffold such as polyglycerols. This optimizing trivalent ligand for multi-trimeric presentation may afford high affinity inhibitor for IAV.

Moreover, polyglycerol scaffolds were easily functionalized with the desired carbohydrates with varying degrees of functionalization shown in the second part of this thesis. When PGs were fully functionalized with Man and FL, the binding affinity was in nanomolar range with commercially available dimeric MBL and DC-SIGN. A study comparing native proteins will more interesting and might lead to even better binders than with the dimeric MBL and DC-SIGN. Efficient binders of MBL and DC-SIGN will be of great therapeutic interest. These can further be investigated for MBL complement inhibition followed by other associated possible biomedical applications. Similarly, DC-SIGN binders can be explored for the pathogen-cell binding inhibition using HIV or Ebola virus particles in cell-based assays.

These multivalent glycoconjugates are of therapeutic interest in drug design and discovery for various other C-type lectins.

7 Abstract and Kurzzusammenfassung

Abstract

This thesis focused on the design, synthesis, and evaluation of multivalent glycoconjugates for lectin binding. The first part discusses the optimization of trivalent sialosides based on functionalizable rigid and flexible core having different lengths of polyethylene glycol spacer for targeting hemagglutinin trimeric (HA₃) glycoproteins on the surface of influenza virus. All the synthesized compounds were screened using hemagglutination inhibition assay (HAI) and microscale thermophoresis (MST). The rigid adamantane-based trivalent sialosides with hexaethylene glycol (EG₆) linker showed a binding affinity in low micromolar range with $K_i = 30 \mu\text{M}$.

The second part of this thesis discusses the synthesis and evaluation of a series of polyglycerol based (linear and hyperbranched) mannosides and fucosyllactosides for C-type lectin binding. Polyglycerol polymers are highly water soluble, biocompatible, and easily functionalizable. Polyglycerol based multivalent glycoconjugates were synthesized using a copper assisted click reaction of azido fucosyllactoside and azido mannoside derivative with the propargylated polyglycerol with different degrees of functionalization. These glycoconjugates were tested for binding with mannose binding lectin (MBL) and DC-SIGN using biophysical techniques i.e., microscale thermophoresis (MST) and surface plasmon resonance (SPR), respectively. The most potent candidates for MBL and DC-SIGN binding were 100% functionalized hPG- and LPG- based mannosides, respectively, with the dissociation constant (K_d) in nanomolar range. Nanomolar binder for DC-SIGN was approximately 23,000-fold more active than the monovalent mannose with K_d of 3.5 mM. Further on, these multivalent architectures can further be investigated and optimized for the therapeutic application for C-type lectins.

Kurzzusammenfassung

Der Fokus dieser Arbeit war das Design, die Synthese und die Evaluation von Lektinbindenden multivalenten Glykokonjugaten.

Im ersten Teil wird die Optimierung von trivalenten Sialosiden auf der Basis von funktionalisierbaren starren oder flexiblen Kernen und verschiedenen langen Polyethylenglycol-Spacern für die Bindung an Hemagglutinin-Trimere (HA3) auf der Oberfläche von Influenzavirus diskutiert. Die Bindungseigenschaften der synthetisierten Verbindungen wurden mittels Hämagglutinations-Inhibitions-Assays (HAI) und Mikroskalenthermophorese (MST) analysiert. Die starren trivalenten Sialoside auf Adamantan-Basis mit Hexaethylenglykol (EG6)-Linker eine zeigten Bindungsaffinität im niedrigen mikromolaren Bereich mit einer Bindungskonstante (K_i) von $30 \mu\text{M}$.

Der zweite Teil dieser Arbeit befasst sich mit der Synthese und Bewertung einer Reihe von linearen und hyperverzweigten Mannosiden auf Polyglycerin-Basis und Fucosyllactosiden für die Bindung von Lektinen vom C-Typ. Polyglycerin-basierte Polymere sind wasserlöslich, biokompatibel und leicht funktionalisierbar. Mehrwertige Glykokonjugate auf Polyglycerinbasis wurden unter Verwendung einer kupferassistierten Klickreaktion ausgehend von Azidofucosyllactosid und Azidomannosidderivaten mit propargylierten Polyglycerol mit unterschiedlichem Funktionalisierungsgrad synthetisiert. Diese Glykokonjugate wurden auf Bindung mit Mannose-bindendem Lektin (MBL) und DC-SIGN unter Verwendung biophysikalischer Techniken wie Mikroskalenthermophorese (MST) bzw. Oberflächenplasmonresonanz (SPR) untersucht. Die aussichtsreichsten Kandidaten für die MBL- und DC-SIGN-Bindung waren vollständig funktionalisierte Mannoside auf hPG und lPG Basis mit Dissoziationskonstanten (K_d) im nanomolaren Bereich. Der beste Kandidat für die DC-SIGN Bindung war mit einem K_d von $3,5 \mu\text{M}$ etwa 23.000-fach aktiver als monovalente Mannose. Die synthetisierten multivalenten Architekturen kommen daher für eine zukünftige therapeutische Anwendung in Frage und können für die Bindung von Lektinen vom C-Typ optimiert werden.

References

8 References

- [1] (a) C. Fasting, C. A. Schalley, M. Weber, O. Seitz, S. Hecht, B. Kokschi, J. Darnedde, C. Graf, E.-W. Knapp, R. Haag, *Angewandte Chemie International Edition* **2012**, *51*, 10472-10498; (b) L. L. Kiessling, J. E. Gestwicki, L. E. Strong, *Current Opinion in Chemical Biology* **2000**, *4*, 696-703.
- [2] V. M. Krishnamurthy, L. A. Estroff, G. M. Whitesides, **2006**.
- [3] M. Mammen, S.-K. Choi, G. M. Whitesides, *Angewandte Chemie International Edition* **1998**, *37*, 2754-2794.
- [4] A. Mulder, J. Huskens, D. N. Reinhoudt, *Organic & Biomolecular Chemistry* **2004**, *2*, 3409-3424.
- [5] L. M. Stevers, P. J. de Vink, C. Ottmann, J. Huskens, L. Brunsveld, *Journal of the American Chemical Society* **2018**, *140*, 14498-14510.
- [6] Y. C. Lee, R. T. Lee, *Accounts of Chemical Research* **1995**, *28*, 321-327.
- [7] J. Cervin, A. M. Wands, A. Casselbrant, H. Wu, S. Krishnamurthy, A. Cvjetkovic, J. Estelius, B. Dedic, A. Sethi, K.-L. Wallom, R. Riise, M. Bäckström, V. Wallenius, F. M. Platt, M. Lebens, S. Teneberg, L. Fändriks, J. J. Kohler, U. Yrliid, *PLOS Pathogens* **2018**, *14*, e1006862.
- [8] J. R. Thiagarajah, A. S. Verkman, *Trends in Pharmacological Sciences* **2005**, *26*, 172-175.
- [9] W. B. Turnbull, B. L. Precious, S. W. Homans, *Journal of the American Chemical Society* **2004**, *126*, 1047-1054.
- [10] M. A. Gimbrone, Jr., T. Nagel, J. N. Topper, *The Journal of clinical investigation* **1997**, *99*, 1809-1813.
- [11] L. L. Kiessling, N. L. Pohl, *Chemistry & Biology* **1996**, *3*, 71-77.
- [12] C. P. Dietrich, J. de Paiva, C. T. Moraes, H. K. Takahashi, M. A. Porcionatto, H. B. Nader, *Biochimica et Biophysica Acta (BBA) - General Subjects* **1985**, *843*, 1-7.
- [13] (a) W. J. Lees, A. Spaltenstein, J. E. Kingery-Wood, G. M. Whitesides, *Journal of Medicinal Chemistry* **1994**, *37*, 3419-3433; (b) M. Mammen, G. Dahmann, G. M. Whitesides, *Journal of Medicinal Chemistry* **1995**, *38*, 4179-4190.
- [14] S. Bhatia, M. Dimde, R. Haag, *MedChemComm* **2014**, *5*, 862-878.
- [15] (a) E. A. Merritt, W. G. J. Hol, *Current Opinion in Structural Biology* **1995**, *5*, 165-171; (b) E. Fan, E. A. Merritt, C. L. M. J. Verlinde, W. G. J. Hol, *Current Opinion in Structural Biology* **2000**, *10*, 680-686.
- [16] (a) E. Fan, Z. Zhang, W. E. Minke, Z. Hou, C. L. M. J. Verlinde, W. G. J. Hol, *Journal of the American Chemical Society* **2000**, *122*, 2663-2664; (b) Z. Zhang, E. A. Merritt, M. Ahn, C. Roach, Z. Hou, C. L. M. J. Verlinde, W. G. J. Hol, E. Fan, *Journal of the American Chemical Society* **2002**, *124*, 12991-12998; (c) E. A. Merritt, Z. Zhang, J. C. Pickens, M. Ahn, W. G. J. Hol, E. Fan, *Journal of the American Chemical Society* **2002**, *124*, 8818-8824.
- [17] G. Thoma, R. O. Duthaler, J. L. Magnani, J. T. Patton, *Journal of the American Chemical Society* **2001**, *123*, 10113-10114.
- [18] S.-K. Choi, M. Mammen, G. M. Whitesides, *Journal of the American Chemical Society* **1997**, *119*, 4103-4111.
- [19] K. H. Mortell, R. V. Weatherman, L. L. Kiessling, *Journal of the American Chemical Society* **1996**, *118*, 2297-2298.
- [20] M. D. Disney, J. Zheng, T. M. Swager, P. H. Seeberger, *J Am Chem Soc* **2004**, *126*, 13343-13346.
- [21] (a) X. Li, M. Morimoto, H. Sashiwa, H. Saimoto, Y. Okamoto, S. Minami, Y. Shigemasa, *Polymers for Advanced Technologies* **1999**, *10*, 455-458; (b) M. Morimoto, H. Saimoto, H. Usui, Y. Okamoto, S. Minami, Y. Shigemasa, *Biomacromolecules* **2001**, *2*, 1133-1136.

References

- [22] I. K. Park, J. Yang, H. J. Jeong, H. S. Bom, I. Harada, T. Akaike, S. I. Kim, C. S. Cho, *Biomaterials* **2003**, *24*, 2331-2337.
- [23] H. Sashiwa, Y. Shigemasa, R. Roy, *Macromolecules* **2000**, *33*, 6913-6915.
- [24] (a) M. L. Wolfenden, M. J. Cloninger, *Journal of the American Chemical Society* **2005**, *127*, 12168-12169; (b) E. K. Woller, E. D. Walter, J. R. Morgan, D. J. Singel, M. J. Cloninger, *Journal of the American Chemical Society* **2003**, *125*, 8820-8826.
- [25] (a) Y. H. Jiang, P. Emau, J. S. Cairns, L. Flanary, W. R. Morton, T. D. McCarthy, C. C. Tsai, *AIDS research and human retroviruses* **2005**, *21*, 207-213; (b) M. Witvrouw, V. Fikkert, W. Pluymers, B. Matthews, K. Mardel, D. Schols, J. Raff, Z. Debyser, E. De Clercq, G. Holan, C. Pannecouque, *Molecular pharmacology* **2000**, *58*, 1100-1108; (c) G. Y. K. C. C. Williams, B. D. Kelly, S. A. Henderson, Z. Wu, P. Razzino, in *US Patent 20100292148*, **2010**.
- [26] (a) J. Vonnemann, S. Liese, C. Kuehne, K. Ludwig, J. Dervedde, C. Böttcher, R. R. Netz, R. Haag, *J Am Chem Soc* **2015**, *137*, 2572-2579; (b) M. Calderon, M. A. Quadir, S. K. Sharma, R. Haag, *Advanced materials (Deerfield Beach, Fla.)* **2010**, *22*, 190-218; (c) S. Bhatia, D. Lauster, M. Bardua, K. Ludwig, S. Angioletti-Uberti, N. Popp, U. Hoffmann, F. Paulus, M. Budt, M. Stadtmüller, T. Wolff, A. Hamann, C. Böttcher, A. Herrmann, R. Haag, *Biomaterials* **2017**, *138*, 22-34; (d) I. Papp, C. Sieben, K. Ludwig, M. Roskamp, C. Böttcher, S. Schlecht, A. Herrmann, R. Haag, *Small* **2010**, *6*, 2900-2906.
- [27] (a) Y. H. W. Kim, O. W. , *Am. Chem. Soc., Div. Polym. Chem* **1988**, *29*, 310-311; (b) Y. H. Kim, O. W. Webster, *Journal of the American Chemical Society* **1990**, *112*, 4592-4593.
- [28] (a) D. Wilms, S.-E. Stiriba, H. Frey, *Accounts of Chemical Research* **2010**, *43*, 129-141; (b) C. Gao, D. Yan, *Progress in Polymer Science* **2004**, *29*, 183-275.
- [29] J. M. J. Fréchet, M. Henmi, I. Gitsov, S. Aoshima, M. R. Leduc, R. B. Grubbs, *Science* **1995**, *269*, 1080-1083.
- [30] (a) A. Sunder, R. Hanselmann, H. Frey, R. Mülhaupt, *Macromolecules* **1999**, *32*, 4240-4246; (b) R. Haag, A. Sunder, J.-F. Stumbé, *Journal of the American Chemical Society* **2000**, *122*, 2954-2955.
- [31] R. K. Kainthan, J. Janzen, E. Levin, D. V. Devine, D. E. Brooks, *Biomacromolecules* **2006**, *7*, 703-709.
- [32] C. Siegers, M. Biesalski, R. Haag, *Chemistry* **2004**, *10*, 2831-2838.
- [33] A. Thomas, S. S. Müller, H. Frey, *Biomacromolecules* **2014**, *15*, 1935-1954.
- [34] (a) A. Dworak, I. Panchev, B. Trzebicka, W. Walach, *Polymer Bulletin* **1998**, *40*, 461-468; (b) C. S. Schacht, C. Schuell, H. Frey, T. W. de Loos, J. Gross, *J. Chem. Eng. Data* **2011**, *56*, 2927-2931.
- [35] (a) M. Erberich, H. Keul, M. Möller, *Macromolecules* **2007**, *40*, 3070-3079; (b) M. Hans, P. Gasteier, H. Keul, M. Moeller, *Macromolecules* **2006**, *39*, 3184-3193.
- [36] G. Gunkel, M. Weinhart, T. Becherer, R. Haag, W. T. S. Huck, *Biomacromolecules* **2011**, *12*, 4169-4172.
- [37] D. Taton, A. Le Borgne, M. Sepulchre, N. Spassky, *Macromolecular Chemistry and Physics* **1994**, *195*, 139-148.
- [38] (a) M. Gervais, A.-L. Brocas, G. Cendejas, A. Deffieux, S. Carlotti, *Macromolecules* **2010**, *43*, 1778-1784; (b) A. Labbé, S. Carlotti, C. Billouard, P. Desbois, A. Deffieux, *Macromolecules* **2007**, *40*, 7842-7847.
- [39] J. J. Skehel, D. C. Wiley, *Annual Review of Biochemistry* **2000**, *69*, 531-569.
- [40] (a) D. Henritzi, B. Hoffmann, S. Wacheck, S. Pesch, G. Herrler, M. Beer, T. C. Harder, *Influenza and Other Respiratory Viruses*, *0*; (b) C. E. Samuel, *The Journal of biological chemistry* **2010**, *285*, 28399-28401.

References

- [41] A. H. Reid, J. K. Taubenberger, T. G. Fanning, *Microbes and infection* **2001**, *3*, 81-87.
- [42] (a) E. Vanderlinden, L. Naesens, *Medicinal Research Reviews* **2014**, *34*, 301-339; (b) C. A. Russell, T. C. Jones, I. G. Barr, N. J. Cox, R. J. Garten, V. Gregory, I. D. Gust, A. W. Hampson, A. J. Hay, A. C. Hurt, J. C. de Jong, A. Kelso, A. I. Klimov, T. Kageyama, N. Komadina, A. S. Lapedes, Y. P. Lin, A. Mosterin, M. Obuchi, T. Odagiri, A. D. M. E. Osterhaus, G. F. Rimmelzwaan, M. W. Shaw, E. Skepner, K. Stohr, M. Tashiro, R. A. M. Fouchier, D. J. Smith, *Science* **2008**, *320*, 340-346; (c) T. M. Tumpey, T. R. Maines, N. Van Hoeven, L. Glaser, A. Solorzano, C. Pappas, N. J. Cox, D. E. Swayne, P. Palese, J. M. Katz, A. Garcia-Sastre, *Science* **2007**, *315*, 655-659; d) K. Das, J. M. Aramini, L. C. Ma, R. M. Krug, E. Arnold, *Nature structural & molecular biology* **2010**, *17*, 530-538; e) M. de Graaf, R. A. Fouchier, *Embo j* **2014**, *33*, 823-841.
- [43] (a) G. Chowell, S. M. Bertozzi, M. A. Colchero, H. Lopez-Gatell, C. Alpuche-Aranda, M. Hernandez, M. A. Miller, *The New England journal of medicine* **2009**, *361*, 674-679; (b) R. J. Garten, C. T. Davis, C. A. Russell, B. Shu, S. Lindstrom, A. Balish, W. M. Sessions, X. Xu, E. Skepner, V. Deyde, M. Okomo-Adhiambo, L. Gubareva, J. Barnes, C. B. Smith, S. L. Emery, M. J. Hillman, P. Rivallier, J. Smagala, M. de Graaf, D. F. Burke, R. A. Fouchier, C. Pappas, C. M. Alpuche-Aranda, H. Lopez-Gatell, H. Olivera, I. Lopez, C. A. Myers, D. Faix, P. J. Blair, C. Yu, K. M. Keene, P. D. Dotson, Jr., D. Boxrud, A. R. Sambol, S. H. Abid, K. St George, T. Bannerman, A. L. Moore, D. J. Stringer, P. Blevins, G. J. Demmler-Harrison, M. Ginsberg, P. Kriner, S. Waterman, S. Smole, H. F. Guevara, E. A. Belongia, P. A. Clark, S. T. Beatrice, R. Donis, J. Katz, L. Finelli, C. B. Bridges, M. Shaw, D. B. Jernigan, T. M. Uyeki, D. J. Smith, A. I. Klimov, N. J. Cox, *Science* **2009**, *325*, 197-201.
- [44] W. Weis, J. H. Brown, S. Cusack, J. C. Paulson, J. J. Skehel, D. C. Wiley, *Nature* **1988**, *333*, 426-431.
- [45] (a) S. Tong, X. Zhu, Y. Li, M. Shi, J. Zhang, M. Bourgeois, H. Yang, X. Chen, S. Recuenco, J. Gomez, L.-M. Chen, A. Johnson, Y. Tao, C. Dreyfus, W. Yu, R. McBride, P. J. Carney, A. T. Gilbert, J. Chang, Z. Guo, C. T. Davis, J. C. Paulson, J. Stevens, C. E. Rupprecht, E. C. Holmes, I. A. Wilson, R. O. Donis, *PLOS Pathogens* **2013**, *9*, e1003657; (b) S. Tong, X. Zhu, Y. Li, M. Shi, J. Zhang, M. Bourgeois, H. Yang, X. Chen, S. Recuenco, J. Gomez, L. M. Chen, A. Johnson, Y. Tao, C. Dreyfus, W. Yu, R. McBride, P. J. Carney, A. T. Gilbert, J. Chang, Z. Guo, C. T. Davis, J. C. Paulson, J. Stevens, C. E. Rupprecht, E. C. Holmes, I. A. Wilson, R. O. Donis, *PLoS Pathog* **2013**, *9*, e1003657; (c) M. Hussain, H. D. Galvin, T. Y. Haw, A. N. Nutsford, M. Husain, *Infection and drug resistance* **2017**, *10*, 121-134.
- [46] G. R. Whittaker, *Expert Reviews in Molecular Medicine* **2004**, *3*, 1-13.
- [47] (a) W. Shao, X. Li, M. U. Goraya, S. Wang, J.-L. Chen, *International journal of molecular sciences* **2017**, *18*, 1650; (b) G. W. Both, M. J. Sleight, N. J. Cox, A. P. Kendal, *Journal of virology* **1983**, *48*, 52-60; (c) R. G. Webster, W. G. Laver, G. M. Air, G. C. Schild, *Nature* **1982**, *296*, 115; d) M. Verhoeyen, R. Fang, W. M. Jou, R. Devos, D. Huylebroeck, E. Saman, W. Fiers, *Nature* **1980**, *286*, 771.
- [48] F. Carrat, A. Flahault, *Vaccine* **2007**, *25*, 6852-6862.
- [49] (a) J. Steel, A. C. Lowen, *Current topics in microbiology and immunology* **2014**, *385*, 377-401; (b) A. H. Reid, J. K. Taubenberger, *Journal of General Virology* **2003**, *84*, 2285-2292; (c) M. Richard, S. Herfst, H. Tao, N. T. Jacobs, A. C. Lowen, *Journal of Virology* **2018**, *92*.
- [50] M. von Itzstein, *Nature Reviews Drug Discovery* **2007**, *6*, 967.
- [51] G. A. Landolt, C. W. Olsen, *Animal Health Research Reviews* **2007**, *8*, 1-21.

References

- [52] (a) C. Scholtissek, *European Journal of Epidemiology* **1994**, *10*, 455-458; (b) C. Scholtissek, *Medical Principles and Practice* **1990**, *2*, 65-71.
- [53] (a) M. Orlich, H. Gottwald, R. Rott, *Virology* **1994**, *204*, 462-465; (b) L. S. David, A. S. Dennis, B. Jill, H. B. Ian, C. E. Steve, L. Chang-Won, J. M. Ruth, M.-B. Christian, M. Valentine, C. P. Janice, P. Brundaban, R. Herman, S. Eric, J. A. Dennis, *Emerging Infectious Disease journal* **2004**, *10*, 693.
- [54] M. F. Boni, Y. Zhou, J. K. Taubenberger, E. C. Holmes, *Journal of virology* **2008**, *82*, 4807-4811.
- [55] R. M. DuBois, J. M. Aguilar-Yañez, G. I. Mendoza-Ochoa, Y. Oropeza-Almazán, S. Schultz-Cherry, M. M. Alvarez, S. W. White, C. J. Russell, *Journal of Virology* **2011**, *85*, 865-872.
- [56] B. Isin, P. Doruker, I. Bahar, *Biophysical journal* **2002**, *82*, 569-581.
- [57] D. C. Wiley, J. J. Skehel, *Annu Rev Biochem* **1987**, *56*, 365-394.
- [58] A. García-Sastre, *The American journal of pathology* **2010**, *176*, 1584-1585.
- [59] M. N. Matrosovich, T. Y. Matrosovich, T. Gray, N. A. Roberts, H. D. Klenk, *J Virol* **2004**, *78*, 12665-12667.
- [60] Y. Ha, D. J. Stevens, J. J. Skehel, D. C. Wiley, *Proc Natl Acad Sci U S A* **2001**, *98*, 11181-11186.
- [61] Q. Li, J. Qi, Y. Wu, H. Kiyota, K. Tanaka, Y. Suhara, H. Ohru, Y. Suzuki, C. J. Vavricka, G. F. Gao, *Journal of Virology* **2013**, *87*, 10016-10024.
- [62] S. J. Gamblin, J. J. Skehel, *Journal of Biological Chemistry* **2010**.
- [63] (a) A. S. Monto, *Emerging infectious diseases* **2006**, *12*, 55-60; (b) J. Beigel, M. Bray, *Antiviral research* **2008**, *78*, 91-102; (c) L. Y. Zeng, J. Yang, S. Liu, *Expert opinion on investigational drugs* **2017**, *26*, 63-73; (d) M. T. Osterholm, N. S. Kelley, A. Sommer, E. A. Belongia, *The Lancet Infectious Diseases* **2012**, *12*, 36-44.
- [64] G. A. Poland, R. M. Jacobson, I. G. Ovsyannikova, *Clinical infectious diseases : an official publication of the Infectious Diseases Society of America* **2009**, *48*, 1254-1256.
- [65] M. Matrosovich, H. D. Klenk, *Reviews in medical virology* **2003**, *13*, 85-97.
- [66] (a) J. Yang, M. Li, X. Shen, S. Liu, *Viruses* **2013**, *5*, 352; (b) S. J. Fleishman, T. A. Whitehead, D. C. Ekiert, C. Dreyfus, J. E. Corn, E. M. Strauch, I. A. Wilson, D. Baker, *Science* **2011**, *332*, 816-821.
- [67] F. Li, C. Ma, J. Wang, *Current medicinal chemistry* **2015**, *22*, 1361-1382.
- [68] I. A. Wilson, J. J. Skehel, D. C. Wiley, *Nature* **1981**, *289*, 366.
- [69] M. Waldmann, R. Jirmann, K. Hoelscher, M. Wienke, F. C. Niemeyer, D. Rehders, B. Meyer, *Journal of the American Chemical Society* **2014**, *136*, 783-788.
- [70] N. K. Sauter, M. D. Bednarski, B. A. Wurzburg, J. E. Hanson, G. M. Whitesides, J. J. Skehel, D. C. Wiley, *Biochemistry* **1989**, *28*, 8388-8396.
- [71] G. B. Sigal, M. Mammen, G. Dahmann, G. M. Whitesides, *Journal of the American Chemical Society* **1996**, *118*, 3789-3800.
- [72] A. Tsuchida, K. Kobayashi, N. Matsubara, T. Muramatsu, T. Suzuki, Y. Suzuki, *Glycoconjugate Journal* **1998**, *15*, 1047-1054.
- [73] S.-J. Kwon, D. H. Na, J. H. Kwak, M. Douaisi, F. Zhang, E. J. Park, J.-H. Park, H. Youn, C.-S. Song, R. S. Kane, J. S. Dordick, K. B. Lee, R. J. Linhardt, *Nature Nanotechnology* **2016**, *12*, 48.
- [74] I. Papp, C. Sieben, A. L. Sisson, J. Kostka, C. Bottcher, K. Ludwig, A. Herrmann, R. Haag, *Chembiochem* **2011**, *12*, 887-895.
- [75] D. Lauster, M. Glanz, M. Bardua, K. Ludwig, M. Hellmund, U. Hoffmann, A. Hamann, C. Bottcher, R. Haag, C. P. R. Hackenberger, A. Herrmann, *Angew Chem Int Ed Engl* **2017**, *56*, 5931-5936.

References

- [76] (a) S. Bhatia, L. C. Camacho, R. Haag, *Journal of the American Chemical Society* **2016**, *138*, 8654-8666; (b) V. Bandlow, S. Liese, D. Lauster, K. Ludwig, R. R. Netz, A. Herrmann, O. Seitz, *Journal of the American Chemical Society* **2017**, *139*, 16389-16397.
- [77] T. Ohta, N. Miura, N. Fujitani, F. Nakajima, K. Niikura, R. Sadamoto, C. T. Guo, T. Suzuki, Y. Suzuki, K. Monde, S. I. Nishimura, *Angewandte Chemie International Edition* **2003**, *42*, 5186-5189.
- [78] J. Rao, J. Lahiri, R. M. Weis, G. M. Whitesides, *Journal of the American Chemical Society* **2000**, *122*, 2698-2710.
- [79] M. Yamabe, K. Kaihatsu, Y. Ebara, *Bioconjugate Chemistry* **2018**, *29*, 1490-1494.
- [80] A. N. Zelensky, J. E. Gready, *Febs j* **2005**, *272*, 6179-6217.
- [81] K. Drickamer, M. E. Taylor, *Current opinion in structural biology* **2015**, *34*, 26-34.
- [82] J. C. Hoving, G. J. Wilson, G. D. Brown, *Cellular microbiology* **2014**, *16*, 185-194.
- [83] C. G. Figdor, Y. van Kooyk, G. J. Adema, *Nature Reviews Immunology* **2002**, *2*, 77.
- [84] G. D. Brown, J. A. Willment, L. Whitehead, *Nature Reviews Immunology* **2018**, *18*, 374-389.
- [85] W. I. Weis, K. Drickamer, W. A. Hendrickson, *Nature* **1992**, *360*, 127.
- [86] (a) K. K. Ng, K. Drickamer, W. I. Weis, *The Journal of biological chemistry* **1996**, *271*, 663-674; (b) K. Drickamer, *Nature* **1992**, *360*, 183; (c) W. I. Weis, M. E. Taylor, K. Drickamer, *Immunological Reviews* **1998**, *163*, 19-34.
- [87] <https://www.invivogen.com/review-clr>.
- [88] W. I. Weis, *Current Opinion in Structural Biology* **1997**, *7*, 624-630.
- [89] M. W. Turner, *Immunology Today* **1996**, *17*, 532-540.
- [90] (a) M. W. Turner, *Molecular immunology* **2003**, *40*, 423-429; (b) A. Miller, A. Phillips, J. Gor, R. Wallis, S. J. Perkins, *The Journal of biological chemistry* **2012**, *287*, 3930-3945.
- [91] R. Wallis, K. Drickamer, *The Biochemical journal* **1997**, *325 (Pt 2)*, 391-400.
- [92] W. I. Weis, G. V. Crichlow, H. M. Murthy, W. A. Hendrickson, K. Drickamer, *The Journal of biological chemistry* **1991**, *266*, 20678-20686.
- [93] O. Neth, D. L. Jack, A. W. Dodds, H. Holzel, N. J. Klein, M. W. Turner, *Infection and immunity* **2000**, *68*, 688-693.
- [94] (a) S. Sheriff, C. Y. Chang, R. A. Ezekowitz, *Nature structural biology* **1994**, *1*, 789-794; (b) W. I. Weis, K. Drickamer, *Structure (London, England : 1993)* **1994**, *2*, 1227-1240.
- [95] U. Holmskov, R. Malhotra, R. B. Sim, J. C. Jensenius, *Immunology Today* **1994**, *15*, 67-74.
- [96] O. Neth, D. L. Jack, M. Johnson, N. J. Klein, M. W. Turner, *The Journal of Immunology* **2002**, *169*, 4430-4436.
- [97] J. Epstein, Q. Eichbaum, S. Sheriff, R. A. Ezekowitz, *Current opinion in immunology* **1996**, *8*, 29-35.
- [98] P. N. Nesargikar, B. Spiller, R. Chavez, *European journal of microbiology & immunology* **2012**, *2*, 103-111.
- [99] A. J. Nauta, M. R. Daha, C. v. Kooten, A. Roos, *Trends in Immunology* **2003**, *24*, 148-154.
- [100] M. J. Walport, *New England Journal of Medicine* **2001**, *344*, 1058-1066.
- [101] (a) S. V. Petersen, S. Thiel, L. Jensen, T. Vorup-Jensen, C. Koch, J. C. Jensenius, *Molecular immunology* **2000**, *37*, 803-811; (b) C. Auriti, G. Prencipe, M. Moriondo, I. Bersani, C. Bertaina, Mond, #xec, V. , R. Inglese, *Journal of Immunology Research* **2017**, *2017*, 11.
- [102] (a) M. Noris, G. Remuzzi, *Seminars in Nephrology* **2013**, *33*, 479-492; (b) J. M. Thurman, V. M. Holers, *The Journal of Immunology* **2006**, *176*, 1305-1310; cD.

References

- Ricklin, G. Hajishengallis, K. Yang, J. D. Lambris, *Nature Immunology* **2010**, *11*, 785.
- [103] (a) L. J. Schlapbach, M. Mattmann, S. Thiel, C. Boillat, M. Otth, M. Nelle, B. Wagner, J. C. Jensenius, C. Aebi, *Clinical infectious diseases : an official publication of the Infectious Diseases Society of America* **2010**, *51*, 153-162; (b) M. Scorza, R. Liguori, A. Elce, F. Salvatore, G. Castaldo, *Clinica chimica acta; international journal of clinical chemistry* **2015**, *451*, 78-81.
- [104] L. H. Bouwman, B. O. Roep, A. Roos, *Human Immunology* **2006**, *67*, 247-256.
- [105] H. F. Weisman, T. Bartow, M. K. Leppo, H. C. Marsh, Jr., G. R. Carson, M. F. Concino, M. P. Boyle, K. H. Roux, M. L. Weisfeldt, D. T. Fearon, *Science* **1990**, *249*, 146-151.
- [106] S. M. Shandelya, P. Kuppusamy, M. L. Weisfeldt, J. L. Zweier, *Circulation* **1993**, *87*, 536-546.
- [107] M. Lauterbach, G. Horstick, N. Plum, J. Lotz, E. Lauterbach, L. S. Weilemann, O. Kempfski, *Shock (Augusta, Ga.)* **2007**, *27*, 75-83.
- [108] E. Jordan James, C. Montalto Michael, L. Stahl Gregory, *Circulation* **2001**, *104*, 1413-1418.
- [109] V. I. Pavlov, Y. S. Tan, E. E. McClure, L. R. La Bonte, C. Zou, W. B. Gorsuch, G. L. Stahl, *The American journal of pathology* **2015**, *185*, 347-355.
- [110] M.-O. Skjoedt, P. Roversi, T. Hummelshøj, Y. Palarasah, A. Rosbjerg, S. Johnson, S. M. Lea, P. Garred, *The Journal of biological chemistry* **2012**, *287*, 32913-32921.
- [111] F. Orsini, S. Fumagalli, E. Császár, K. Tóth, D. De Blasio, R. Zangari, N. Lénárt, Á. Dénes, M.-G. De Simoni, *Arteriosclerosis, Thrombosis, and Vascular Biology* **2018**, *38*, 2678-2690.
- [112] (a) D. De Blasio, S. Fumagalli, L. Longhi, F. Orsini, A. Palmioli, M. Stravalaci, G. Vegliante, E. R. Zanier, A. Bernardi, M. Gobbi, M. G. De Simoni, *Journal of cerebral blood flow and metabolism : official journal of the International Society of Cerebral Blood Flow and Metabolism* **2017**, *37*, 938-950; (b) M. Stravalaci, D. De Blasio, F. Orsini, C. Perego, A. Palmioli, G. Goti, A. Bernardi, M. G. De Simoni, M. Gobbi, *Journal of biomolecular screening* **2016**, *21*, 749-757.
- [113] D. A. Kimbrell, B. Beutler, *Nature Reviews Genetics* **2001**, *2*, 256.
- [114] (a) F. Baribaud, S. Pöhlmann, R. W. Doms, *Virology* **2001**, *286*, 1-6; (b) R. Celerino da Silva, L. Segat, S. Crovella, *Human Immunology* **2011**, *72*, 305-311.
- [115] U.-S. Khoo, K. Y. K. Chan, V. S. F. Chan, C. L. S. Lin, *Journal of Molecular Medicine* **2008**, *86*, 861-874.
- [116] L. Wu, V. N. KewalRamani, *Nature Reviews Immunology* **2006**, *6*, 859.
- [117] (a) H. Feinberg, D. A. Mitchell, K. Drickamer, W. I. Weis, *Science* **2001**, *294*, 2163-2166; (b) Y. Guo, H. Feinberg, E. Conroy, D. A. Mitchell, R. Alvarez, O. Blixt, M. E. Taylor, W. I. Weis, K. Drickamer, *Nature structural & molecular biology* **2004**, *11*, 591-598.
- [118] B. J. Appelmelk, I. van Die, S. J. van Vliet, C. M. Vandenbroucke-Grauls, T. B. Geijtenbeek, Y. van Kooyk, *Journal of immunology (Baltimore, Md. : 1950)* **2003**, *170*, 1635-1639.
- [119] S. Menon, K. Rosenberg, S. A. Graham, E. M. Ward, M. E. Taylor, K. Drickamer, D. E. Leckband, *Proceedings of the National Academy of Sciences of the United States of America* **2009**, *106*, 11524-11529.
- [120] D. 10.5772/50627.
- [121] D. A. Mitchell, A. J. Fadden, K. Drickamer, *The Journal of biological chemistry* **2001**, *276*, 28939-28945.

References

- [122] J. Luczkowiak, S. Sattin, I. Sutkevičiūtė, J. J. Reina, M. Sánchez-Navarro, M. Thépaut, L. Martínez-Prats, A. Daggetti, F. Fieschi, R. Delgado, A. Bernardi, J. Rojo, *Bioconjugate Chemistry* **2011**, *22*, 1354-1365.
- [123] C. R. Becer, M. I. Gibson, J. Geng, R. Ilyas, R. Wallis, D. A. Mitchell, D. M. Haddleton, *Journal of the American Chemical Society* **2010**, *132*, 15130-15132.
- [124] P. Kiran, S. Bhatia, D. Lauster, S. Aleksić, C. Fleck, N. Peric, W. Maison, S. Liese, B. G. Keller, A. Herrmann, R. Haag, *Chemistry – A European Journal* **2018**, *24*, 1-14.

9 Appendix

9.1 List of abbreviations

AGE	Allyl glycidyl ether
Approx.	Approximately
Arg	Arginine
Me	methyl
MeOH	methanol
min(s)	minute(s)
NMR	Nuclear Magnetic Resonance
ConA	Concavallin A
CTL	C-type lectins
Cryo TEM	Cryo transmission electron microscopy
CT	Cholera toxin
C1-INH	C1 esterase inhibitor
CTLD	C-type lectin like domain
CRP	C-reactive protein
CRD	Carbohydrate recognition domain
DB	Degree of branching
DC-SIGN	Dendritic cell-specific ICAM-3-grabbing non-integrin
DF	Degree of functionalization
DLS	Dynamic light scattering
DNA	Deoxy ribose nucleic acid
dPG	Dendritic polyglycerol
E. COLI	Escherichia Coli
EEGE	Ethoxyethyl glycidyl ether
EM	Effective molarity
HA	Hemagglutinin
HA ₃	Hemagglutinin trimer
HIV	Human immunodeficiency virus
hMBL	Human Mannose binding lectin
HSV	Herpes simplex virus
IAV	Influenza A virus
ICAM-1	Intracellular adhesion molecule-1
IL	Interleukin

Appendix

ITC	Isothermal titration calorimetry
Kd	Dissociation constant
IPG	Linear polyglycerol
mAbs	Monoclonal antibody
MASP	Mannan-binding lectin- associated serine protease
Map19	MBL-associated protein of 19 kDa
MD	Molecular dynamics
MBP	Mannose binding protein
MST	Microscale thermophoresis
M.Wt	Molecular weight
mRNA	Messenger ribose nucleic acid
NA	Neraminidase
NAI	Nuraminidase inhibitor
OEG	Oligoethylene glycol
PAMAM	Poly(amido-amine)
PAA	Polyacrylamide
PDI	Polydispersity index
PPOK	Potassium 3-phenylpropanolate
nPG	Polyglycerol based nanogel
PPOK	potassium 3-phenylpropanolate
PPE	Poly(p-phenylene ethynylene)
PPI	Poly(ethylenimine)
PLL	Poly-L-lysine
PEG	Polyethylene glycol
RBC	Red blood cell
rhMBL	Recombinant human MBL
RNA	Ribose nucleic acid
ROMP	Ring opening metathesis polymerization
ROMBP	Ring-opening metathesis polymerization
SiRNA	Small interfering RNA
SA	Sialic acid
SCVP	Self-condensing vinyl polymerization
sLe ^x	Sialylated LewisX
sMAP	Small MBL-associated protein

Appendix

sCR1	Soluble complement receptor type-1
SPR	Surface plasmon resonance
^t BGE	tert-butyl glycidyl ether
TBI	Traumatic brain injury
TCC	Terminal complement complex
NOct ₄ Br	Tetraoctylammoniumbromid
ⁱ Bu ₃ Al	Triisobutylaluminum
TMP	Trimethylolpropane
TMSGE	Trimethylsilyl glycidyl ether
VCAM-1	Vascular cell adhesion molecule-1

9.2 Publication and conference contributions

Publications

Pallavi Kiran,^[+] Sumati Bhatia,^[+] Daniel Lauster, Stevan Aleksić, Carsten Fleck, Natalija Peric, Wolfgang Maison, Susanne Liese, Bettina G. Keller, Andreas Herrmann, Rainer Haag* *Chem. Eur. J.* 2018, 24, 1–14. Exploring Rigid and Flexible Core Trivalent Sialosides for Influenza Virus Inhibition. [+] authors contributed equally. <https://doi.org/10.1002/chem.201804826>,^[+] Authors contributed equally.

Poster Presentations

- (1) European Winterschool on Physical Organic Chemistry, Bressenone, Italy (February 2016), *Multivalent Macromolecules as inhibitors of Influenza virus*; P.Kiran, S. Bhatia, and R. Haag
- (2) Workshop by SFB765, Freie University Berlin, Germany (August 2016), *Multivalent Macromolecules as inhibitors of Influenza virus*; P. Kiran, S. Bhatia, and R. Haag
- (3) PhD workshop by SFB765, Hannover, Germany (August 2016), *Multivalent Macromolecules as inhibitors of Influenza virus*; Pallavi Kiran, Sumati Bhatia, Wolfgang Maison and Rainer Haag
- (4) SFB765 Doktorandentag at Freie University Berlin, Germany (February 2017), *Multivalent Macromolecules as inhibitors of Influenza virus*; Pallavi Kiran, Sumati Bhatia, Wolfgang Maison and Rainer Haag
- (5) NanoBioMater 2017 Summer School & International Conference by University of Stuttgart, Germany (June 2017), *Multivalent Macromolecules as inhibitors of Influenza virus*; Pallavi Kiran, Sumati Bhatia, Daniel Lauster, Andreas Herrmann, Rainer Haag
- (6) ICMS Outreach Symposium at Technical university of Eindhoven, Netherland (January 2018), *Multivalent Sialylated Polyglycerol Derivatives Inhibit Influenza Virus Propagation*; Pallavi Kiran, Shalini Kumari, Sumati Bhatia, Daniel Lauster, Kai Ludwig, Christoph Böttcher, Alf Hamann, Andreas Herrmann, Rainer Haag

Appendix

- (7) SFB765 Doktorandentag, Freie University Berlin, Germany (March 2018), *Multivalent Sialylated Polyglycerol Derivatives Inhibit Influenza Virus Propagation*; Pallavi Kiran[#], Shalini Kumari[#], Sumati Bhatia, Daniel Lauster, Kai Ludwig, Christoph Böttcher, Alf Hamann, Andreas Herrmann, Rainer Haag
- (8) Workshop on Symposium on Cooperative Effects in Chemistry, Muenster, Germany (April 2018), *Multivalent Sialylated Polyglycerol Derivatives Inhibit Influenza Virus Propagation*; Pallavi Kiran, Shalini Kumari, Sumati Bhatia, Daniel Lauster, Kai Ludwig, Christoph Böttcher, Alf Hamann, Andreas Herrmann, Rainer Haag

9.3 Curriculum vitae

For reasons of data protection, the curriculum vitae is not published in the electronic version